

Optimized position for a sponson on the Fairplayer with respect to the ship performance

D. Spaans

Delft University of Technology



Optimized position for a sponson on the Fairplayer with respect to the ship performance

by

D. Spaans

to obtain the degree of Master of Science
at the Delft University of Technology,

Degree programme: Master Marine Technology
Specialisation: Ship Hydromechanics
Student number: 4155793
Graduation date: November 2, 2017
Project duration: November 14, 2016 – November 2, 2017
Thesis committee: Prof. dr. ir. A.P. van 't Veer, TU Delft, Graduation professor
Ir. J. den Haan, TU Delft, University daily supervisor
Ir. K. van der Heiden, Jumbo Maritime, Company daily supervisor

This thesis is confidential and cannot be made public until November 2, 2022.

An electronic version of this thesis is available at <http://repository.tudelft.nl/>.

Preface

This graduation thesis is the end product of my master Marine Technology at Delft University of Technology. This thesis report is the outcome of my work on the optimized position for a sponson on the Fairplayer. The Fairplayer is one of the J-Class heavy lift vessels from Jumbo Maritime, which headquarters is positioned in Schiedam, The Netherlands. This is also the office where I performed my research.

First of all I would like to thank Jumbo Maritime for giving me the opportunity to work on my master thesis. The company has a pleasant working atmosphere and when asked, help was happily provided. The first person I would like to thank personally is Kasper van der Heiden, my supervisor from Jumbo Maritime. He gave me the freedom to completely define my own subject and guided me through the project. A special thanks goes to Joost den Haan, who looked critically at my project and asked the right questions to keep me sharp. The next person I would like to thank is Erik Rotteveel. He helped me with creating concepts in Rhinoceros and the resistance calculations in RAPID. I would also like to thank Christian Veldhuis from MARIN for the support with RAPID. Furthermore I would like to thank the other students at Jumbo for their humour during the breaks.

Finally, I want to thank my friends and family for supporting me during my studies. Even when things were more difficult they supported me. I wish you much fun reading this report and hope you enjoy it.

D. Spaans
Delft, November 2017

Abstract

Jumbo Maritime is a heavy lift shipping and offshore transportation & installation contractor. The Fairplayer is one of their J-class vessels that is capable of performing offshore installation work. The vessel has a DP2 system and two 900 ton Huisman cranes. Due to the insufficient static stability a stabilization pontoon is required to increase the lifting capacity from 1000 ton to the maximum capacity of 1800 ton. This stabilization pontoon can only be used in the harbour or in calm waters and cannot be used in rough offshore conditions. The limited lifting capacity in offshore conditions is a missed opportunity to make use of the Fairplayer in a wider segment of the offshore installation market.

The static stability of the Fairplayer can be increased by the use of a sponson. A sponson is an extension on the side of the hull. A widening of the hull decreases the operating range of the two cranes, which are placed on starboard side. For this reason the sponson is only placed at portside. It is expected that this sponson generates an increase of the ship resistance and therefore a dual draft vessel is investigated. A dual draft vessel changes the draft when the operation of the vessel has changed. The Fairplayer with a sponson as a dual draft vessel sails to the port without having an increased resistance. During the offshore installation operation the Fairplayer fills the ballast tanks to increase the draft of the vessel and thereby the static stability.

A concept study is done to the application of a sponson on the Fairplayer, where the main variation in vertical position of the sponson on the operational profile was investigated. From this concept study it is concluded that a vertical position of the sponson around or even below the waterline is preferred. Therefore the goal of this thesis was to investigate the influence of the position and shape of a sponson on the Fairplayer with respect to the resistance.

There are multiple methods to calculate the resistance of the Fairplayer with a sponson. Methods such as CFD and model testing are expensive and time consuming, which are not feasible to use for the amount of concepts in this research. The empirical method set up by Holtrop & Mennen gives an estimation based on formulas for different resistance components. The formulas are based on resistance data from model tests and full scale vessels obtained in the past. The Fairplayer with a sponson is a hull shape which is significantly different than the hull shapes used to set up the method. By analysing the different resistance components it is concluded that the wave-making resistance is the only resistance component, which has trouble estimating. Another method to calculate the resistance is the potential flow theory program RAPID. The software RAPID is developed at MARIN and solves the potential flow problem by an iterative procedure, based on a raised-panel method. The program calculates the wave-making resistance of a vessel, but does not take the viscous effects into account. In this research an adjusted Holtrop-Mennen method is set up, which combines the Holtrop-Mennen method and the wave-making resistance calculations with RAPID.

This method uses five steps to calculate the percentage increase of the total resistance. Step 1 is the basis calculation of the Fairplayer without a sponson at a draft of 7.5 meter with the Holtrop-Mennen method. Step 2 is the calculation of the increase in the wave-making resistance for the Fairplayer with a sponson using the program RAPID. In step 3 the frictional resistance is calculated based on the ITTC-57 flat plate friction formula. Also the change of the form factor ($1 + k$), due to the change of the hull shape is estimated. In step 4 the change of other resistance components due to the concept with a sponson are calculated. The appendage resistance does not change, because the rudders and bilge keel of the vessel do not change. The model-ship correlation coefficient changes, because of the increase of the wetted area of the concept. The final step (step 5) combines all resistance components and calculates the percentage increase compared to the basis calculation as done in step 1.

The influence of the position and shape on the resistance of the Fairplayer with a sponson is obtained from three different variation studies. In this study only one variable is changed in five consecutive concepts in order to see the influence. The three variables that are tested are the longitudinal starting position, the length over width ratio and the vertical starting position of the sponson. From this study it can be concluded that

the frictional resistance and the model-ship correlation resistance both have a similar increase in resistance for all concepts. This means that a concept with a different the position and shape of the sponson does not have a significant effect on these two resistance components. On the other hand, the wave-making resistance seems to be of significant influence. The wave-making resistance varies from an increase of 8 to 200% between the concepts. The longitudinal position of the sponson leads to an interference of the wave system of the sponson with the wave system generated by the vessel itself. This interference can result in an increase of the wave height by the coincide of two wave crests. A coincide of a wave crest and wave trough can result in a decrease of the wave height. From the variation of the length over width ratio of the sponson it is concluded that a higher ratio results in a decrease of the wave-making resistance. A side note needs to be made that the influence of the longitudinal position of the front and aft shoulder of the sponson could lead to an interference of the wave systems that results in a higher resistance. The total resistance increases rapidly when the vertical starting position is lower, but a lower vertical starting position means that the conversion in a dual draft vessel cannot be obtained.

The final design of the sponson on the Fairplayer is 5 meter wide and 60 meter long. This sponson has a vertical starting position of 5.8 meter, which means that the operational profile of the vessel changes. The vessel sails in ballast condition on a draft of 5.5 meter without an increase of resistance due to the sponson. The vessel sails with cargo on deck at the transit draft of 7.5 meter due to the insufficient static stability at a draft of 5.5 meter. The increase of the total resistance of the Fairplayer with a sponson is 7%. This increase in resistance results in a decrease of 3% on the maximum speed, which becomes 16.5 knots.

It can be concluded that the Fairplayer with a sponson leads to an increase of the lifting capacity from 1000 ton to 1800 ton. The drawback is that the vessel encounters a decrease of the maximum speed with 3% to a speed of 16.5 knots, when the vessel sails with cargo on deck. The calculation method should be validated with a CFD calculation or a model test. A financial analysis has to decide if the increase in revenues due to the larger crane capacity weighs up to the initial investment and the longer transit times due to the reduced speed.

Contents

Preface	iii
Abstract	v
List of Figures	xi
List of Tables	xv
Nomenclature	xv
1 Introduction	1
1.1 Jumbo Maritime	1
1.2 Problem introduction	1
1.3 Previous research	3
1.4 Sponson	3
1.5 Basis of the concept	5
1.6 Research question	7
1.7 Boundaries of the research	7
1.8 Operational profile	8
1.9 Document structure	9
2 Literature	11
2.1 Ship definitions	11
2.2 Lift operation	12
2.3 Resistance	14
2.3.1 Decomposition of the total resistance	15
2.4 Holtrop-Mennen resistance prediction method	15
2.5 Computational techniques	18
2.5.1 Computational techniques for viscous flows	18
2.5.2 Potential flow theory	19
2.6 RAPID	24
2.7 Slamming	25
3 Concept study	27
3.1 Concept boundaries	28
3.1.1 Current design	28
3.1.2 Static stability	28
3.1.3 Cargo stored on deck	28
3.1.4 SPS regulation	29
3.1.5 Feasibility	29
3.2 Concept criteria	30
3.2.1 Loss of stability	30
3.2.2 Resistance	30
3.2.3 CAPEX	31
3.2.4 Motion behaviour	31
3.2.5 Ballast water	32
3.2.6 Deck area	34
3.2.7 Maintenance	34

3.3	Concepts overview	34
3.3.1	Concept 1: Long sponson around the waterline	34
3.3.2	Concept 2: Long sponson above the waterline	35
3.3.3	Concept 3: Long sponson below the waterline	35
3.3.4	Concept 4: Short sponson above the waterline	36
3.3.5	Concept 5: Vertically movable sponson	37
3.4	Concept selection	38
3.4.1	Conclusions of the concept study	40
4	Resistance calculation method	43
4.1	Methods to calculate the resistance of the Fairplayer	43
4.1.1	Comparison between Holtrop-Mennen, CFD and RAPID	44
4.2	Input options in RAPID	47
4.2.1	Calculation of the transom flow	47
4.2.2	Asymmetrical calculation	50
4.2.3	Grid study	51
4.3	Adjusted Holtrop-Mennen method for the resistance calculation	54
5	Results of the adjusted Holtrop-Mennen method	59
5.1	Systematic concept variation	59
5.2	Results of the adjusted Holtrop-Mennen method	61
5.3	Conclusions of the adjusted Holtrop-Mennen method	66
5.4	Speed of the Fairplayer with a sponson	69
6	Conclusions and recommendations	73
6.1	Conclusions	73
6.2	Recommendation	75
	Bibliography	77
A	Factsheet Fairplayer	79
B	Previous research	85
C	Resistance prediction method by Holtrop & Mennen	87
C.1	Raw data from the Holtrop-Mennen method	91
C.2	Evolution of the Holtrop-Mennen method from 1977 to 1984	92
D	RAPID calculation	95
D.1	Adjustment of the 3D model	95
D.2	Grid generation	96
D.3	Calculation	97
D.4	Calculation with a sponson	101
D.5	First calculations of a sponson with RAPID	103
E	Variation concepts	109
E.1	Concept a1	110
E.2	Concept a2	111
E.3	Concept a3	112
E.4	Concept a4	113
E.5	Concept a5	114
E.6	Concept b1	115
E.7	Concept b2	116
E.8	Concept b3	117
E.9	Concept b4	118
E.10	Concept b5	119
E.11	Concept c1	120
E.12	Concept c2	121
E.13	Concept c3	122
E.14	Concept c4	123
E.15	Concept c5	124

E.16 Concept d1	125
F Results of the adjusted Holtrop-Mennen method	127

List of Figures

1.1	Competition analysis of the current fleet of heavy lift vessels. [1]	2
1.2	Examples of the use of a pontoon to increase the static stability.	3
1.3	The principle of a dual draft vessel.	4
1.4	The concept a dual draft vessel with one sponson.	4
1.5	L-Class vessel tested at MARIN.	5
1.6	The important locations for the ship's stability.	5
1.7	The important dimensions for the calculation of the moment of inertia of the waterplane.	7
1.8	Weather data locations for motion analysis.	8
2.1	Definition of ship motions.	11
2.2	Situation 'before lift'.	12
2.3	Situation 'lift off'.	13
2.4	Situation 'crane out'.	13
2.5	Range of vessels from the Holtrop-Mennen method.	16
2.6	Pressure variation due to streamline curvature. [17]	20
2.7	Pressure and velocity distribution along a 2D body [17].	21
2.8	Direction, phase speed and length of the wave components in three-dimensional cases [17].	22
2.9	The near-field disturbance and the free wave systems for the wedge hull [17].	23
2.10	The location of the panels on the hull and above the free surface in RAPID [20].	25
3.1	Overview of the variables of the sponson in top view.	27
3.2	Overview of the variables of the sponson in front view.	27
3.3	Schematic representation of the two different cases where a loss of stability can occur.	30
3.4	The amount of ballast water for a range of drafts.	33
3.5	The time needed to submerge from a draft of 5.5 meter.	33
3.6	Concept 1: Long sponson around the waterline (T = 5.5 meter).	34
3.7	Concept 2: Long sponson above the waterline (T = 7.5 meter).	35
3.8	Concept 3: Long sponson below the waterline (T = 7.5 meter).	36
3.9	Concept 4: Short sponson above the waterline (T = 7.5 meter).	36
3.10	Concept 5: Vertically movable sponson.	37
3.11	The three levels in the hierarchy of the AHP method.	38
3.12	The 9-point scale, which can be used to compare the criteria in the AHP method.	38
4.1	Schematic overview of four resistance calculation methods.	44
4.2	Comparison of the wave pattern from the CFD and RAPID calculation (T = 6.5 meter).	47
4.3	Different configurations of the free surface.	48
4.4	Froude number of the transom at a speed of 17 knots.	49
4.5	Wave pattern comparison for panels behind the transom.	50
4.6	Wave pattern of a calculation with an asymmetric hull in RAPID.	51
4.7	Hull surface grid study of the Fairplayer.	52
4.8	Free surface grid study of the Fairplayer.	52
4.9	Hull surface grid study of the Fairplayer with a sponson.	53
4.10	Free surface grid study of the Fairplayer with a sponson.	53
4.11	The wave pattern of the Fairplayer at a draft of 7.5 meter.	55
4.12	The underwater ship of the symmetric Fairplayer with sponsons.	56
4.13	The underwater ship of the adjusted hull with sponsons.	56
5.1	Defenitions of the six variables which define the dimensions of the sponson.	60

5.2	Increase of the individual resistance components w.r.t. the Fairplayer, when the longitudinal position of the sponson is varied.	61
5.3	Wave pattern comparison of the variation in longitudinal position of the sponson.	63
5.4	Increase of the individual resistance components w.r.t. the Fairplayer, when the length over width ratio of the sponson is varied.	64
5.5	Wave pattern comparison of the variation in length over width ratio of the sponson.	65
5.6	Increase of the individual resistance components w.r.t. the Fairplayer, when the vertical position of the sponson is varied.	66
5.7	Rhinoceros 3D model of concept b4.	68
5.8	'Crane out' phase during the lifting operation of the Fairplayer with a sponson.	69
5.9	The resistance of the Fairplayer with a sponson as function of the speed.	70
6.1	Rhinoceros 3D model of the final concept (concept b4) of the Fairplayer with a sponson.	75
B.1	Four concepts defined by P. Harenberg [6].	85
C.1	Stern shape coefficient C_{stern}	88
C.2	Approximate $1 + k_2$ values.	89
D.1	3D model of the J-class vessel the Fairplayer.	95
D.2	3D model of the J-class vessel the Fairplayer without rudders and propeller.	96
D.3	3D model of the J-class vessel the Fairplayer, which is used to create a grid for RAPID.	96
D.4	3D model of the J-class vessel the Fairplayer with a grid for RAPID.	97
D.5	Window with the dimensions of the imported panel file of the hull.	97
D.6	Window with the speed of the vessel and the water depth can be seen.	98
D.7	Panel file of the J-class vessel the Fairplayer in ParaView.	98
D.8	Input window for the generation of the free surface in RAPID.	99
D.9	Input window for the start of the calculation in RAPID.	99
D.10	Window with all the information about the calculation in RAPID.	100
D.11	Output window with all the information about the iterations of the calculation in RAPID.	100
D.12	Contours of the sponson in the hull of the Fairplayer in Rhinoceros.	101
D.13	Intersection of the contours with the hull of the Fairplayer in Rhinoceros.	101
D.14	Transition of the sponson to the hull of the Fairplayer in Rhinoceros.	102
D.15	Contour lines to create one surface at the side of the sponson in Rhinoceros.	102
D.16	Panels of the free surface for the Fairplayer with a sponson.	102
D.17	Wave pattern of the Fairplayer with a sponson calculated with RAPID.	103
D.18	Rhinoceros 3D model of the first test concept.	104
D.19	Wave pattern of the first concept with a sponson calculated with RAPID.	104
D.20	Rhinoceros 3D model of the test concept with an open aft of the sponson.	105
D.21	Wave pattern of the concept with an open aft of the sponson calculated with RAPID.	105
D.22	Free surface grid study for the concept with a sponson with an open aft.	106
D.23	Free surface grid of the concept with an open aft of a sponson.	106
E.1	Rhinoceros 3D model of concept a1.	110
E.2	Wave pattern of concept a1 as calculated with RAPID.	110
E.3	Rhinoceros 3D model of concept a2.	111
E.4	Wave pattern of concept a2 as calculated with RAPID.	111
E.5	Rhinoceros 3D model of concept a3.	112
E.6	Wave pattern of concept a3 as calculated with RAPID.	112
E.7	Rhinoceros 3D model of concept a4.	113
E.8	Wave pattern of concept a4 as calculated with RAPID.	113
E.9	Rhinoceros 3D model of concept a5.	114
E.10	Wave pattern of concept a5 as calculated with RAPID.	114
E.11	Rhinoceros 3D model of concept b1.	115
E.12	Wave pattern of concept b1 as calculated with RAPID.	115
E.13	Rhinoceros 3D model of concept b2.	116
E.14	Wave pattern of concept b2 as calculated with RAPID.	116

E.15 Rhinoceros 3D model of concept b3.	117
E.16 Wave pattern of concept b3 as calculated with RAPID.	117
E.17 Rhinoceros 3D model of concept b4.	118
E.18 Wave pattern of concept b4 as calculated with RAPID.	118
E.19 Rhinoceros 3D model of concept b5.	119
E.20 Wave pattern of concept b5 as calculated with RAPID.	119
E.21 Rhinoceros 3D model of concept c1.	120
E.22 Wave pattern of concept c1 as calculated with RAPID.	120
E.23 Rhinoceros 3D model of concept c2.	121
E.24 Wave pattern of concept c2 as calculated with RAPID.	121
E.25 Rhinoceros 3D model of concept c3.	122
E.26 Wave pattern of concept c3 as calculated with RAPID.	122
E.27 Rhinoceros 3D model of concept c4.	123
E.28 Wave pattern of concept c4 as calculated with RAPID.	123
E.29 Rhinoceros 3D model of concept c5.	124
E.30 Wave pattern of concept c5 as calculated with RAPID.	124
E.31 Rhinoceros 3D model of concept d1.	125
E.32 Wave pattern of concept d1 as calculated with RAPID.	125

List of Tables

1.1	Main characteristics of the Fairplayer.	2
1.2	Main characteristics of the pontoons.	3
1.3	Offshore weather locations.	8
3.1	Operatibility of the four concepts and the Fairplayer when lifting 900 ton [6].	32
3.2	Operatibility of the four concepts when lifting 1800 ton [6].	32
3.3	Comparison of the different criteria in a matrix	39
3.4	The matrix with 'concept priorities' for each criteria.	39
3.5	The consistency ratio's for the different matrices.	40
3.6	Eigenvector with the weighted criteria.	40
3.7	Results of the Analytic Hierarchy Process.	40
4.1	The Holtrop-Mennen resistance calculation of the Fairplayer at a draft of 6.5 meter.	45
4.2	Results of the CFD calculation, the RAPID calculation and the Holtrop-Mennen method.	45
4.3	The total resistance of the three methods.	45
4.4	Amount of panels on the hull surface in the grid study.	51
4.5	The Holtrop-Mennen resistance calculation of the Fairplayer at a draft of 7.5 meter.	54
5.1	Main variables of the fifteen concepts of the sponson.	60
5.2	Main characteristics of the sponson on the Fairplayer	68
C.1	Raw data from the Holtrop-Mennen method of 1984.	91
C.2	Evolution of the Holtrop-Mennen method.	93
E1	Increase of the resistance components as percentage of the Fairplayer for the different concepts.	127
E2	Values of the resistance components for the different concepts calculated with the adjusted Holtrop-Mennen method.	128
E3	Resistance components for the extra iteration of the concept from the Fairplayer with a sponson.	128

Nomenclature

Abbreviations

AHP	Analytic Hierarchy Process
CAPEX	Capital expenditures
CFD	Computational Fluid Dynamics
COB	Center of buoyancy
COG	Center of gravity
CPP	Controllable pitch propeller
DDS	Deepwater Deployment System
DP2	Dynamic positioning 2
DPR	Daily Progress Report
ITTC	International Towing Tank Conference
LCB	Longitudinal center of buoyancy
MCR	Maximum continuous rating
RAO	Response Amplitude Operator
RAPID	RAised Panel Iterative Dawson
SOLAS	Safety Of Life At Sea
SPS	Special Purpose Ship

Greek Symbols

α	Angle of the rudder	[<i>rad</i>]
η_{tr}	Depth of the transom	[<i>m</i>]
λ	Wave length	[<i>m</i>]
λ_1	Largest eigenvalue of the matrix	[-]
∇	Displacement	[<i>m</i> ³]
ν	Kinematic viscosity	[<i>m</i> ² / <i>s</i>]
ϕ	Roll motion	[<i>rad</i>]
ϕ	Velocity potential	[-]
ψ	Yaw motion	[<i>rad</i>]
ρ	Density	[<i>kg/m</i> ³]
ρ_w	Sea water density	[<i>kg/m</i> ³]
θ	Direction of the wave	[<i>deg</i>]

θ	Pitch motion	[<i>rad</i>]
ζ	Wave elevation	[<i>m</i>]
Latin Symbols		
$1 + k$	Form factor	[-]
$1 + k_2$	Form factor of the appendages	[-]
a	Air gap	[<i>m</i>]
A_m	Cross-sectional area	[<i>m</i> ²]
A_{BT}	Transverse area of the bulb	[<i>m</i> ²]
$A_{sponson}$	Waterplane area of the sponson	[<i>m</i> ²]
A_T	Area of the transom	[<i>m</i> ²]
A_{vessel}	Waterplane area of the vessel	[<i>m</i> ²]
AR	Aspect ratio	[-]
B	Width of the vessel	[<i>m</i>]
b	Span of the rudder	[<i>m</i>]
$b_{sponson}$	Width of the sponson	[<i>m</i>]
BM	Distance from COB to M	[<i>m</i>]
c	Constant	[-]
c	Velocity of the wave	[<i>m/s</i>]
C_B	Block coefficient	[-]
C_F	Frictional resistance coefficient	[-]
C_L	Lift coefficient	[-]
C_P	Prismatic coefficient	[-]
C_r	Residual resistance coefficient	[-]
C_t	Total resistance coefficient	[-]
C_{Di}	Induced drag coefficient	[-]
CI	Consistency index	[-]
CR	Consistency ratio	[-]
D_i	Induced drag force	[<i>N</i>]
$F_{gravity}$	Gravitational force	[<i>N</i>]
F_{ni}	Froude number based on the immersed transom	[-]
F_n	Froude number	[-]
F_x	Force in x-direction	[<i>N</i>]
g	Gravitational constant	[<i>m/s</i> ²]
GM	Metacentric height	[<i>m</i>]

h	Shift in reference point of the load	[m]
I_t	Transverse moment of inertia of the waterplane	[m^4]
KB	Distance from keel to COB	[m]
KG	Distance from keel to COG	[m]
L	Length of the vessel	[m]
L	Lift force	[N]
L_{pp}	Length between the perpendiculars	[m]
L_R	Parameter reflecting the length of the run	[m]
$l_{sponson}$	Length of the sponson	[m]
L_{wl}	Length of the waterline	[m]
M	Metacenter	[m]
M_{st}	Stability moment	[Nm]
n	Size of the matrix	[-]
n_x	Normal vector in x-direction	[-]
p	Pressure	[Pa]
p_∞	Undisturbed pressure	[Pa]
P_{load}	Mass of the load	[kg]
R_r	Roughness correction	[N]
R_v	Viscous resistance	[N]
R_{APP}	Appendage resistance	[N]
R_A	Model-ship correlation resistance	[N]
R_B	Bulbous bow resistance	[N]
R_F	Frictional resistance	[N]
R_n	Reynolds number	[-]
R_{total}	Total resistance	[N]
R_{TR}	Transom immersion resistance	[N]
R_W	Wave-making resistance	[N]
RI	Random index	[-]
S	Wetted area of the vessel	[m^2]
S_{APP}	Wetted area of the appendages	[m^2]
S_{rudder}	Projected wetted area of the rudder	[m^2]
T	Draft of the vessel	[m]
t	Time	[s]
u	Velocity in x-direction	[m/s]

V	Velocity of the vessel	[m/s]
v	Velocity in y-direction	[m/s]
w	Velocity in z-direction	[m/s]
x	Surge motion	[m]
y	Half width of the vessel	[m]
y	Sway motion	[m]
z	Heave motion	[m]
z	Vertical direction	[m]



Introduction

1.1. Jumbo Maritime

Jumbo Maritime is a heavy lift shipping and offshore transportation & installation contractor. Jumbo has been in this field of work for more than 45 years. After the standardization of cargo size by the introduction of pallets and containers, Jumbo's founding father saw an opportunity in the transport of cargo that did not fit into a container. The first ship was the mv Stellaprima, which was equipped with four 12 ton derricks. From that moment in 1968, Jumbo became a pioneer in the heavy lift shipping industry. The existing fleet contains of ten vessels, where two of the J-class vessels are capable of performing offshore installation work. These two vessels (Jumbo Javelin and Fairplayer) are equipped with a dynamic positioning (DP2) system, two 900 ton Huisman cranes and a Deepwater Deployment System (DDS). The DP2 system allows the ship keep position at sea and therefore to perform offshore installation work. The Deepwater Deployment System enables the cranes to lower loads up to 3000 meter water depth.

1.2. Problem introduction

The maximum lifting capacity of the Fairplayer is limited to 1000 ton in offshore conditions, due to the insufficient static stability. This can be seen as a missed opportunity to use the Fairplayer in a wider segment of the offshore installation market. The economic crisis and the consequent reduced demand for offshore installation work, results in a growth of competition in the offshore installation market. Jumbo Maritime is active in different segments of the offshore installation market, namely Offshore Heavy Lifting, Subsea Lifting Operations and Floater and Mooring Installations [21]. Typical offshore operations performed by Jumbo Maritime are the installation of fixed facilities such as piled foundations, templates, conductors, jackets and topsides. Also FPSO Mooring Systems can be installed with the vessels. Within Jumbo Maritime, it is expected that these markets will shift towards the installation of heavier equipment. Competition analysis, which can be found in figure 1.1, has shown that vessels with a DP system and a lifting capacity within the range between 1000 and 1800 ton are rare [1]. Most of the other vessels in this range are jack-up vessels or heavy lift barges, which have the disadvantage of a large resistance during transit.

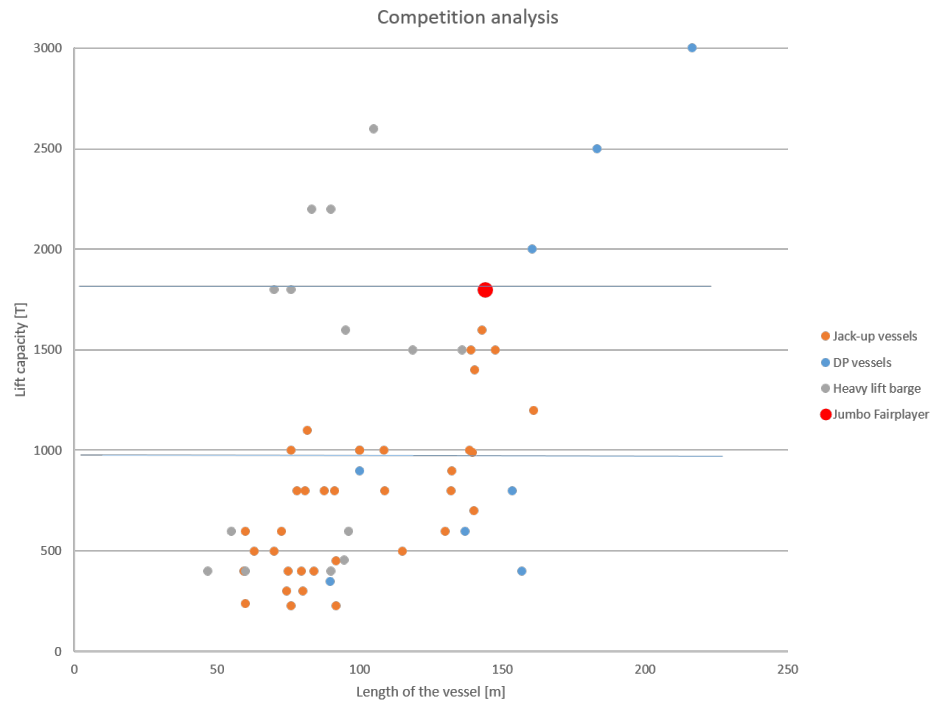


Figure 1.1: Competition analysis of the current fleet of heavy lift vessels. [1]

In order to compete in this market with one of the existing vessels, it is chosen to perform a research to adjust the Fairplayer. The Fairplayer is one of the two J-class vessels of Jumbo Maritime that can perform offshore installation work. Besides the DP2 system and the DDS, the Fairplayer also has a helicopter landing platform. The main characteristics of the Fairplayer can be found in table 1.1 and the fact sheet can be found in appendix A.

Table 1.1: Main characteristics of the Fairplayer.

Length o.a.	144.1 m
Breadth moulded	26.7 m
Depth to Main Deck	14.1 m
Draft	8.1 m
Displacement (at 7.5 m)	20120 Te
Speed (transit)	17 knots
Accommodation	80 POB
Mast Cranes	2 x 900 Te

Due to the insufficient static stability of the Fairplayer it cannot use its entire crane capacity in offshore lifting operations. The Fairplayer is currently equipped with two 900 ton cranes, which can perform a combined lift of 1800 ton. The maximum combined lifting capacity of the vessel in offshore conditions is limited to 1000 ton. The maximum lifting capacity can be achieved in the harbour or at calm seas by using pontoons. A pontoon is attached to the side of the vessel where stabilizer slots are placed, this can be seen in figure 1.2. The pontoons have a height of 3.7 meter, which is very limited for the use in heavier offshore conditions. In order to fulfil the demand in the offshore market, the J-class vessel Fairplayer need to be modified to be able to perform lifting operations with the maximum lifting capacity of 1800 ton.



(a) Pontoon attached to the vessel in the harbour. (b) Lifting operation with a pontoon on calm sea.

Figure 1.2: Examples of the use of a pontoon to increase the static stability.

The Fairplayer has two pontoons stored on deck, which can be attached alongside the ship to increase the static stability. The dimensions of the pontoons can be found in table 1.2. The pontoons can be attached to each other to even further increase the stability.

Table 1.2: Main characteristics of the pontoons.

	Pontoon 1	Pontoon 2
Length [m]	11	10.5
Width [m]	8	5
Height [m]	3.7	3.7
Weight [ton]	69.40	30.40

1.3. Previous research

The increase of operability of the Fairplayer has already led to several studies. This has been done by T. van Schalkwijk [25] and P. Harenberg [6]. The work of T. van Schalkwijk was aimed on the increase of the workability for offshore lifting operations by reducing the roll motion. The main conclusion was that the workability could be increased by the installation of Magnus rotors or anti-roll tanks on board. The installation of Magnus rotors leads to a reduction of the roll motion during the lifting operation in a wide range of wave conditions and is therefore preferred over anti-roll tanks. The installation of such a system cannot be applied to increase the lifting capacity of the Fairplayer, but can be used to reduce the roll motion.

The work of P. Harenberg was focused on the analysis of four concepts to increase the static stability and therefore increase the maximum lift capacity. These four concepts can be found in appendix B. From these concepts, two concepts (concept 3 and 4) were investigated in detail. Concept 3 is a broadening of the vessel by adding an extension to both sides of the hull. This broadening of the hull started at the bottom of the vessel and results in a large increase of the resistance during sailing. Also the static stability during transit increases, which results in larger ship accelerations. Concept 4 is the application of an offshore pontoon to create extra stability. It turned out that this pontoon could not be installed in rough offshore wave conditions, because of large ship and pontoon motions. This results in a pontoon that needs to be attached in the harbour and needs to be dragged to the offshore location. The large resistance during transit results in a maximum speed of 7.5 knots. Concluding, both concepts result in an increase of the offshore lifting capacity and in a workability comparable to the current Fairplayer. The disadvantage of both concepts is the increased resistance during transit. The relatively fast transit speed of the vessels is a strength for Jumbo Maritime, which makes these concepts not applicable.

1.4. Sponson

A concept developed by the innovation department of Jumbo is to build a dual draft vessel by the application of sponsons [15]. Sponsons are extensions placed at the sides of the hull. When applying these sponsons above the waterline, an increase of the waterline surface is obtained when increasing the draft of the vessel. The draft of the vessel can be changed by (de)ballasting the ballast tanks of the vessel, which can be seen in figure 1.3.

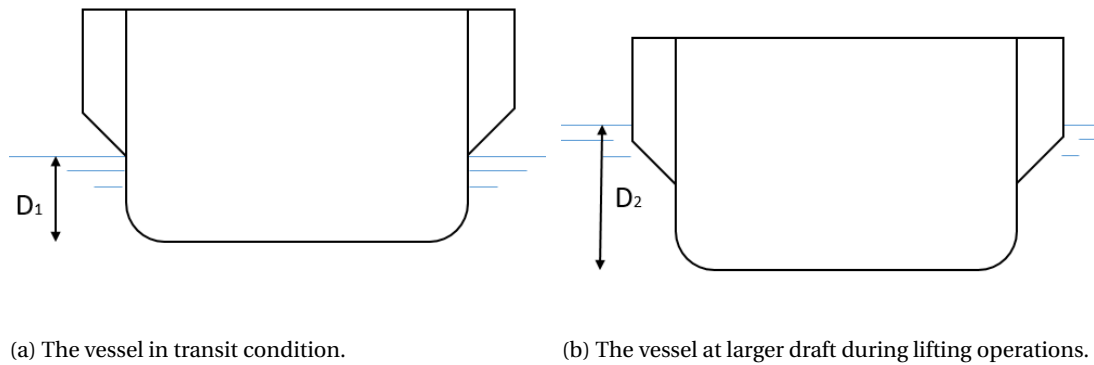


Figure 1.3: The principle of a dual draft vessel.

The adjustment of sponsons at both sides of the hull also has a negative effect. The construction of the vessel is designed to withstand the forces from the load in the two cranes, which are positioned at starboard side. For this reason the cranes cannot be shifted. The maximum capacity of the cranes is limited by the working radius of the cranes as can be seen in appendix A. The maximum lifting capacity of one crane is 900 ton can be used until a working radius of 25 meter at starboard side and 27.5 meter at portside. Lifting operations at starboard side of the vessel are only done for the shipping of long cargo which does not fit between the cranes. In the offshore installation the cargo is smaller and is lifted at starboard side. A sponson at the side of the crane (starboard) results in a large minimum working radius for the cranes. When the working range of the vessel increases, the moment that is created by the load increases as well. This larger moment needs to be compensated by ballast water, which can be a limited factor during the operation. This trade-off resulted in a variation by only applying a sponson at portside, which can be seen in figure 1.4. The cranes can lift the cargo at starboard side and the portside is equipped with a sponson in order to increase the static stability. Besides the increase of stability, the deck area increases as well, which has a positive effect on the amount and size of cargo that can be transported.

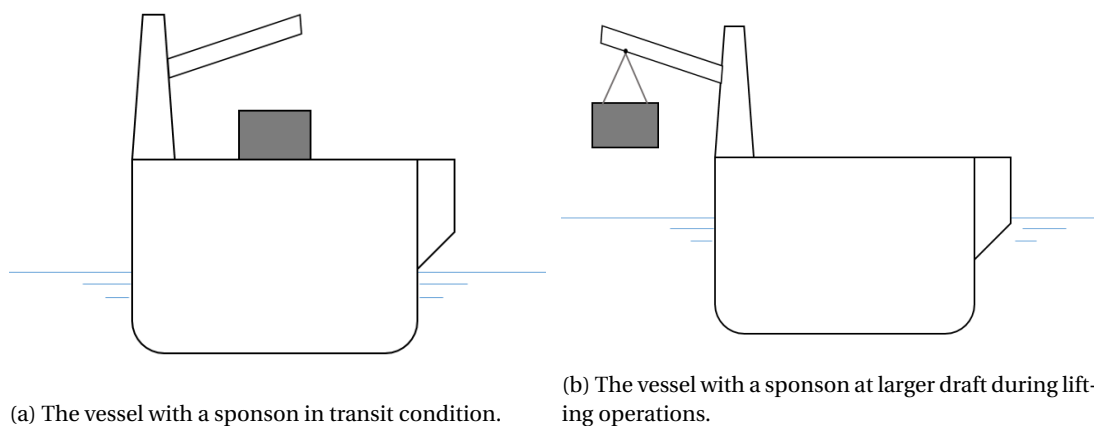
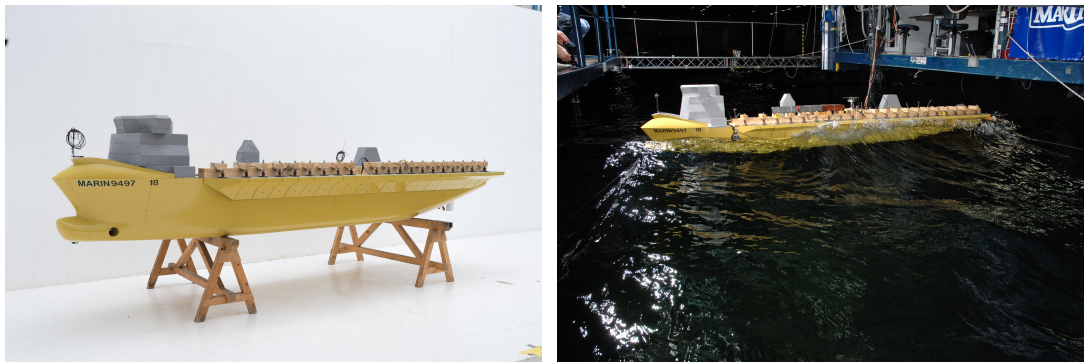


Figure 1.4: The concept a dual draft vessel with one sponson.

An asymmetric hull is not applied on a wide scale. A research is done during the concept phase of a new type of vessel (L-class) with a sponson for Jumbo Maritime. This concept has a sponson at the maindeck in order to create a larger deck area, which can be seen in figure 1.5 [2]. This was positioned far above the waterline, but the class society required results from model tests on the slamming behaviour of this concept. The model tests showed that the concept has a good motion behaviour in severe wave conditions, where it turned out to have two different natural roll frequencies. If the vessel was excited in one of the natural roll frequencies, the motion was damped when the vessel rolled over to the other side. The slamming forces on the sponson are measured and the construction is dimensioned to withstand these forces. Jumbo decided

to stop the design process of the L-class vessel, due to the declining demand in the offshore and shipping market.



(a) Sponson of the L-Class vessel.

(b) Model test, beam waves (heading 270 deg).

Figure 1.5: L-Class vessel tested at MARIN.

1.5. Basis of the concept

Static equilibrium

The equilibrium of a ship floating in water can be described by Archimedes's principle [22] and can be found in equation 1.1. The weight of the ship must be in a vertical equilibrium with the buoyancy force, which is equal to the weight of the displaced water. This can be expressed as in equation 1.1.

$$F_{gravity} = \rho_w \cdot g \cdot \nabla, \quad (1.1)$$

where $F_{gravity}$ is the gravitational force of the vessel, ρ_w is the density of water, g is the gravity acceleration and ∇ is the displacement of the vessel.

The most important locations for defining the static stability of a ship are given in figure 1.6. The buoyancy force acts on a line through the center of buoyancy, COB , indicated by B in figure 1.6. The weight of the ship acts in the center of gravity, COG , indicated by G in figure 1.6. When cargo is placed on the deck of the ship, the total mass increases and therefore the draft of the ship increases until the buoyancy and gravity force are in equilibrium again.

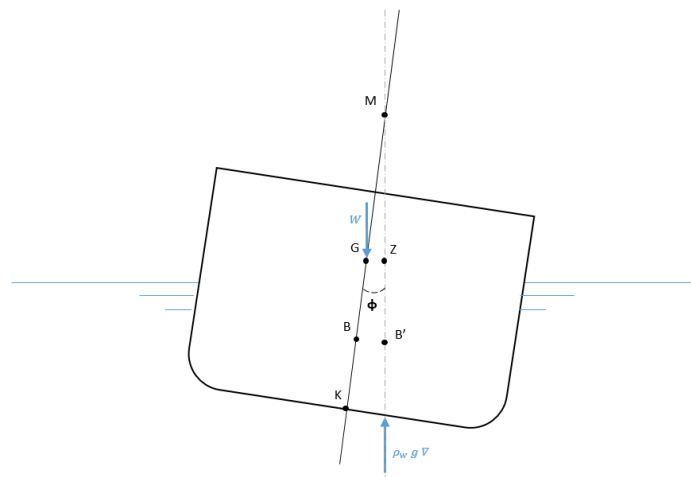


Figure 1.6: The important locations for the ship's stability.

The metacenter, M , is the intersection point of the symmetric axis in upright position and the line through the buoyancy force when the ship is at a heeling angle which approaches zero. This can be seen in figure 1.6.

The static stability of a ship is defined by the metacentric height (GM), which is the distance from the COG until the metacenter M .

The value of GM gives insight in the ships stability [22]. If the GM is larger than zero, the ship forces back to its initial position after a disturbance, which is not the case if the GM is negative. The stability moment that is created when the ship is under a small roll angle can be calculated with equation 1.2.

$$M_{ST} = \rho_w \cdot g \cdot \nabla \cdot GZ, \quad (1.2)$$

which can be seen as the bouyancy force times the distance GZ . If the static stability (GM) increases, the distance GZ also increases if the vessel is under a small heel angle. This means that with a higher GM , the stability moment increases and the accelerations of the vessel increase. The fraction of GM/B is a measure for the motion behaviour of the vessel. A too high fraction results in a small natural roll period, which means the accelerations in roll motion are high. A relative low GM/B fraction results in a larger natural period and therefore the ship behaves more smooth. The class society prescribes a minimal intitial metacentric height, GM , of at least 0.15 meter [23]. Jumbo Maritime uses a minimal metacentric height of at least 1.2 meter during transit with cargo, to guarantee safety for the crew and the valuable cargo. For sailing without cargo on deck a minimal metacentric height of 1.0 meter is used [16]. The GM can be calculated from equation 1.3.

$$GM = KB + BM - KG, \quad (1.3)$$

where KB and KG are the distances from the keel to the COB and the COG respectively. If assumed that the heel angles of the ship are very small, the vertical movement of the COB can be neglected. Then the BM can be calculated by equation 1.4.

$$BM = \frac{I_t}{\nabla}, \quad (1.4)$$

where I_t is the transverse moment of inertia of the waterplane area and ∇ the displacement of the ship. This is only applicable for heel angles smaller than ten degrees. If the heel angle becomes larger, the vertical movement of the COB need to be taken into account, which can be done with Scribanti's formula [22]. Another assumption is that the sides of the ship are perpendicular to the waterline. This means that at small angles the volume that comes out of the water is equal to the volume that goes into the water. For ships that have a rapidly changing waterplane area these equations are not valid.

Increase of static stability by a sponson

The static stability is defined as the value of GM , which can be calculated with equation 1.3. There are three options to increase the GM , by increasing the KB or BM or by decreasing the KG . The placement of the sponson as described in paragraph 1.4, uses this in order to increase the static stability. By increasing the draft of the vessel during a lifting operation, the KB increases. The increase of draft at an offshore location can only be achieved by increasing the weight of the vessel by filling the ballast tanks. The KG value can either increase or decrease, depending on the position of the ballast tanks that are filled. The BM can be calculated according to equation 1.4. In order to increase the BM , either the I_t should increase or ∇ should decrease. The concept with a sponson is based on the submersion of the vessel with a sponson, so the displacement definitely increases. This means that the moment of inertia of the waterplane area needs to increase more than the displacement does. The moment of inertia of the waterplane area changes due to the sponson. The moment of inertia of a vessel with a sponson can be calculated by calculating the individual moments of inertia and combine them with Steiner's rule [7]. The moment of inertia of the waterplane of a vessel can be calculated with equation 1.5 [22].

$$I_{t, vessel} = 2 \cdot \int_{x=0}^{x=L} \frac{1}{3} y^3 dx, \quad (1.5)$$

where L is the length of the vessel and y is the half width of the vessel. The moment of inertia of the waterplane area of a sponson, which can be simplified as a square box can be calculated with equation 1.6.

$$I_{t, sponson} = \frac{l_{sponson} \cdot b_{sponson}^3}{12}, \quad (1.6)$$

where $l_{sponson}$ is the length and $b_{sponson}$ is the width of the sponson. The total moment of inertia of the waterplane area can now be calculated with Steiner's rule and can be seen in equation 1.7.

$$I_{t, vessel \text{ with sponson}} = I_{t, vessel} + d_{vessel}^2 \cdot A_{vessel} + I_{t, sponson} + d_{sponson}^2 \cdot A_{sponson}, \quad (1.7)$$

where d_{vessel} and $d_{sponson}$ are the distances from the new centerline of the vessel to the centerline of the vessel and sponson respectively. These distances can be seen in figure 1.7. A_{vessel} and $A_{sponson}$ are the waterplane areas of the vessel and sponson respectively.

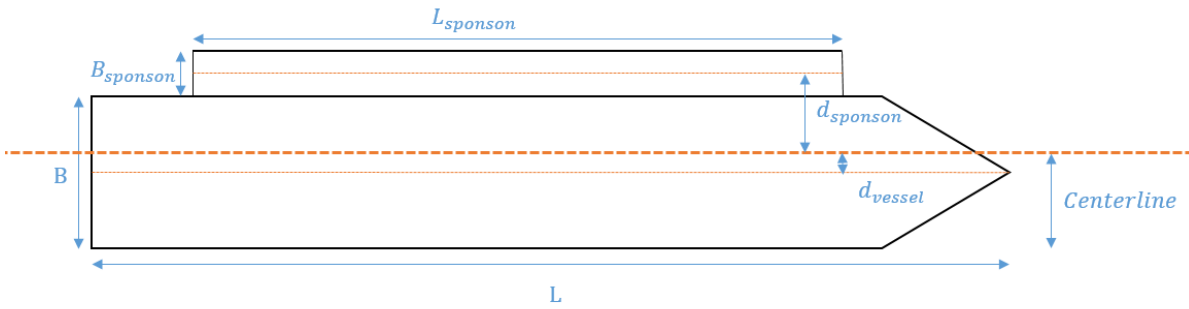


Figure 1.7: The important dimensions for the calculation of the moment of inertia of the waterplane.

The moment of inertia of the waterplane of the Fairplayer with a sponson needs to be calculated from a new centerline. This centerline is the median of the waterplane area and is calculated with equation 1.8.

$$Centerline = \frac{\left(A_{vessel} \cdot \frac{B}{2} + A_{sponson} \cdot \left(B + \frac{B_{sponson}}{2} \right) \right)}{A_{vessel} + A_{sponson}}, \quad (1.8)$$

in which B is the width of the Fairplayer, $B_{sponson}$ is the width of the sponson.

1.6. Research question

The problem as described in paragraph 1.2 needs to be formulated so research can be carried out. The application of a sponson at the portside of the Fairplayer is analysed to increase the static stability. The goal of this research is to find out what the influence of a sponson is on the resistance of the vessel.

The main question that needs to be answered in this thesis is:

What is the influence of the position and shape of a sponson on the Fairplayer with respect to the resistance?

1.7. Boundaries of the research

Boundaries need to be specified in order to avoid an overload of work. The thesis focuses on the hydrodynamic side of the applicability of sponson rather than the structural dimensioning of this sponson. Therefore

the structural dimensions of the sponson does not need to be calculated. The motion behaviour of the Fairplayer is not analysed in this research, because a research on this has already been done [6]. This thesis does not include a financial analysis, because it is an initial research carried out to this concept.

It is known that there is a patent on the concept of a dual draft vessel by GustoMSC Resources B.V. and Seaway Heavy Lifting Engineering B.V. [27]. The concept, which is investigated during this master thesis, could have some conflicts with the claim in the patent. This means that from a juristic point of view this concept and the patent need to be compared. It is not part of this thesis to check if this concept is patented or not.

1.8. Operational profile

The vessels of Jumbo operate all over the world. In most cases, the vessel is not at the location of the cargo, so the vessel needs to sail to the port without cargo. From this harbour, the vessel sails to the next port or offshore location with cargo on board. After delivering the cargo on the location, the vessel sails empty to the next port for a new job. The Fairplayer is used as an Offshore Installation vessel and will therefore only sail with cargo to the offshore location and sails back empty. From this operational profile, it can be concluded that the vessel sails empty for more than 50% of the time. This can be taken into account during the design phase of the vessel with a sponson.

Offshore Locations

A study of the weather data of seven different offshore locations is performed by BMT ARGOSS [18]. The seven locations with meteorological data are locations where Jumbo performs offshore installation work. As can be seen, these offshore locations are widespread, which means that the vessel will sail all over the world to perform offshore installation work. The weather locations can be found in figure 1.8.



Figure 1.8: Weather data locations for motion analysis.

The offshore locations are labelled with a number from L1 to L7. The offshore locations can be found in table 1.3.

Table 1.3: Offshore weather locations.

Index	Location	Coordinates
L1	Offshore Brazil	23.5158° S, 41.0611° W
L2	North Sea	56.1878° N, 2.8107° E
L3	North Sea	54.9484° N, 7.7966° E
L4	South Africa	35.1167° S, 22.5333° E
L5	North Sea	56.7828° N, 2.1106° E
L6	North Sea	61.2167° N, 0.6667° E
L7	NW Australia	19.9200° S, 115.3000° E

1.9. Document structure

This report starts with a literature study in chapter 2. In chapter 3 a concept study is done to the main variations of the vertical position of the sponson. The vertical position of the sponson has an influence on the operational profile and the performance of a dual draft vessel. From this concept study two concepts are preferred. Both concepts have the sponson positioned partly under the waterline. The increase of resistance of the Fairplayer with a sponson is an important criteria for Jumbo Maritime and therefore an adjusted Holtrop-Mennen method is set up in this research. This adjusted Holtrop-Mennen method is executed in five steps, which are explained in chapter 4. The method is used to calculate the influence of the shape and longitudinal position of the sponson on the resistance of the Fairplayer. The systematic variation of the shape and position of the sponson and the results from this are shown and discussed in chapter 5. The final concept of the Fairplayer with a sponson is also explained and discussed in this chapter. In chapter 6 the conclusions of this research are listed. Also recommendations are given for further research that needs to be carried out to see how the sponson influences the performance of the Fairplayer.

2

Literature

This chapter provides the literature used in this research. In paragraph 2.1 the motions of the vessel are defined. In paragraph 2.2 the different phases in the lift operation at Jumbo are described. The division of the resistance of a ship into components and the different methods to calculate this resistance are explained in paragraph 2.3. One of the methods to predict the resistance of a ship is the method developed by Holtrop & Mennen, which are explained in paragraph 2.4. Another method to calculate the resistance is with the use of computational techniques, which are discussed in paragraph 2.5. The computer program RAPID is introduced in paragraph 2.6. A sponson on the vessel can result in an increase of the amount of slamming as described in paragraph 2.7.

2.1. Ship definitions

The motions of a ship are described by three translations of the ship's center of gravity and three rotations about the axes [13]. The three translations are called surge (in longitudinal x -direction), sway (in lateral y -direction) and heave (in vertical z -direction). The three rotations are called roll (around the x -axis), pitch (around the y -axis) and yaw (around the z -axis). These six ship motions and the corresponding positive directions can be seen in figure 2.1. These six degrees of freedom are summed in the vector \vec{x} of equation 2.1.

$$\vec{x} = \begin{bmatrix} x \\ y \\ z \\ \phi \\ \theta \\ \psi \end{bmatrix} \quad (2.1)$$

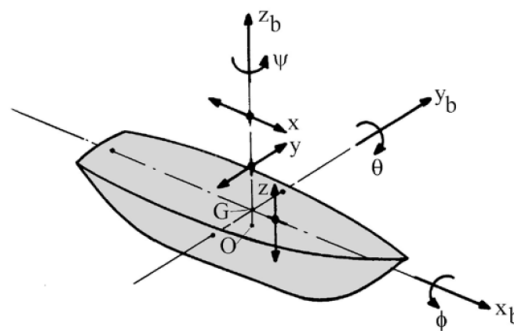


Figure 2.1: Definition of ship motions.

2.2. Lift operation

As described Jumbo Maritime performs shipping operations as well as offshore installation work. When the client asks Jumbo to execute offshore installation work, the Jumbo Javelin or Fairplayer sails to the port where the clients equipment is stored and lifts the cargo with its own cranes on board. After this the ship sets sail to the offshore location where the installation work needs to be done. The weather forecast is monitored to find an interval in the weather forecast which is suitable for the installation work. When the ships enters the specific location the preparations for the lift are carried out. The lift operation takes place when the crew is ready and the environmental conditions are within the operational limits. When the installation is finished, the ship sets sail to its next project.

The static stability of the lift operations is evaluated in three different stages of the lift operation at sea. When the ship is at the offshore location, the ship's dynamic positioning system is turned on and preparations are done to perform the offshore lift. This means that the ballast tanks are filled with water, in order to decrease the height of the center of gravity. This stage is called 'before lift', during this stage the GM is very high and therefore the motions of the vessel will become more rough. The situation 'before lift' is shown in figure 2.2. The period of time that the vessel is in this stage of the lifting process is limited.

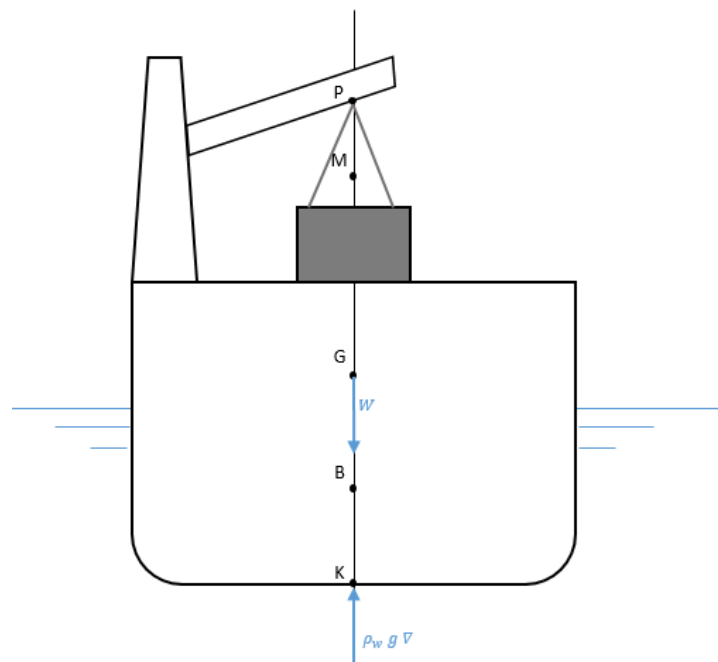


Figure 2.2: Situation 'before lift'.

The second stage during the lift operations is when the cargo is lifted from the deck. This phase is called 'lift off' and results in a change of center of gravity in height. At the time of a lift of the cargo from the deck, the point of reference for the weight of the cargo shifts all the way up to the crane tip, which means a vertical shift in COG and a reduction of the GM value. The vertical shift in COG (G_0G_1) can be calculated as follows [13]:

$$G_0G_1 = \frac{P_{load} \cdot h}{\rho_w \cdot \nabla}, \quad (2.2)$$

where P_{load} is the mass of the load, h is the shift in reference point of the load and ∇ is the displacement of the ship. The situation 'lift off' is shown in figure 2.3, in which the vertical shift of the center of gravity (G_0G_1) and the shift in reference point of the load (h) are drawn in red.

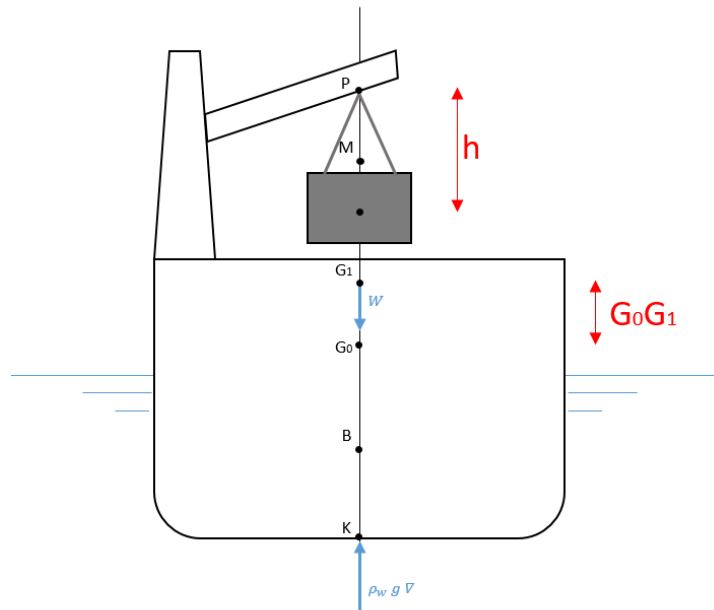


Figure 2.3: Situation 'lift off'.

The third stage during the lift operations is when the crane is turned outwards and the cargo is positioned above the water. In this situation, the reference point for the weight of the cargo shifts outwards and needs to be compensated by ballast water at the other side of the hull to prevent a heel angle. The difference compared to the 'lift off' situation is the position of the reference point P. This point is situated with a large arm compared to midship, which means that a small roll motion will result in large accelerations at this point. This situation 'crane out' is shown in figure 2.4.

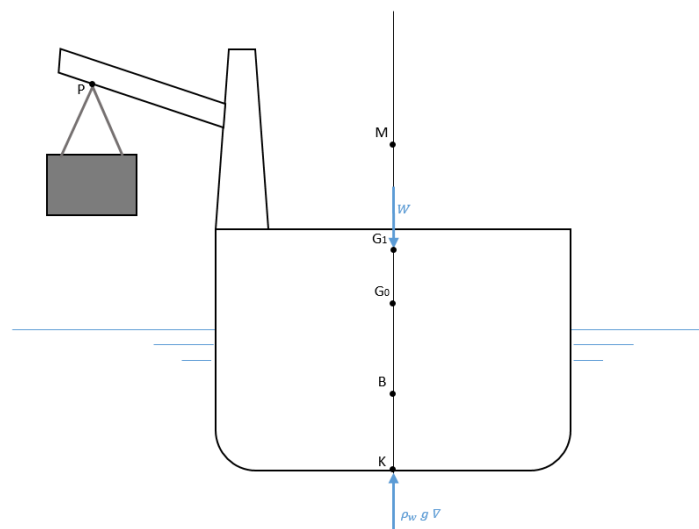


Figure 2.4: Situation 'crane out'.

Kahn Rule

The engineers of Jumbo Maritime have set up a rule of thumb called the 'Kahn-rule' for the minimum GM during the lifting operation [14]. The 'Kahn-rule' is defined as a function of the load (P_{load}) which will be

lifted. According to the 'Kahn-rule' the minimum GM during lifting should be:

$$GM = 1.0 + 1.5 \cdot \left(\frac{P_{load}}{1800} \right). \quad (2.3)$$

This rule of thumb is set up during the test lift of 1800 ton with the Fairplayer. A GM in this order of magnitude results in a relatively small heel angle when the cranes turn, because the stability moment created by the buoyancy force is sufficient in small heel angles, as explained in paragraph 1.5. A smaller GM results in a larger heel angle, which is not preferred based on the experience of the captains of Jumbo.

2.3. Resistance

During the design phase of a ship the resistance of a ship can be predicted in three different ways [17]. The three methods are:

- Model testing
- Computational techniques
- Empirical methods

Model testing

In model tests, a scale model of the ship is towed in a water tank. The resistance of the scale model is measured and needs to be scaled to the full scale hull. Model tests are rather time-consuming, compared to empirical methods and potential flow calculations. Especially if a number of hull shapes need to be iterated to come to a final design. The production of a scale model and hiring a towing tank is expensive.

Computational techniques

The fast development of computer technology resulted in computational techniques in ship hydrodynamics. These techniques can give an insight in the fluid flow around the vessel. The full Navier-Stokes equations need to be solved to analyse the viscous flow around a vessel. The governing equations that need to be solved can be found in paragraph 2.5. The computational power for solving the Navier-Stokes equations is considerably larger than for potential flow methods. Potential flow methods do not take the viscosity of the fluid into account and are calculated with Panel Methods. This means that the fluid flow is only solved on the boundaries of the domain (hull surface and free surface). Calculating the non-viscous flow is mainly used to optimize the local shape of the hull, especially in the forebody of the vessel. The equations that need to be solved can be found in paragraph 2.5.2.

Empirical methods

A method to get a quick resistance estimation is the use of empirical methods. There are two different types of empirical methods: systematic series and formulas based on unsystematic data. In a systematic series a systematic variation on the main particulars of a parent model is made and the resistance of all these models is obtained by model tests. The data is used to set up regression formulas which are dependent on the main particulars. The same can be done for unsystematic data.

There are several different methods to predict the resistance of ships. Watson [28] describes five prediction methods commonly used.

The method by Rear Admiral D.W. Taylor of the U.S. Navy is known as Taylor's method. This method is based on the division between the friction and the residuary resistance. The residuary resistance is plotted in graphs which are based on main dimensions of the vessel. The friction resistance is based on an equation of the speed and wetted surface. The Taylor method gave quite an accurate estimate of the resistance in the days of the publication, but the equations are not dependent on the longitudinal center of buoyancy (LCB) and the distinction between a single-screw and twin-screw vessel. These two variables are both recognised as influencing the resistance [28].

A second method mentioned is the Ayre's C2 method. The method is based on a series of hull forms. The method gives an estimation of the effective brake horsepower needed to deliver, based on the speed, displacement of the vessel and a constant. This constant is plotted, based on the speed and length. Corrections are

made for block coefficient and position of the LCB. The method will only give an estimation of the effective break horsepower and does not split the total resistance in different components.

A third method that can be used to determine the resistance is the method of Moor. The method gives a dimensionless value for the total ship resistance coefficient. This dimensionless value is given for a standard ship with dimensions of 122 x 16.76 x 7.93 (or 5.5 for twin-screw ships) meter for a range of block coefficients, *LCB* positions and velocities. For other ship dimensions a correction graph is given and formulas are based on this graphs. This method is set up for both single-screw and twin-screw ships.

A fourth method described in Watson [28] is the method of Guldhammer and Harvard. This method defines the total resistance R_t as in equation 2.4.

$$R_t = \frac{1}{2} \cdot C_t \cdot \rho_w \cdot S \cdot V^2, \quad (2.4)$$

where S is the wetted area and V is the velocity of the vessel. The total resistance component (C_t) is split up in two different coefficients: the residual resistance coefficient and the frictional resistance coefficient ($C_t = C_r + C_f$). The frictional resistance coefficient is obtained from the ITTC-57 flat plate friction line. The residual resistance coefficient is obtained from graphs, which are based on the position of *LCB*. For other positions of *LCB* an any variation of B/T , corrections are made.

The fifth method is the method developed by Holtrop & Mennen and is described in detail in paragraph 2.4.

2.3.1. Decomposition of the total resistance

The resistance of a vessel can generally be split into two main components: wave resistance and viscous resistance [17]. These two components can also be subdivided into components. The wave-making resistance can be split into the wave pattern and the wave breaking resistance. The viscous resistance can be split into four components: flat plate friction, roughness effects, form effect on friction and form effect on pressure. The six different components will be discussed further.

Wave-making resistance

When the vessel moves through the water surface, water particles are disturbed from their original position and waves are generated. If this disturbance becomes too large, the waves may be steep enough to break down into eddies and foam. The energy which is removed from the wave system is found in the wake of the ship and is called the wave breaking resistance. The remaining energy is radiated away through the wave system and is called the wave pattern resistance.

Viscous resistance

The flat plate friction can be described as the friction of a flat plate with the same wetted surface as the ship. This means that the flat plate friction is only the tangential forces between the solid surface and the water. The roughness of the surface effects the skin friction of the vessel. For model ships this roughness effects can be neglected but for full scale vessel, this always leads to a resistance increase. As the flow approaches the vessel, it has to go around the hull, which leads to a local velocity of the water which is different than the undisturbed flow. At the bow and stern of the ship, the velocity is reduced, but over the main part of the hull there is a velocity increase. This leads to an increase in the friction as compared to the flat plate, which is called the form effect on friction. The form effect on pressure is caused by a pressure difference between the foreship and the aftship. The boundary layer around the aftship causes a displacement of the streamlines outwards. The pressure at the aft end of the hull is then reduced and the integrated pressures over the hull will not cancel, as described in paragraph 2.5.2. This is a form effect on pressure with a viscous origin.

2.4. Holtrop-Mennen resistance prediction method

In paragraph 2.3 five different ways of predicting the ship resistance with empirical methods are mentioned. A commonly used empirical method is the method developed by Holtrop & Mennen [8], [10], [11] and [9]. The method is based on the evaluation of model test and trial results. From this data a numerical description of the ship's resistance is developed as well as propulsion properties and scale effects between model and full size ship. The range of vessels on which this empirical method is based, can be found in figure 2.5 [8]. The

J-Class vessel Fairplayer has a $\frac{L}{B}$ ratio of 5.1 and a C_P of 0.75. C_P is the prismatic coefficient can be calculated with equation 2.5.

$$C_P = \frac{\nabla}{L_{pp} \cdot A_m}, \quad (2.5)$$

where ∇ is the displacement, L_{pp} is the length between the perpendiculars and A_m is the cross-sectional area.

As can be seen in figure 2.5, the Fairplayer is slightly outside the range of general cargo vessels, but still within the range of tankers and bulkcarriers. The amount of vessels on which the method is based is increased from 1977 until 1984, which makes it plausible that the method can also be used just outside the range.

Type of ship	F_n max.	C_P		L/B		Number of ships			
		min.	max.	min.	max.	single screw		twin screw	
						model	full scale	model	full scale
Tankers, bulkcarriers	0.24	0.73	0.85	5.1	7.1	48	13	3	2
General cargo	0.30	0.58	0.72	5.3	8.0	21	17	3	2
Fishing vessels, tugs	0.38	0.55	0.65	3.9	6.3	35	--	3	2
Container ships, frigates	0.45	0.55	0.67	6.0	9.5	6	--	18	1
Various	0.30	0.56	0.75	6.0	7.3	7	6	3	3
Total						117	36	30	10

Figure 2.5: Range of vessels from the Holtrop-Mennen method.

The method is described in a number of papers, where the first one published in 1977 [8]. In this paper the resistance is divided into the wave-making and the viscous resistance. In the successive paper, the wave-making resistance is expanded by making it dependent on more variables [10]. Also the resistance of a bulbous bow is taken as a separate component. In 1982 [11] and 1984 [9], the breakdown of the resistance is extended. The total resistance can now be calculated as given in equation 2.6. In appendix C the complete method described by Holtrop & Mennen can be found. In appendix C the results of the Holtrop-Mennen method for the Fairplayer can be found. Also the evolution of the results for the Fairplayer over the years is shown.

$$R_{total} = R_F + R_{APP} + R_W + R_B + R_{TR} + R_A \quad (2.6)$$

where:

- R_F = frictional resistance according to the ITTC-57 formula
- R_{APP} = appendage resistance
- R_W = wave-making resistance and wave breaking resistance
- R_B = additional pressure resistance of bulbous bow
- R_{TR} = additional pressure resistance due to transom immersion
- R_A = model-ship correlation resistance

The frictional resistance R_F is determined from the flat plate friction formula, which is corrected for the ship form. The flat plate friction resistance is based on the resistance of a flat plate of equal length and wetted surface and at the same speed of the vessel. The correction for the hull form is expressed as a fraction of the flat plate resistance. The frictional resistance can be calculated with equation 2.7.

$$R_F = \frac{1}{2} \cdot \rho_w \cdot V^2 \cdot C_F \cdot (1 + k) \cdot S \quad (2.7)$$

where ρ_w is the water density, V the velocity of the vessel, C_F the coefficient of frictional resistance and S the total wetted surface. The friction coefficient C_F is calculated from the ITTC-57 formula with equation 2.8 and is dependent on the Reynolds number R_n . The form factor $(1 + k)$ can be calculated with equation 2.9.

$$C_F = \frac{0.075}{(\log R_n - 2)^2} \quad (2.8)$$

$$1 + k = 0.93 + 0.487118 \cdot c_{14} \cdot \left(\frac{B}{L_{wl}}\right)^{1.06806} \cdot \left(\frac{T}{L_{wl}}\right)^{0.46106} \cdot \left(\frac{L_{wl}}{L_R}\right)^{0.121563} \cdot \left(\frac{L_{wl}^3}{\nabla}\right)^{0.36486} \cdot (1 - C_P)^{-0.604247} \quad (2.9)$$

in this formula B and T are the moulded breadth and draft, respectively. L_{wl} is the length on the waterline and ∇ is the displacement volume. C_P is the prismatic coefficient and L_R is defined as shown in equation 2.10. The coefficient C_{14} takes into account the stern shape of the vessel [9].

$$L_R = L_{wl} \left(1 - C_P + 0.06 \cdot C_P \cdot \frac{LCB}{(4 \cdot C_P - 1)}\right) \quad (2.10)$$

where LCB is the longitudinal position of the center of buoyancy forward of $0.5L$ as percentage of L .

The formula for the wave-making resistance is split into two ranges for the speed of the vessel (below and above $F_n = 0.5$). The Fairplayer has a maximum speed of $F_n = 0.24$, which means that the formula for low and moderate speeds can be used. The formula for the wave-making resistance can be found in equation 2.11.

$$R_W = c_1 \cdot c_2 \cdot c_5 \cdot \nabla \cdot \rho_w \cdot g \cdot e^{(m_1 \cdot F_n^d + m_4 \cdot \cos(\lambda \cdot F_n^{-2}))} \quad (2.11)$$

the coefficients (λ , c_1 , c_2 , c_5 , m_1 and m_4) in equation 2.11 are dependent on the main dimensions of the vessel, such as B , T , C_P and ∇ and can be found in appendix C. d is a constant and is equal to -0.9 . ∇ is the displacement of the vessel. The wave-making resistance is also dependent on the Froude number (F_n).

The appendage resistance can be determined with equation 2.12.

$$R_{APP} = 0.5 \cdot \rho_w \cdot V^2 \cdot S_{APP} \cdot (1 + k_2)_{eq} \cdot C_F \quad (2.12)$$

in this formula is S_{APP} the wetted area of the appendages. The form factor $(1 + k_2)$ changes between different appendages and need to be estimated and combined [9]. C_F is the same flat plate friction coefficient as calculated with equation 2.8.

The additional resistance due to the bulbous bow near the water surface can be calculated with equation 2.13.

$$R_B = 0.11 \cdot e^{(-3 \cdot P_B^{-2})} \cdot F_{ni}^3 \cdot A_{BT}^{1.5} \cdot \frac{\rho_w \cdot g}{(1 + F_{ni}^2)} \quad (2.13)$$

where P_B is a coefficient which is dependent on the emergence of the bow and F_{ni} is the Froude number based on the immersions of the bow. The formulas for this can be found in appendix C. A_{BT} is the transverse cross section of the bulb.

The additional pressure resistance due to the immersed transom can be determined with equation 2.14.

$$R_{TR} = 0.5 \cdot \rho_w \cdot V^2 \cdot A_T \cdot c_6 \quad (2.14)$$

where c_6 is dependent on the Froude number based on the transom immersion F_{nT} , A_T is the area of the transom and is explained in detail in appendix C.

The last resistance component defined by Holtrop & Mennen [9] is the model-ship correlation resistance R_A , which can be calculated with equation 2.15. This resistance component is introduced to describe the effect of the hull roughness and the still-air resistance.

$$R_A = \frac{1}{2} \cdot \rho_w \cdot V^2 \cdot S \cdot C_A \quad (2.15)$$

2.5. Computational techniques

As described in paragraph 2.3 there are two different methods of calculating the flow around a ship, namely with the Navier-Stokes equations as in CFD and the potential flow method. The governing equations of those two methods will be explained.

2.5.1. Computational techniques for viscous flows

In the computational technique for viscous flows the governing equations of the flow around a ship are the continuity equation and the Navier-Stokes equation [17]. These two equations constitute a closed system for the pressure, and the three velocity components. For the derivation of the equations in this paragraph, the Cartesian coordinate system recommended by the ITTC is used. The ship is considered to be fixed and the inflow of fluid is uniform and from ahead.

The continuity equation can be derived by considering the mass flows through the faces of the infinitesimal element $dxdydz$. The mass inflow in the x -direction is $\rho u dydz$. The outflow can be written as:

$$\left[\rho u + \frac{\partial}{\partial x} \rho u dx \right] dydz. \text{ This results in the net outflow of: } \frac{\partial}{\partial x} \rho u dxdydz.$$

This can be done for the y and z -direction in the same way. In the element no mass is created or disappeared, so the total net transport of mass out of the element must be zero. This leads to equation 2.16.

$$\frac{\partial}{\partial x} \rho u dxdydz + \frac{\partial}{\partial y} \rho v dxdydz + \frac{\partial}{\partial z} \rho w dxdydz = 0 \quad (2.16)$$

With ρ constant, the continuity equation for incompressible flows can be rewritten as in equation 2.17.

$$\frac{\partial u}{\partial x} + \frac{\partial v}{\partial y} + \frac{\partial w}{\partial z} = 0 \quad (2.17)$$

The Navier-Stokes equations can be seen as Newton's second law to the infinitesimal fluid element $dxdydz$. The complete derivation of the Navier-Stokes equations can be found in [17]. The Navier-Stokes equation in the three directions can be found in equation 2.18. The left-hand side of the three equations represent the accelerations of a fluid particle in the x , y and z directions. The right-hand side represent the forces on the element per unit of mass. The first term appears because of the pressure gradients and the last one because of viscous forces. There is an extra term in the z -equation, which represents the gravity effects.

$$\begin{aligned}
\frac{\partial u}{\partial t} + u \frac{\partial u}{\partial x} + v \frac{\partial u}{\partial y} + w \frac{\partial u}{\partial z} &= -\frac{1}{\rho} \frac{\partial p}{\partial x} + \nu \left(\frac{\partial^2 u}{\partial x^2} + \frac{\partial^2 u}{\partial y^2} + \frac{\partial^2 u}{\partial z^2} \right) \\
\frac{\partial v}{\partial t} + u \frac{\partial v}{\partial x} + v \frac{\partial v}{\partial y} + w \frac{\partial v}{\partial z} &= -\frac{1}{\rho} \frac{\partial p}{\partial y} + \nu \left(\frac{\partial^2 v}{\partial x^2} + \frac{\partial^2 v}{\partial y^2} + \frac{\partial^2 v}{\partial z^2} \right) \\
\frac{\partial w}{\partial t} + u \frac{\partial w}{\partial x} + v \frac{\partial w}{\partial y} + w \frac{\partial w}{\partial z} &= -\frac{1}{\rho} \frac{\partial p}{\partial z} - g + \nu \left(\frac{\partial^2 w}{\partial x^2} + \frac{\partial^2 w}{\partial y^2} + \frac{\partial^2 w}{\partial z^2} \right)
\end{aligned} \tag{2.18}$$

The Navier-Stokes and continuity equations require conditions on the boundaries of the computational domain for the unknowns velocities and pressure. There are three kinds of boundaries: solid surfaces, water surfaces and 'infinity'.

The solid surface boundary conditions are also called the 'no-slip' condition. This means that the velocity difference between the two phases are smoothed out. For example on the hull surface boundary condition can be written as follows: $u = v = w = 0$, whereas on a point fixed to the earth it can be written as: $u = V$, $v = w = 0$.

The water surface boundary condition can be split into two parts: the dynamic boundary condition and the kinematic boundary condition. The dynamic boundary condition means that the normal force equilibrium between water and air, so the pressures must be equal. The kinematic boundary condition contains the fact that there is no flow through the surface. This means that the vertical velocity of a water particle at the surface must be equal to the derivative of the wave height with respect to time: $w = \frac{\partial \zeta}{\partial t}$, where ζ describes the free surface.

The boundary condition 'infinity' contains that the all disturbances must go to zero at infinity: $u = V$, $v = w = 0$ and $p = p_\infty$, where p_∞ is the undisturbed pressure.

2.5.2. Potential flow theory

As described in paragraph 2.3.1, the total resistance can be split into the wave-making resistance and the viscous resistance. These two phenomena occur simultaneously physically and interactions between the two exist. The separation of the resistance into two components is a simplification but can be seen as an useful approach in practice [17].

A common way to analyse the flow around a vessel is to use potential flow theory. Potential flow theory is based on the flow description by the Navier-Stokes equations (2.18) and the continuity equation (2.16), but does not take into account the viscosity. If the viscous terms in equation 2.18 are dropped, the set of equations that remains are called the Euler equations (2.19).

$$\left(\frac{\partial}{\partial t} + u \frac{\partial}{\partial x} + v \frac{\partial}{\partial y} + w \frac{\partial}{\partial z} \right) \vec{v} = \nabla \left(-\frac{p}{\rho} - gz \right) \tag{2.19}$$

where $\nabla = \left(\frac{\partial}{\partial x} \frac{\partial}{\partial y} \frac{\partial}{\partial z} \right)^T$ is the gradient operator. From this the Bernoulli equation can be derived as is done in [17]. The Bernoulli equation can be found in equation 2.20.

$$\frac{1}{2}(u^2 + v^2 + w^2) + \frac{p}{\rho} + gz = \text{constant along a streamline} \tag{2.20}$$

Without further conditions the constant may differ from one streamline to another.

The next simplification is to suppose that the flow is irrotational. This means that the vorticity, the curl of the velocity vector, is zero throughout the flow field. This can be seen in equation 2.21.

$$\vec{\omega} = \nabla \times \vec{v} = 0 \tag{2.21}$$

This is an acceptable assumption if the inviscid flow is uniform far upstream [17]. In a viscous flow vorticity is being generated at solid boundaries due to wall friction. For irrotational flows, the velocity potential, $\phi(x, y, z)$ can be introduced as a scalar function so that the gradient of the velocity potential is the velocity 2.22. This can be considered as a potential flow.

$$\vec{v}(x, y, z) = \nabla\phi \quad (2.22)$$

Potential flows are described by two main equations. These are the Bernoulli equation and the Laplace equation. The Bernoulli equation can be further simplified as can be seen in [17]. The Bernoulli equation holds with a constant that is the same for the entire field and not just along a streamline, which is given in equation 2.23.

$$\frac{1}{2}\nabla\phi \cdot \nabla\phi + \frac{p}{\rho} + gz = \text{constant} \quad (2.23)$$

The second equation is the Laplace equation. Start with the continuity equation and substitute the velocity potential, which gives the Laplace equation for the velocity potential.

$$\frac{\partial^2\phi}{\partial x^2} + \frac{\partial^2\phi}{\partial y^2} + \frac{\partial^2\phi}{\partial z^2} = 0 \quad \text{or} \quad \nabla^2\phi = 0 \quad (2.24)$$

Concluding, the Bernoulli equation (2.23) and the Laplace equation (2.24) can be used to replace the complicated set of the continuity equation (2.16) and the Navier-Stokes equation (2.18) by using a scalar, the velocity potential. Because the Laplace equation does not contain the pressure, the equations are uncoupled. This means that the potential (and thereby the velocity field) can be solved first and after that the pressure can be found from the Bernoulli equation.

Inviscid flow around a body

Consider a body in 2D, which is placed in a potential (inviscid) flow, without a free surface. The body can be seen as an infinite-draft ship and the flow is undisturbed far ahead of the body. When the flow approaches the body, the straight streamlines have to bend sideward to flow around the body. At the fore shoulder the streamlines turn back to follow the middle part of the body. At the aft of the body, the streamlines bend inward and thereafter outward to adjust to the parallel flow behind the body. This can be seen in figure 2.6 [17].

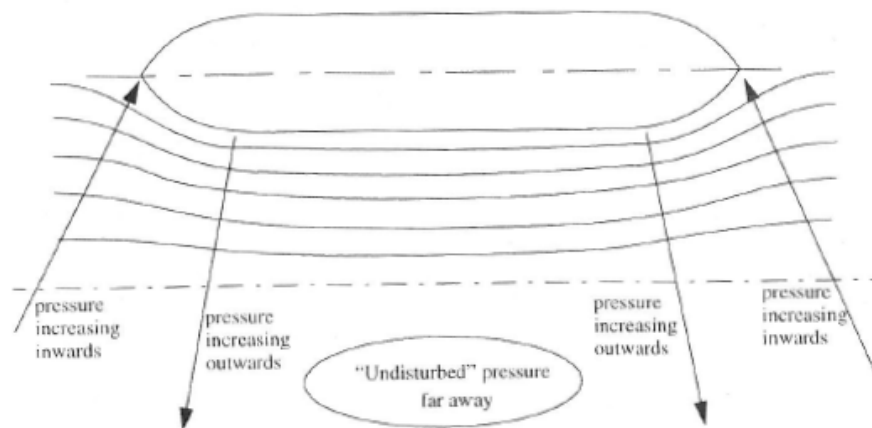


Figure 2.6: Pressure variation due to streamline curvature. [17]

As can be seen, the curvature of the streamlines at the bow and stern is away from the body and at the shoulders the curvature is towards the body. This results in an increase of the pressure at the bow and stern and a decrease toward the body at the shoulders. The streamlines have the same type of curvature further away from the body. Sufficiently far from the body, all streamlines will have straightened out and the flow can be considered as undisturbed. The pressure at the bow and stern of the body will increase from the far field towards the body. At the bow of the body, the streamline will be prevented from bending and the velocity of the flow drops to zero. The pressure will increase until the stagnation pressure. At the stern of the body, the

pressure will also increase until the stagnation pressure and the velocity will decrease. Around the shoulders of the body, the pressure will decrease and the velocity of the flow will increase. This can be seen in figure 2.7. The assumptions done in potential theory about the viscosity and the vorticity will result in a high pressure at the stern. In practice, the pressure will not reach the stagnation pressure due to viscosity of the fluid. If the curvature of the body is too large, the flow will separate and the pressure will even drop further, which can also be seen in figure 2.7.

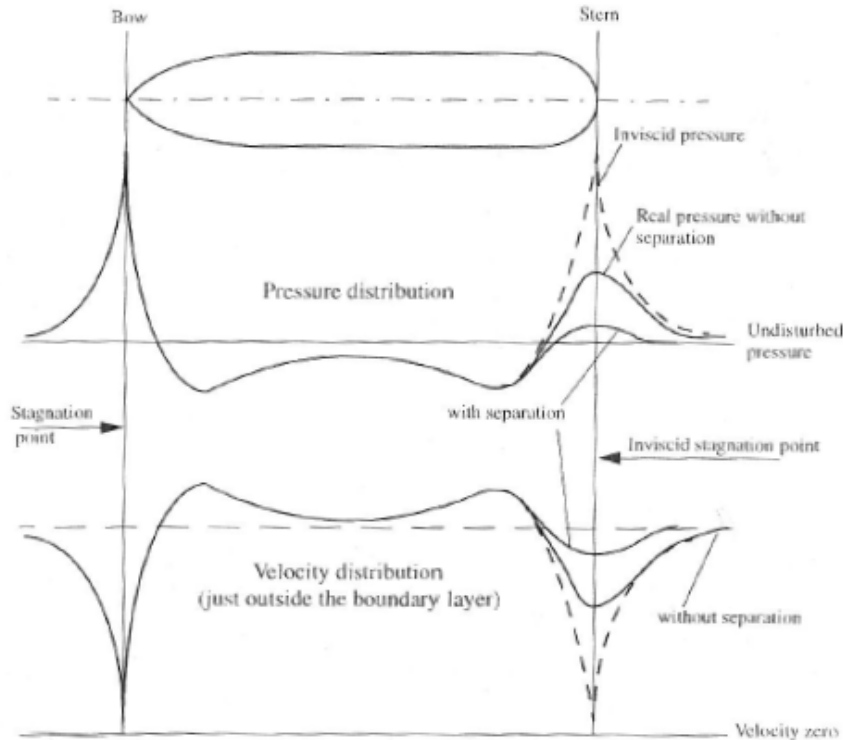


Figure 2.7: Pressure and velocity distribution along a 2D body [17].

In the case of a 3D body, the streamlines normal to the body will stay the same. But there is also a curvature in planes parallel to the surface. At the bow of the body, there will also be a stagnation point. On the 3D body, the same pressure distribution can be seen as in the 2D case. At the bow and stern there will be high pressure regions and low pressure regions will be noticed around the shoulders. In the bottom part of the bow, the curvature of the streamlines is large, which results in a large pressure gradient outward and the pressure at the hull will be low.

The pressure distribution on the hull can give the resistance component by integrating the pressure in longitudinal direction ($F_x = \int_S p \cdot n_x dS$). Because the closed body is considered a inviscid flow, without a free surface, d'Alembert's paradox applies: the total force is exactly zero [17].

Free-surface waves

The non-viscous flow around a vessel gives useful insights as described in paragraph 2.5.2, it does not give a wave pattern or wave resistance. Understanding the generation of a wave pattern and its relation with the hull form, will help to design for minimum wave resistance. A ship wave pattern is made up of a superposition of wave systems which are generated by different parts of the hull and propagating in various directions.

A local disturbance, such as the bow of a ship, generates a continuous set of wave components propagating in various directions ($-\pi/2 < \theta < +\pi/2$), where θ is the angle between the centerline and the wave [17]. The waves with a small angle with respect to the ships direction are called transverse waves and those with a large angle ($\theta > 35$ deg) are called diverging waves. The wave length λ can be calculated with the dispersion relation as can be found in equation 2.25.

$$\lambda = \frac{2 \cdot \pi \cdot c^2}{g}, \quad (2.25)$$

in which c is the velocity of the wave. The wave length of diverging waves is smaller due to the decrease of the velocity of the waves. The wave velocity of a diverging wave can be written as: $c = V \cdot \cos \theta$, which results in the dispersion relation for diverging waves as can be found in equation 2.26

$$\lambda(\theta) = \frac{2 \cdot \pi \cdot c^2}{g} = 2 \cdot \pi \cdot Fn^2 \cdot L \cdot \cos^2 \theta, \quad (2.26)$$

in which L is the length of the vessel and Fn is the Froude number. The direction, phase speed and length of the wave components can be seen in figure 2.8.

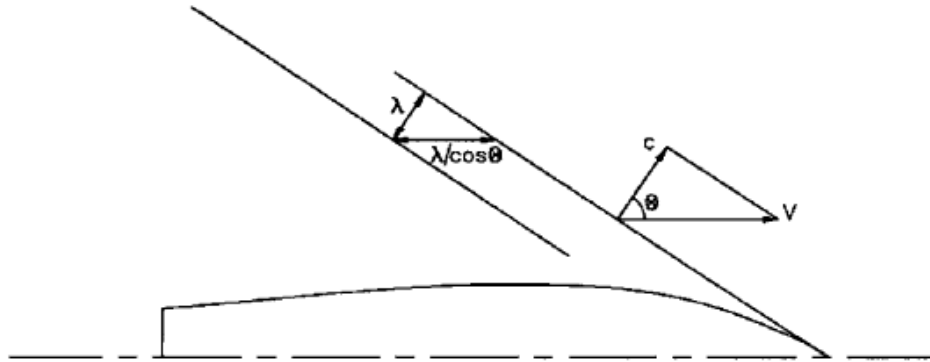


Figure 2.8: Direction, phase speed and length of the wave components in three-dimensional cases [17].

Wave interference

As described in paragraph 2.5.2 the pressure distribution varies along the hull. Surface waves can be considered to be generated by pressure disturbances. The high pressures at the bow and stern will generate a wave system starting with a crest, whereas the low pressures at the shoulders will generate a wave system starting with a trough.

The interference of the different wave systems can be described by the example from a paper by Wigley [17]. The ship can be seen as a double wedge with a parallel midship. The wave systems generated by the different parts of the hull (bow, shoulders and stern) contain transverse and diverging components. In this example, the wave profile along the hull is considered, which is dominated by the transverse waves. The wave profile along the hull can be seen in figure 2.9 and contains of five contributions:

1. A near-field disturbance of the surface, with positive peaks at the bow and stern and negative peaks at the shoulders.
2. The bow wave system, starting with a crest.
3. The fore shoulder wave system, starting with a trough.
4. The aft shoulder wave system, also starting with a trough.
5. The stern wave system, starting with a crest.

The total wave profile along the hull is approximated by the sum of these five systems. The sharp corners at the bow, stern and shoulders result in fixed positions of the origins of this wave systems. As the speed increases, the wave length of the individual wave systems increase and the crests/troughs shift downstream. At different speeds the total wave profile will thus continuously change in shape. If the crests of two or more wave systems coincide, the wave height increases. If a crest and trough of two wave systems coincide, the waves cancel.

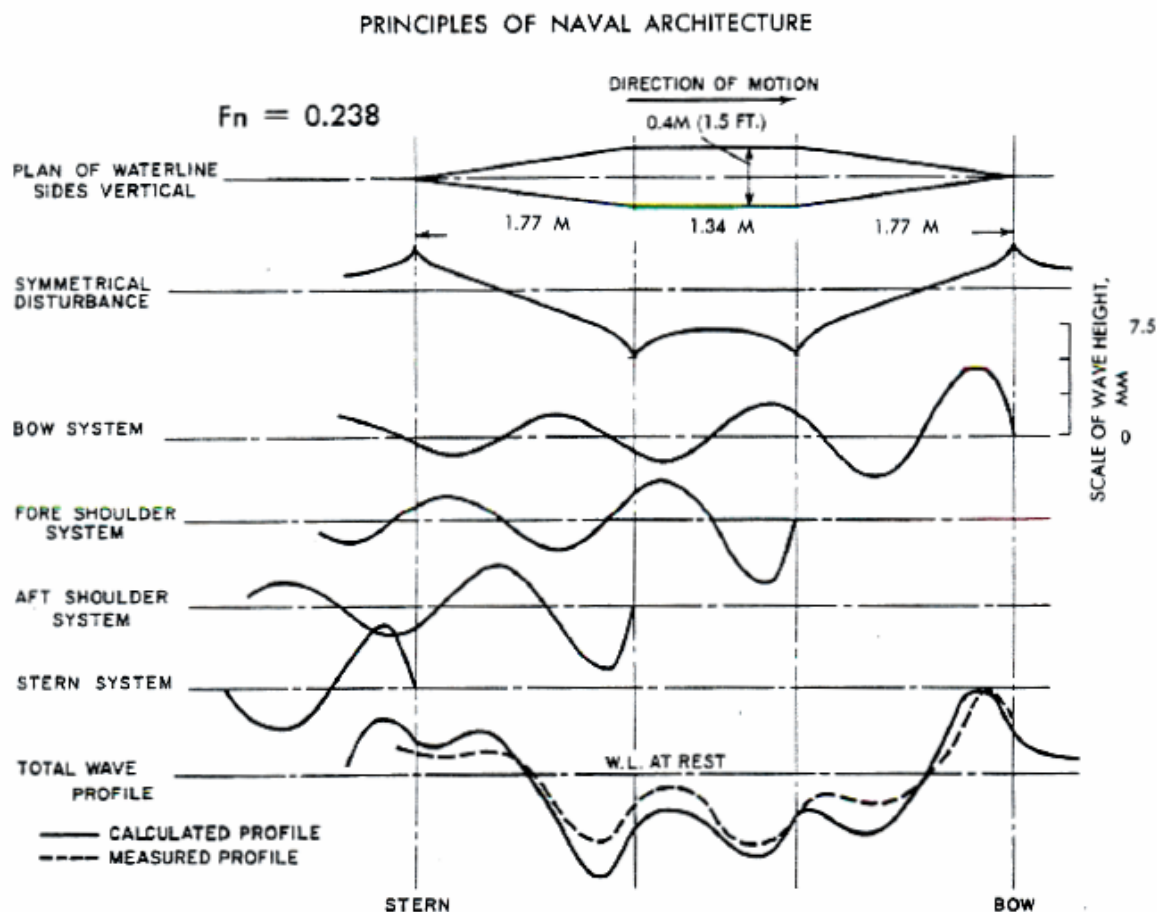


Figure 2.9: The near-field disturbance and the free wave systems for the wedge hull [17].

Ship-shape forms have smooth waterlines without sharp discontinuities. The wave pattern can still be described by the interference of the five wave systems as described above. The wave systems of the shoulder cannot be tied to definite points, due to the gradual slope of the shoulder. Also a bulbous bow will generate a wave system, which interferes with the wave systems. Adding a sponson to the hull also leads to wave systems generated from the shoulders of the sponson. At each speed, the wave length changes and therefore the interference changes.

Wave-making resistance

The wave-making resistance can be calculated in two different ways [17]. The first method is by integrating the longitudinal pressure distribution along the hull, when considering an inviscid flow, as described in paragraph 2.5.2. In this paragraph, the non-viscous flow around a body was analysed without a free surface, which lead to d'Alembert's paradox. When taking into account the free surface, the wave pattern results in a pressure distribution over the hull. The wave-making resistance can be calculated as the net longitudinal force along the hull, as can be seen in equation 2.27.

$$R_W = - \int \int_S p \cdot n_x \cdot dS, \quad (2.27)$$

in which S is the wetted area of the hull, n_x is the longitudinal component of the outward normal on the hull surface and p is the pressure. The wave-making resistance does not include any viscous effects on the pressure, due to the assumption of the non-viscous flow.

The second method to obtain the wave-making resistance is from the wave energy. The wave pattern generated by the ship contains wave energy that radiates out and aft of the hull. This wave energy need to

be generated and maintained by the ship and can therefore be used to calculate the wave-making resistance. The wave-making resistance can be calculated with equation 2.28.

$$R_W = \frac{1}{2} \cdot \pi \cdot \rho \cdot V^2 \int_{-\frac{\pi}{2}}^{+\frac{\pi}{2}} (A(\theta)^2 + B(\theta)^2) \cdot \cos^3 \theta \, d\theta, \quad (2.28)$$

in which A and B are wave spectrum functions. The functions can be represented in an one-dimensional free-wave spectrum, because of the fixed relation between the wave length, speed and direction. In this spectrum the amplitude ($\sqrt{A(\theta)^2 + B(\theta)^2}$) is plotted against the direction (θ).

As can be seen in equation 2.28, the resistance is an integration over the free-wave spectrum and is dependent on the wave amplitude squared. The weighting factor $\cos^3 \theta$ shows that transverse waves are far more important for wave resistance than divergent waves. This means that reducing the amplitude of the transverse waves, by optimizing the wave interference, has a positive effect on the wave resistance [17].

2.6. RAPID

The program RAPID calculates the still-water wave pattern and the steady non-viscous flow around the ship hull [20]. The main results of the program are the wave pattern, the wave profile along the hull, the pressure distribution and streamline direction on the hull, the resistance and the dynamic trim and sinkage. The program can be used for estimating the quality of the design from the wave-making point of view and the main restrictions are listed below [20].

The main restrictions of RAPID are:

- RAPID can only calculate ship-like hull forms.
- RAPID does not include wave breaking, spray and viscous effects.
- RAPID does not explicitly model planing effects.
- RAPID does not model the effect of the propeller.
- RAPID may fail in cases that display extensive and violent wave breaking in reality.

The problem that is solved is the inviscid flow around the ship hull and at the free surface. Mathematically, the problem is defined by the Laplace equation for the velocity potential as described in equation 2.24 and the boundary conditions on the hull and the wave surface. This mathematically problem is solved with a 'panel method', which means that panels are placed on the boundaries of the flow domain (the hull surface and the free surface around the hull). In each panel center a collocation point is selected, which contains an unknown source strength. These source strengths provides a matrix of equations and when solved, the flow field and pressure distribution can be derived.

This matrix of equations needs to be calculated with an iterative approach. From one iteration to the next an improved estimate of the wave surface and velocity field is computed. After a number of steps no further (significant) changes occur and a converged solution is obtained, which satisfies all boundary conditions.

The panels of the free surface are located at a distance above the wave surface, which also explains the name RAPID (RAised Panel Iterative Dawson). In contrast to the panels on the hull which are placed directly at the hull surface. The location of the panels on the hull and above the free surface can be seen in figure 2.10.

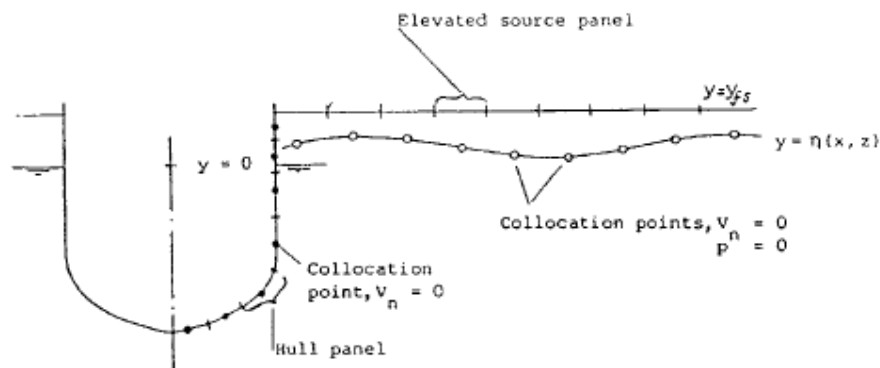


Figure 2.10: The location of the panels on the hull and above the free surface in RAPID [20].

The problem needs to be solved in a two step procedure. The flow field is uniform and the wave surface is flat. In the first step the wave surface changes and wave crest can intersect the panels. In this case the panels need to be repositioned in such way that the distance to the wave surface stays equal. The second step is the repositioning of the hull, which need to be done due to the dynamic pressure distribution. The changing pressure distribution results in trim and sinkage of the hull, which again can have an effect on the wave surface. This iterative process continue until a converged solution is obtained.

The results of the calculation are written in different output files and can also be shown in RAPID. RAPID uses two different methods to calculate the resistance of the vessel. The first method is by integrating the pressures over the hull (Rw1 value), as described with equation 2.27 in paragraph 2.5.2. The second method is by computing the wave energy, and from this the wave resistance, in a cross section behind the transom. This results in a Rw3 value as described with equation 2.28 in paragraph 2.5.2. These two methods, and therefore Rw1 and Rw3 value, should give the same result. However these values are not always the same due to different methods of calculating. This can be explained by uncertainties in the two methods, for example the panel size or panel orientation. The Rw1 value should provide the best absolute value of the wave-making resistance if there is a nice transom flow. The Rw3 value is best used in a relative way for comparing different hull shapes. In general, the Rw3 value is more sensitive to small hull changes [20]. RAPID calculates the wave-making resistance based on potential flow theory and only give a rough estimation of the frictional resistance, based on the ITTC formula and a fixed form factor.

The practical steps that are done in order to create a panel file (.pan file) and calculation in RAPID is described in appendix D.

2.7. Slamming

The impact from the sea surface on the ship is called slamming. Slamming occurs mainly when sailing in waves. The bow comes out of the water and has an impact on the next wave. Slamming does not only occur at the bow of the vessel, but can occur everywhere on a structure that is near the water surface. Slamming is a sudden deceleration of a volume of fluid, which causes a force on the structure. Therefore, these slamming loads need to be taken into account in the structural design of the vessel. Besides the structural requirements that comes with slamming, it is also an important reason for a shipmaster to reduce the ship's speed [5].

Det Norske Veritas (DNV) set up a 'recommended practice' how environmental loads on the structure should be taken into account and among other things also slamming forces [3]. The slamming force on the vessel is a time and location dependent phenomenon. The location of the slamming can be determined on the basis of the instantaneous air gap. The instantaneous air gap is dependent on the still-water air gap, the wave elevation and the motions of the vessel. It is defined by equation 2.29.

$$a(x, y, t) = a_0 + z(x, y, t) - \zeta(x, y, t), \quad (2.29)$$

where a_0 is the still-water air gap, the gap between the mean water level and the structure. $z(x, y, t)$ is the vertical displacement of the vessel on the specific location. $\zeta(x, y, t)$ is the wave elevation on the location of interest. The equation is time and location dependent and a time domain analysis need to be done in order

to see if and how often slamming occurs. When the instantaneous air gap becomes negative ($a(x, y, t) < 0$), an impact between the wave and the structure can be noticed.

The surface elevation is not only depending on the incoming waves, but also the diffracted and radiated waves should be taken into account. The total wave elevation can be written as the sum of these three:

$$\zeta = \zeta_{Incoming} + \zeta_{Radiated} + \zeta_{Diffracted}.$$

Wave-in-deck loads on a floating structure

The approaches for the horizontal and vertical wave-in-deck forces described in the 'recommended practice' [3] are applicable for a deck fixed to a platform and cannot be used for a floating structure. There are three main differences between a floating structure and a fixed deck:

- The motion of the floating structure contributes to the relative impact velocity and acceleration.
- The deck height varies in time and space.
- The impact will to some extent influence the motion of the floating structure.

These three items should be taken into account. For example, a wave diffraction program could be used to calculate the motion and the relative fluid kinematics and from this the slamming forces.

3

Concept study

The conversion of the Fairplayer into a dual draft vessel can be done by a sponson at various vertical positions. A concept study is done to investigate the influence of the vertical position of the sponson on the operational profile and the performance of the Fairplayer. Also the feasibility of the concepts is taken into account. In this study five different concepts designs are set up and analysed.

A sponson on the Fairplayer can be designed in multiple ways. The sponson can be schematically seen in figure 3.1 and 3.2. There are four variables that can be varied in order to change the concept, namely: the length, width, height of the transition and the starting height of sponson.

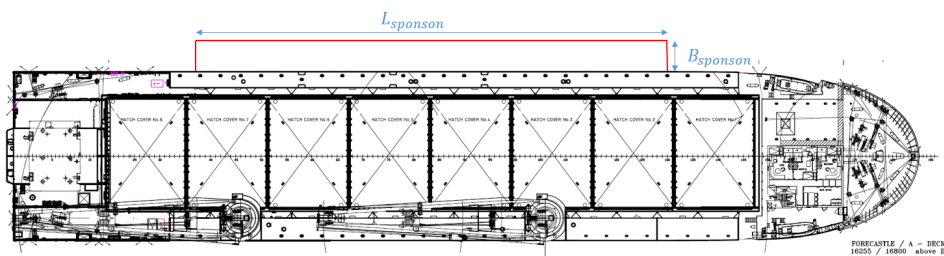


Figure 3.1: Overview of the variables of the sponson in top view.

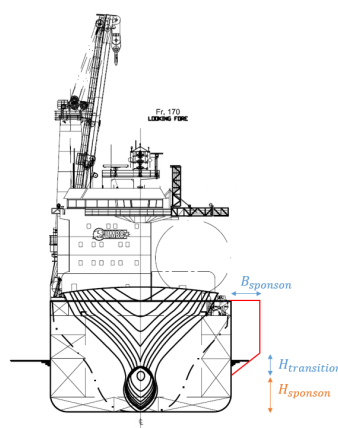


Figure 3.2: Overview of the variables of the sponson in front view.

The front and back of the sponson, as can be seen in figure 3.1, are drawn as perpendicular lines. In the concept design this is done in order to simplify the first stability calculations. In the final design phase this is made as a curved transition in order to reduce resistance in sailing conditions.

The four variables, which define the shape of the sponson, all have an influence on the final design specifications, such as building costs, ship speed and motion behaviour. To compare different concepts, boundary conditions and design criteria are set up. The boundary conditions are set up to obtain a framework for the concepts, this is done in paragraph 3.1. The criteria on which the concept is tested can be found in paragraph 3.2. The concept analysis can be found in paragraph 3.4, in which also conclusions are drawn about this concept study.

3.1. Concept boundaries

The concept of the J-class vessel with a sponson needs to stay within certain boundaries in order to keep the concept realistic and feasible. These boundaries are listed below and are described in this paragraph.

- Current design
- Static stability
- Cargo stored on deck
- SPS regulation
- Feasibility

3.1.1. Current design

The concept of the sponson on the J-class vessel is a conversion of the current vessel. The current design should be kept in mind when developing concepts, because the main dimensions of the vessel cannot be changed easily. The J-class vessel has two different design drafts, namely 7.5 and 8.1 meter. The minimum draft on which the vessel can sail safely in ballast condition is 5.5 meter and from the Daily Progress Report (DPR) it can be seen that the J-class sails most of the time on a draft lower than 6.5 meter. The moulded depth of the vessel is 14.1 meter.

3.1.2. Static stability

In order to increase the maximum lifting load in offshore conditions, the static stability must increase. The minimum static stability (GM) during a lift operation is defined by the 'Kahn-rule', which is set up by Jumbo engineers and can be found in equation 2.3. The second aspect that influences the GM is the shift of the load during the 'lift off'. The reduction of the GM due to this 'lift off' can be found in equation 2.2. These two equations can be combined into one equation for the minimum required GM . This can be found in equation 3.1 and as could be seen, the minimal GM is dependent on the load in the crane, the distance that the COG of the load shifts and the displacement of the vessel. The sponson will be designed on the maximum load (P_{load}), which is 1800 ton and the vertical shift of the COG of the load is 40 meter. The only variable in this equation is the displacement (∇), which is dependent on the dimensions of the sponson and the draft of the vessel.

$$GM_{minimal} = 1.0 + 1.5 \cdot \left(\frac{P_{load}}{1800} \right) + \frac{P_{load} \cdot h}{\rho_w \cdot \nabla}. \quad (3.1)$$

In order to increase the static stability, the waterplane area of the vessel must increase. The length and width of the sponson are dependent variables, as can be seen in equation 1.6.

The concept of a sponson is based on the controlled submersion of the vessel in order to increase the waterline area and therefore the static stability. The lifting operations need to be carried out at a draft where the sponson has vertical sides. With these vertical sides, the static stability remains the same, even when the vessel is under a small list angle or trim angle.

3.1.3. Cargo stored on deck

The maximum combined load of the cranes on the vessel is 1800 ton (2x 900 ton) and when performing the lift with the fly-jib, the maximum combined load is 1400 ton (2x 700 ton). It can be desirable to transport more than one piece of cargo to an offshore location. The cargo is expected to be carried on the deck of the vessel and will therefore result in an increase of the center of gravity. The requirement is set that the minimum

amount of cargo on deck is two loads of 1800 ton or three loads of 1400 ton. During this analysis the most conservative situation is taken into account, which is three 1400 ton loads stored on main deck. For offshore installation work the amount of cabins in the accommodation is not sufficient and an extra accommodation unit needs to be stored on deck.

3.1.4. SPS regulation

The SPS regulations are intended to provide safety regulations for special purpose ships, equivalent to that required by the International Convention for the Safety of Life at Sea in 1974 [12]. The J-class vessels are designed and built as heavy lift vessels and therefore the IMO Special Purpose Ship (SPS) code is not taken into account. The last few years governments allowed only vessels that were SPS compliant to perform offshore installation work. In the past, Jumbo Maritime could submit a special request to Lloyds Register. After approval by the class society Jumbo Maritime could carry out offshore installation work.

These regulations are intended for new built vessel as well as vessels who get a large modification. Because the application of a sponson can be seen as a major modification, the regulations for SPS need to be taken into account. The code is taken into account as a design restriction for the sponson.

The basis for the SPS regulations can be described as follows: Personnel on board the ship, who are not required for normal navigation, engineering and maintenance or engaged to provide services for the persons carried on board need to be treated as passenger. Because these personnel are required for the operations on board the ship, these personnel are expected to have a fair knowledge of the layout of the ship and have received training in safety procedures and the handling of the ship's safety equipment. These vessels do not need to fully comply with the SOLAS regulations for passenger vessels, but must comply to the SPS regulations.

The number of special personnel that needs to be carried on board the Fairplayer is 140. By analysing the regulations, it turned out that this would not lead to a restriction on the dimensions of the sponson. One important aspect of the SPS regulation is the damage stability, which is determined with a probabilistic damage stability calculation. Probabilistic damage stability calculations are done with computer software, where the ship with its watertight compartments is modelled. The program calculates the probability that the vessel sinks if a compartment is flooded and this is extended to all compartments and combinations of compartments. In the end, these probabilities are summed and need to be below a probability defined in the regulations. The SPS regulations for the list angle in case of a flooding are stricter than the regulations for a heavy lift vessel. A study is carried out by Jumbo Maritime in order to investigate the changes that need to be made to the Fairplayer in order to comply with the SPS regulations [26]. In this study four modifications options are required:

- Spitting the hold transversely at frame 132, creating two holds.
- Connecting the double bottom outside tanks with instantaneous cross flooding pipes.
- Splitting the lower side tanks.
- Raising the tank vents to 13.8 meter.

A sponson placed at one side of the ship could have a positive effect on the damage stability. The probability of a hit at the underwater part of this side can be lower due to the hull shape. If the damage is at the other side of the vessel, the sponson can be used as ballast tank to avoid large heeling angles. To find out if a sponson could be beneficial in case of a damage, a damage stability calculation needs to be done.

3.1.5. Feasibility

The concepts need to be made in such a way that it is feasible construct. The materials and ideas need to be proven in the past. Very new and innovative ideas could have unforeseen drawbacks, which could lead to large costs or even dangerous situations during lifting operations. This need to be avoided by concepts that are feasible to build, maintain and operate.

3.2. Concept criteria

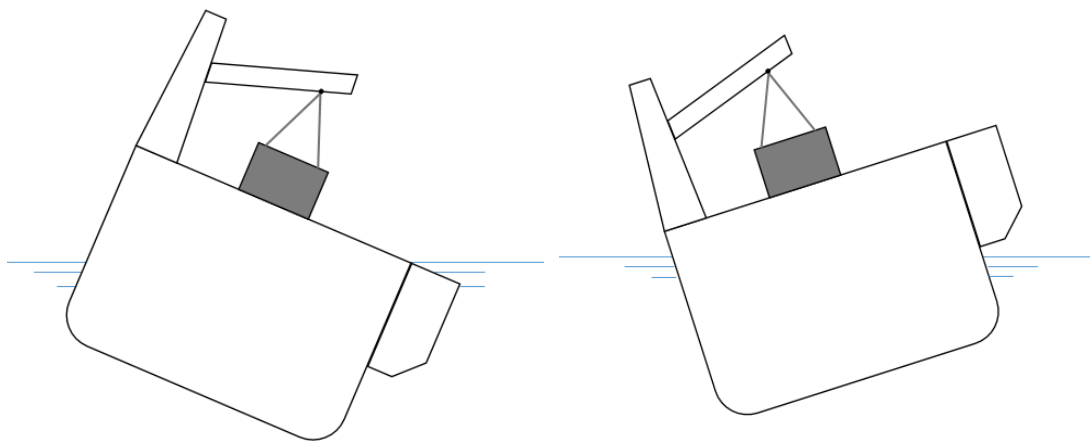
The different concepts are tested on different criteria. These criteria are listed below and will be explained in detail in this paragraph.

- Loss of stability
- Resistance
- CAPEX
- Motion behaviour
- Ballast water
- Deck area
- Maintenance

3.2.1. Loss of stability

Safety is a very important aspect within Jumbo Maritime and Jumbo Maritime has an excellent reputation for the lifting and transport operations. In order to maintain this reputation, the risk on a loss of stability of the vessel with a sponson must be minimized.

The vessel with a sponson can lose the stability when the deck comes in the water or the sponson comes completely out of the water. This can be seen in figure 3.3. From the experience of the Jumbo engineers the maximum allowable list and trim angles are 1.5 degrees. This maximum allowable angles are based on the dynamic response of the load in the crane and the maximum allowable load of the cranes. With a list angle of 1.5 degrees, the maximum vertical change of the waterline is 0.80 meter. It can happen that the weather suddenly changes during a lifting operation, therefore a margin on this minimum dimensions is favourable.



(a) Loss of stability due to the submersion of the deck. (b) Loss of stability due to the sponson come out of the water.

Figure 3.3: Schematic representation of the two different cases where a loss of stability can occur.

3.2.2. Resistance

The resistance of a ship is discussed in paragraph 2.3 and is dependent on different main parameters. By adding a sponson to the Fairplayer the resistance only increases if the sponson is partly submerged during transit conditions. This will only be the case with some of the concepts, which will be described in paragraph 3.3. If one of the concepts has a sponson partly submerged this has an effect on the resistance, which results in a higher fuel consumption at the same speed. This higher fuel consumption has an effect on the operational

costs of the vessel. Another disadvantage of the increased resistance could be that the design speed of the vessel cannot be achieved.

It is hard to predict the exact influence of the sponson on the resistance. Based on engineering practice it can be said that the wider the sponson and the more the sponson is submerged, the higher the resistance will be. The main parameters of a sponson have an effect on different components of the resistance. The wetted surface has a relation with the viscous resistance, which will increase when the wetted surface increases. The wave resistance is dependent on the hull shape and the position of the shoulders. Also the position in height of the sponson has an influence on the viscous and wave making resistance of the vessel. If the concept turns out to have the sponson partly submerged during transit, the extra resistance that this causes needs to be calculated.

3.2.3. CAPEX

As described in paragraph 1.7 this research does not contain a financial analysis. When setting up different concepts it is important to keep the capital expenditures (CAPEX) in mind. The total building costs for this concept can be split into two parts. The first one is the construction of the sponson. The costs are dependent on the size of the sponson, which means that a larger sponson results in larger building costs. Besides that, the capacity in the ballast tanks is not enough to submerge the vessel until a draft of more than 9 meter and also compensate for the heel angle caused by the load in the crane during the 'crane out' phase. This means that if the operating draft of the vessel increases, the amount of extra ballast tanks must increase as well. In paragraph 3.2.5 the current ballast capacity and current ballast pump capacity are analysed. Depending on the concept, either the ballast tank capacity or the ballast pump capacity must increase or both.

The vessel is designed for two different drafts, namely 7.5 and 8.1 meter. When the draft of the vessel increases, it needs to be checked if the ship's construction needs to be strengthened. The limiting factor here is the longitudinal bending moment of the vessel. A sponson at one side of the vessel leads to a stiffer cross-sectional area, which has an advantage to withstand the longitudinal bending moment. The vessel needs to get a certificate for the larger design draft by the class society, in order to be allowed to perform lifting operations.

3.2.4. Motion behaviour

The motion behaviour of the vessel needs to be analysed in two different situations. The first situation is during the transit. The vessel must sail to an offshore location with the cargo on board or needs to sail from this offshore location to the port. The second situation is during the offshore lifting operation. During the offshore lifting operation the vessel is at a larger draft and the static stability is therefore different.

During the transit of the vessel, the sponson is completely or partly out of the water, which means that slamming and high accelerations could occur. The slamming on the sponson is explained later in this paragraph. High accelerations due to the submersion of the sponson can only be calculated by performing a time-domain simulation of the vessel in a seaway. It can be said that the change in width of the vessel has an impact on the accelerations of the vessel. If the length of the sponson and the transition stays the same, the larger the width, the more the change in width, which leads to higher accelerations.

The motion behaviour of the vessel during the lifting operation is dependent on the response amplitude operator (RAO) of the vessel and the wave spectrum. From this an operability study can be performed as described in [6].

Slamming

The dimensions of the sponson also have an influence on the slamming behaviour, as described earlier in paragraph 2.7. Impact from the slamming forces on the structure needs to be taken into account in the design process and can be calculated by calculating the motions and relative fluid kinematics with a wave diffraction program. From the operational point of view, noise from slamming and high acceleration could be a reason to reduce the speed of the vessel or change the course. The position and shape of the sponson has an influence on the slamming behaviour. From equation 2.29, it can be seen that the air gap between the sponson and the water has a strong relation with the slamming behaviour. It can be said that more slamming occurs if the air gap between the water surface and the sponson is smaller.

Operational limits

The operability of a vessel can be calculated by performing a study to the motions of the vessel in a range of wave conditions. These wave conditions are dependent on the offshore location and the period of the year.

An operability study is done at Jumbo Maritime [6], for the Fairplayer with an increase of static stability. The four concepts that are studied can be found in appendix B. The motion behaviour of the four concepts is calculated and the operability in the seven offshore locations described in paragraph 1.8 is calculated. The operability of the four concepts as percentage of the time can be found in table 3.1 for the case of a lift of 900 ton and 3.2 for the case of a lift of 1800 ton.

Table 3.1: Operability of the four concepts and the Fairplayer when lifting 900 ton [6].

Fairplayer - 900 ton	Original	Concept 1	Concept 2	Concept 3	Concept 4
Before lift off					
Average operability [%]	50	49	50	50	50
After lift off					
Average operability [%]	57	43	47	60	50
Out reach					
Average operability [%]	60	49	53	60	57

Table 3.2: Operability of the four concepts when lifting 1800 ton [6].

Fairplayer - 1800 ton	Original	Concept 1	Concept 2	Concept 3	Concept 4
Before lift off					
Average operability [%]	-	38	39	45	42
After lift off					
Average operability [%]	-	43	45	47	40
Out reach					
Average operability [%]	-	52	54	57	55

As can be seen in table 3.1, the workability with a load of 900 ton is about the same for all four concepts. Concept 3 is the concept with extension at both sides of the vessel and has the best operability at the seven locations. In table 3.2 the same conclusion can be drawn, concept 3 has the best operability, but the others do not differ much.

The extensions of concept 3 [6] can be compared with a sponson, so it is expected that the Fairplayer with a sponson has a similar motion behaviour and operability during lifting operations. A motion analysis and operability study needs to be carried out in order to draw exact conclusions about the operability.

3.2.5. Ballast water

Ballast water is required to submerge to a larger draft and to compensate for the heeling moment created by the load when the crane is at its outreach. From the stability booklet [23], the displacement of the vessel over a range from 3 until 8,5 meter can be found. The amount of ballast water needed for a specific draft can be calculated with equation 3.2. The lightweight of vessel is 9537 ton and in this analysis the weight of the cargo is assumed to be zero. The other tanks and equipment contain all tanks such as fresh water, fuel, oil and grey water tanks. The maximum amount of ballast water in the current vessel is 11500 ton. All tanks, when not taking into account the ballast water tanks, have a total mass of 2247 ton. With this information the line in graph 3.4 is drawn.

$$\text{Ballast water} = \text{displacement} - \text{lightweight} - \text{cargo} - \text{other tanks and equipment} \quad (3.2)$$

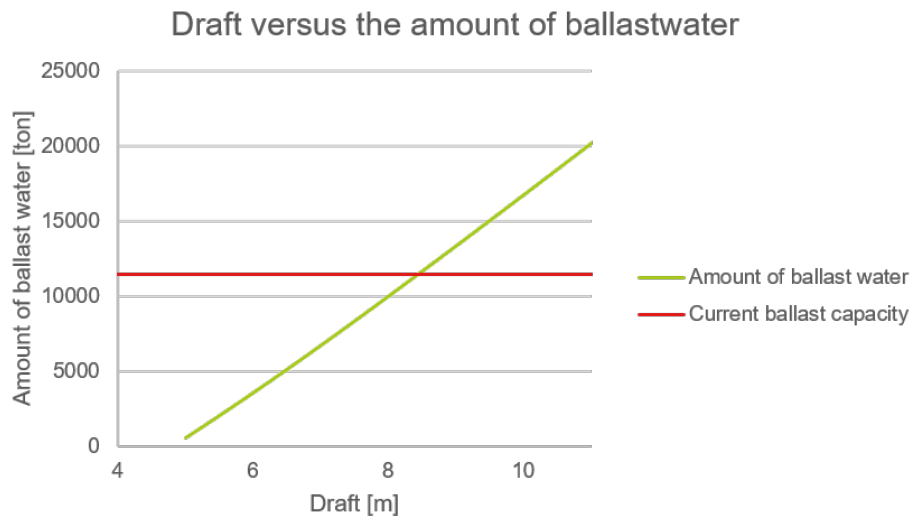


Figure 3.4: The amount of ballast water for a range of drafts.

As can be seen, the maximum ballast capacity is only enough to submerge the vessel to a draft of 8.5 meter. This is when no cargo is stored on deck and the trim of the vessel is not taken into account. So when the trim of the vessel needs to be controlled, the maximum draft is even lower. In order to increase the draft to 10 meter, the ballast capacity need to increase with almost 50%. This ballast tanks need to be placed in the cargo hold, which reduces the space for cargo.

The current ballast pump capacity consist of three bilge ballast pumps ($700 \frac{m^3}{h}$), two general service pumps ($175 \frac{m^3}{h}$) and an emergency bilge pump ($260 \frac{m^3}{h}$). In figure 3.5, the time that the J-Class vessel needs to submerge to a certain draft from the initial draft of 5.5 meter is given. It takes more than 4.5 hours to submerge from a draft of 5.5 meter until 8.5 meter with the current ballast capacity of three bilge ballast pumps (in total $2100 \frac{m^3}{h}$).

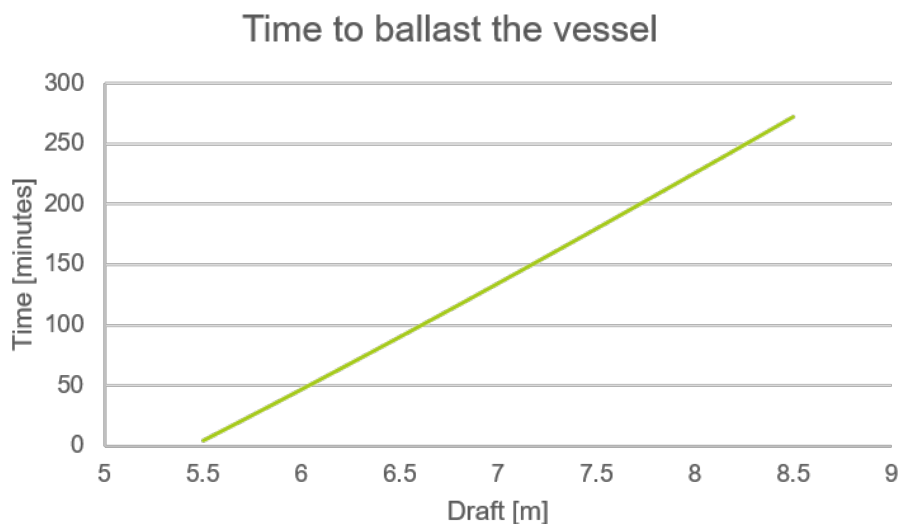


Figure 3.5: The time needed to submerge from a draft of 5.5 meter.

If one of the concepts need to submerge to a larger draft, extra ballast tanks are needed to ensure that the draft can be achieved. The sponson creates an even large buoyancy, but can also accommodate for more

ballast water tanks. It can even be favourable to fill the sponson with ballast water during lifting operations, because it can create a counteracting moment when the crane is in the 'reach out' position.

3.2.6. Deck area

The application of a sponson leads to a larger deck area. An increase in deck area is beneficial for the amount or the size of the cargo that is transported. The maximum load on the extra deck area of the sponson is dependent on the shape of the sponson and the strength the construction of the sponson.

3.2.7. Maintenance

Besides the building costs of the sponson, the maintenance costs are also very important. The maintenance costs and time to perform maintenance can be significant if the concept is very complex or has moving parts. The time that the crew needs to perform maintenance is time that the vessel cannot sail or cannot perform lifting operations and therefore reduces the revenues of the vessel.

3.3. Concepts overview

Five concepts of the vessel with a sponson are set up and analysed. The five concepts are created within the concept boundaries. From these five concepts an operational profile is sketched and the advantages and disadvantages are listed.

3.3.1. Concept 1: Long sponson around the waterline

This concept is based on a sponson just above the waterline and along the length of the vertical side of the vessel, which can be seen in figure 3.6. This length results in a width that could be as small as possible. The sponson starts at a height of 5.5 meter, so the vessel can sail on a draft of 5.5 meter without having an increased resistance. The vertical side of the sponson starts at 7.0 meter, which results in a vertical side of 7.1 meter. The draft of 5.5 meter can only be achieved when the vessel is empty or with a limited amount of cargo, but the operational profile shows that this is more than 50% of the time as described in paragraph 1.8. If the vessel sails with cargo, which reaches the maximum crane capacity of 1800 ton, the static stability of the vessel is negative. The ship needs to ballast until the sponson is partly under the waterline and the waterline area is increased. The vessel can sail at a draft of 7.5 meter, where the side of the sponson is vertical. The lift operations will be performed at a draft of 8.5 meter, where the side of the sponson is vertical. The ballast capacity is sufficient to submerge to this draft, as explained in paragraph 3.2.5. Slamming could be an issue while sailing at 5.5 meter draft, but can be avoided by increasing the draft to 7.5 meter.

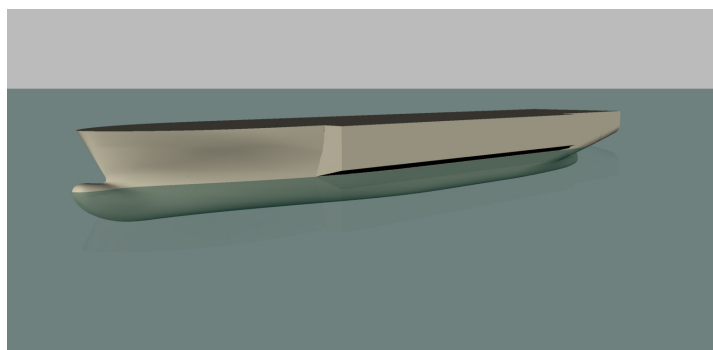


Figure 3.6: Concept 1: Long sponson around the waterline (T = 5.5 meter).

Advantages:

- The vertical side at the lifting draft from waterline to deck is large.
- A transit draft of 5.5 m without extra resistance.
- The ballast tank capacity to submerge the vessel to the lifting draft is sufficient.

Disadvantages:

- At the transit draft slamming could be a limited factor.
- During sailing with cargo the sponson results in additional resistance.

3.3.2. Concept 2: Long sponson above the waterline

This concept is based on a sponson far above the water and along the length of the vertical side of the vessel, which can be seen in figure 3.7. The main advantage of this concept is that only the vessel above the draft of 7.5 meter is changed. The sponson starts at a height of 7.5 meter and has a vertical side from a height of 9.0 meter. This means that the vertical side of the sponson is 5.1 meter. The vessel can sail with cargo on a draft until 7.5 meter without having an increased resistance. During the lifting operations, the vessel needs to submerge to a draft of 10.5 meter. This is also one of the disadvantages of this concept, the existing ballast capacity is not sufficient to submerge to this draft. This means that additional ballast tanks need to be installed in the cargo hold so the hold cannot or can only partly be used for cargo. Besides that, the hull is not designed for a draft of 10 meter, so the strength of the hull need to be checked. The operational profile of the vessel will not change significantly, because it only needs to submerge when performing the installation work. This increasing draft can be a limited factor in ports with a limiting depth.

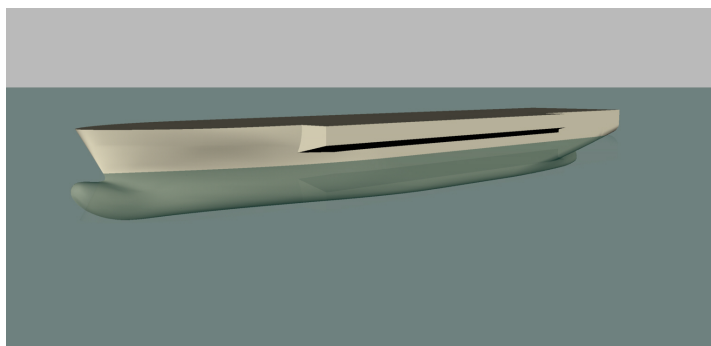


Figure 3.7: Concept 2: Long sponson above the waterline (T = 7.5 meter).

Advantages:

- No increase of resistance until a draft of 7.5 meter.
- The probability of slamming is reduced due to an increase of the air gap.

Disadvantages:

- Large amount of ballast water needed to get to the lifting draft.
- Small vertical side during the lifting operations.
- Strengthening of the hull needs to be checked.

3.3.3. Concept 3: Long sponson below the waterline

This concept is based on a sponson that starts just above the bilge keel, which can be seen in figure 3.8. The sponson starts at a height of 2 meter and has a vertical side from about 5 meter. This concepts does not have a draft on which the vessel can sail without an increased resistance. The static stability for lifting operations can be obtained at every draft, which means that even in shallow waters the vessel can perform its lifting operations. A large disadvantage is the high static stability of the vessel, even when the vessel is empty, which results in a 'stiff' vessel as described in paragraph 1.5.

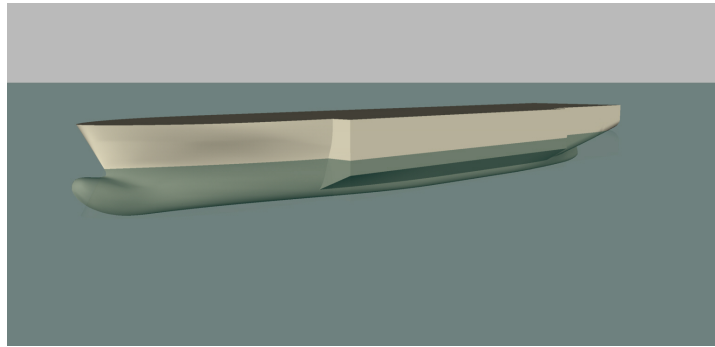


Figure 3.8: Concept 3: Long sponson below the waterline ($T = 7.5$ meter).

Advantages:

- Obtain the static stability on a shallow draft.
- Large vertical side of the sponson during the lifting operation.
- Slamming at the bottom of the sponson is eliminated.

Disadvantages:

- The high static stability results in a 'stiff' vessel.
- An increase of resistance at every draft.

3.3.4. Concept 4: Short sponson above the waterline

This concept is based on a sponson far above the waterline, but is a variant of concept 2 in paragraph 3.3.2. As can be seen in equation 1.6 the width has a positive effect on the static stability. This means that the length of the sponson can be significantly decreased if the width is increased. The width of the sponson is expected to have a negative effect on the resistance and is therefore limited in the other concepts. The sponson is positioned far above the waterline and will only be submerged when the vessel is performing its lifting operations. The sponson starts at a height of 7.5 meter and has a vertical side from 9.0 meter. The vertical side is also 5.1 meter. The increased width of the sponson could lead to a loss of stability at a smaller heel angle. The limited amount of ballast capacity has the same disadvantages as concept 2.

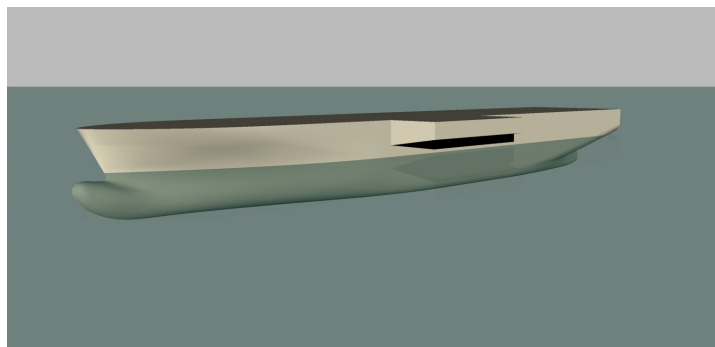


Figure 3.9: Concept 4: Short sponson above the waterline ($T = 7.5$ meter).

Advantages:

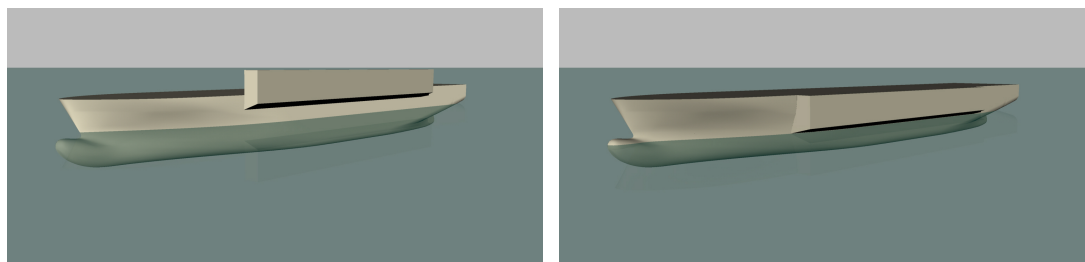
- No increase of resistance until a draft of 7.5 meter.
- The probability of slamming is reduced due to an increase of the air gap.

Disadvantages:

- Large amount of ballast water needed to get to the lifting draft.
- Small vertical side during the lifting operations.
- Strengthening of the hull needs to be checked.

3.3.5. Concept 5: Vertically movable sponson

This concept is based on a sponson that can be moved in vertical direction, which can be seen in figure 3.10. The sponson is placed on a rail system and is positioned at the top when the vessel is empty or sails with its cargo to the offshore location. The sponson can be lowered when the vessel is arrived at the offshore location. This concept has the advantages of concept 2 and 4, where the vessel can sail without an increase of resistance and has the advantage of concept 1 and 3, where the vessel does not need extra ballast tanks in order to submerge to the lifting draft. The main disadvantage is that the rail construction will be very expensive, because it needs to transfer all the forces from the sponson to the hull. Also the maintenance costs of this system are much higher compared to the other concepts.



(a) Sponson in upper position during sailing ($T = 7.5$ meter).

(b) Sponson in lower position during the lifting operations ($T = 5.5$ meter).

Figure 3.10: Concept 5: Vertically movable sponson.

Advantages:

- An increase of static stability when needed.
- No increase of resistance until a draft of 7.5 meter.
- The probability of slamming is reduced due to an increase of the air gap.

Disadvantages:

- Building costs of the system are high.
- Maintenance costs of the system are higher compared to the other concepts.
- No extra deck space, due to the movable construction and no overhanging cargo.

3.4. Concept selection

In order to choose between the different concepts, a design tool is used. The design tool that is used is the Analytic Hierarchy Process (AHP) developed by T.L. Saaty [24]. The AHP method is a method of making a single selection from a group of concepts. The method uses a pair-wise comparison, which means that it only compares two items. This is relatively easy to perform.

The AHP uses a three level hierarchy, which can be seen in figure 3.11.

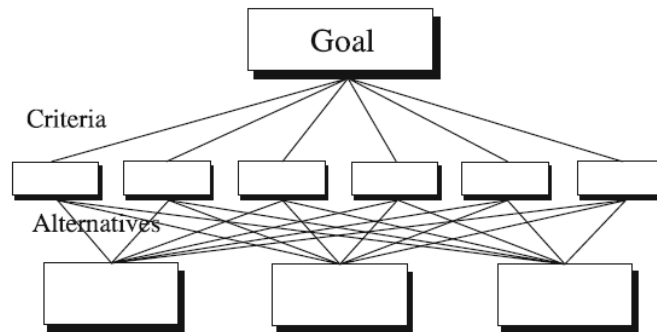


Figure 3.11: The three levels in the hierarchy of the AHP method.

On the bottom level the different alternatives or concepts are placed and on the level in the middle the different criteria. This all for the goal, which is on top of the hierarchy. In this case the goal is to choose one of the concepts. During this analysis there are 5 concepts designed, which are described in paragraph 3.3. The criteria are defined in paragraph 3.2.

The problem is split into a series of pairwise comparisons. For each of these comparisons ask what the first criteria (A) relates to the second criteria (B). For this a 9-point scale is used to compare the criteria. This 9-points scale can be found in figure 3.12.

Definition	Intensity
1	A and B equally important
3	A is weakly more important than B
5	A is strongly more important than B
7	A is very strongly more important than B
9	A is extremely or absolutely more important than B

Figure 3.12: The 9-point scale, which can be used to compare the criteria in the AHP method.

In figure 3.12 only the odd numbers are shown, the even numbers can also be used and will be an interpolation between the intensities. If the criteria B is more important than A, the reciprocal can be used (for example 1/3). All these comparisons can be placed in a matrix. For the design criteria this matrix can be found in table 3.3.

Table 3.3: Comparison of the different criteria in a matrix

	Loss of stability	Resistance	CAPEX	Motion behaviour	Ballast water	Deck space	Maintenance
Loss of stability	1,00	3,00	5,00	3,00	7,00	9,00	3,00
Resistance	0,33	1,00	3,00	1,00	7,00	9,00	1,00
CAPEX	0,20	0,33	1,00	0,33	5,00	7,00	0,33
Motion behaviour	0,33	1,00	3,00	1,00	7,00	9,00	1,00
Ballast water	0,14	0,14	0,20	0,14	1,00	5,00	0,14
Deck space	0,11	0,11	0,14	0,11	0,20	1,00	0,11
Maintenance	0,33	1,00	3,00	1,00	7,00	9,00	1,00

There are two notes that can be made, the diagonal always contains ones and the matrix is reciprocal ($a_{i,j} = \frac{1}{a_{j,i}}$). In order to check if the matrix is consistent, a consistency index (CI) can be calculated. This consistency index can be calculated with equation 3.3, where λ_1 is the largest eigenvalue of the matrix and n is the size of the matrix.

$$CI = \frac{\lambda_1 - n}{n - 1} \geq 0 \quad (3.3)$$

This consistency index can be compared to a random index (RI) as described in [24]. This random index is dependent on the number of criteria. This comparison is expressed in a consistency ratio (CR), which can be calculated with equation 3.4.

$$CR = \frac{CI}{RI} \quad (3.4)$$

For this consistency ratio an acceptable limit is set on $CR \leq 0.1$. Which basically says that the consistency index is 10 times better than the random index.

This analysis is done in order to find the weighted criteria, but the concepts need to be analysed in the same way. The concepts are compared to each other on every criteria. The matrices can be checked on consistency as described before and the eigenvectors can be used as a ranking of the concepts for each of the criteria. These eigenvectors can be put into one large matrix called the 'concept priorities', which can be found in table 3.4. A higher value means that the concept is more preferred.

Table 3.4: The matrix with 'concept priorities' for each criteria.

	Loss of stability	Resistance	CAPEX	Motion behaviour	Ballast water	Deck space	Maintenance
Concept 1	0,41	0,13	0,89	0,27	0,51	0,50	0,63
Concept 2	0,08	0,57	0,18	0,58	0,09	0,75	0,47
Concept 3	0,79	0,05	0,38	0,07	0,21	0,40	0,39
Concept 4	0,06	0,57	0,18	0,55	0,09	0,18	0,47
Concept 5	0,44	0,57	0,04	0,53	0,82	0,06	0,05

The consistency ratio's for the different matrices can be found in table 3.5.

Table 3.5: The consistency ratio's for the different matrices.

	Consistency ratio
Criteria	0,07
Loss of stability	0,03
Resistance	0,08
CAPEX	0,10
Motion behaviour	0,06
Ballast water	0,07
Deck space	0,04
Maintenance	0,03

The normalized eigenvector associated with the largest eigenvalue of the matrix turns out to be the best way of weighting options [24]. The eigenvector of the matrix in table 3.3 can be seen in table 3.6. Again, the criteria with the highest score has the highest priority.

Table 3.6: Eigenvector with the weighted criteria.

	Criteria weights
Loss of stability	0,76
Resistance	0,36
CAPEX	0,17
Motion behaviour	0,36
Ballast water	0,07
Deck space	0,04
Maintenance	0,36

3.4.1. Conclusions of the concept study

In order to find a final result, the 'concept priorities' can be multiplied by the 'criteria weights' as seen in equation 3.5.

$$[\text{concept priorities}] \cdot [\text{criteria weights}] = [\text{result}] \quad (3.5)$$

The results can be found in table 3.7.

Table 3.7: Results of the Analytic Hierarchy Process.

	Results
Concept 1	0,90
Concept 2	0,71
Concept 3	0,88
Concept 4	0,66
Concept 5	0,82

From this Analytic Hierarchy Process it can be concluded that two concepts have about the same score, which can be found in table 3.7. These two concepts are concept 1 and 3, which are concepts where the sponson is partly submerged during transit. These two concepts have a good score on the loss of stability, which means that chance of the loss of stability is lower than the other concepts. This safety aspect is very important for Jumbo Maritime, but the same counts for the relatively high transit speed of the vessels. The two concepts have a low score on the resistance, as can be seen in table 3.4. In this stage of the research the resistance is not calculated exactly and only assumptions based on engineering practice are made.

In this study concept 1 and 3 turn out to be very feasible concepts, except for the increase in resistance. In order to get a better insight in the increase of the resistance, this needs to be calculated. The concept study mainly focused on the vertical position of the sponson, but the shape and longitudinal position of the sponson could also be of influence on the resistance of the Fairplayer with a sponson. To see if the increase of

resistance of concepts 1 and 3 is not a too large drawback, a method is set up to calculate the resistance, but also to obtain information about the optimal shape and longitudinal position of the sponson as is described in chapter 4. In this study the operational profile of concept 1 is taken into account. This means that the draft at which the resistance should be calculated is 7.5 meter.

4

Resistance calculation method

The increase of resistance of the vessel with a sponson is an important criteria for Jumbo Maritime. As described in paragraph 2.3 there are multiple ways of predicting the still water resistance in an early stage of the design process, each of these methods are discussed in paragraph 4.1. This leads to a first estimation of the increased resistance of the Fairplayer with a sponson, with an adjusted Holtrop-Mennen method as set up in this research. The adjusted Holtrop-Mennen method is divided into a five step plan for calculating the resistance of the Fairplayer with sponson and is discussed in paragraph 4.3.

4.1. Methods to calculate the resistance of the Fairplayer

There are multiple ways to calculate the resistance of a vessel, which are described in paragraph 2.3. Each of these methods is discussed for its applicability in this research. The first method mentioned is model testing, which is a rather time-consuming and expensive method for this research. In this stage of the research, multiple hull shapes need to be compared, which makes model testing not the most suitable method. The second method mentioned is the use of empirical methods. Empirical methods are based on resistance data of vessel, which are tested in the past. A vessel with a sponson has a completely different hull shape than the conventional hull shapes which are used to set up the empirical methods. This need to be taken into account if an empirical method is used and therefore assumptions need to be made to be able to use the formulas. The method of Holtrop & Mennen is an extensive method, which gives a division into six different resistance components and is commonly used in ship design. The third method is the use of computational techniques. There are two main methods to use computational techniques for the prediction of the resistance of a vessel. The two main methods are Computational fluid dynamics (CFD) and potential flow theory programs, such as RAPID. A CFD code solves the Navier-Stokes equations as described in paragraph 2.5.1 and takes the viscosity of the fluid into account, whereas in potential flow theory this is not the case.

From this it can be seen that model testing is not applicable in this research. The three main methods left are: The method of Holtrop-Mennen, CFD calculations and RAPID calculations. Each of this methods has limitations and drawbacks, therefore an adjusted Holtrop-Mennen method is set up in this research to give a first estimation of the increased resistance. In figure 4.1 the four methods to calculate the resistance of the Fairplayer without a sponson, with one sponson and with two sponsons are shown. For each of these methods the limitations are discussed.

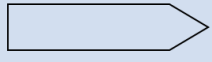




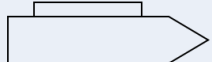





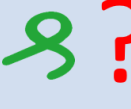



	Holtrop-Mennen method	CFD	RAPID	Adjusted Holtrop-Mennen method
Base case Fairplayer 				
Fairplayer with two sponsons 				
Fairplayer with sponson 				

Figure 4.1: Schematic overview of four resistance calculation methods.

In figure 4.1 it is shown if the calculation method can be used for the types of vessel in the left column. The method of Holtrop & Mennen can be used for a wide variation of vessels within certain boundaries as described in paragraph 2.4. The Fairplayer without a sponson can therefore be calculated with this method. The Fairplayer with a sponson has a drastically changing dimensions (i.a. B , C_B , C_M , C_P). The calculation with Holtrop-Mennen for the Fairplayer with sponson is done and is shown in table C.2. The wave-making resistance calculated with Holtrop-Mennen is among others dependent on the width of vessel, B , and the prismatic coefficient, C_P , which have changed due to the sponson. It is expected that the wave-making resistance would increase due to the sponson, but the Holtrop-Mennen calculation results in a decrease of 50%, which makes the outcome of the calculations unreliable. This is the reason why these boxes in figure 4.1 have large question marks as well as a check mark.

CFD calculations are expensive, time consuming and Jumbo Maritime does not have CFD software in-house. In the design process of the Fairplayer Van Oossanen performed a CFD calculation with the software FINE/MARINE to calculate the resistance of the vessel [30]. This calculation can be used in the comparison with the RAPID calculation and the Holtrop-Mennen method. In this research it is not feasible to perform CFD calculations with a number of different concepts of the Fairplayer with a sponson.

The calculations with RAPID are quicker to perform than CFD calculations and are therefore preferred to use to calculate a large amount of concepts. The version available for this research could only perform symmetric calculations and can therefore only be used to calculate the Fairplayer with two sponsons. As described in paragraph 2.6 the potential flow theory program RAPID only calculates the wave-making resistance. For the frictional resistance only a rough estimation is given, based on the ITTC-1957 flat plate friction formula and a standard form factor. This frictional resistance is therefore not adequate and a better estimation of the form factor needs to be done.

All three methods described cannot give a (reliable) result of the increased resistance of a sponson on the Fairplayer. Therefore a method is set up in this research to combine the Holtrop-Mennen method and the RAPID calculation into one. It is chosen to use the results of the RAPID calculations to give an estimation of the increase in wave-making resistance and use the Holtrop-Mennen method for the frictional resistance. A five step plan is set up to give a first estimation of the influence of the Fairplayer with a sponson, which is described in paragraph 4.3.

4.1.1. Comparison between Holtrop-Mennen, CFD and RAPID

The results of the calculations with RAPID, CFD and Holtrop-Mennen all have a different background and to investigate if the calculations are all within a certain range, the results are compared. The Fairplayer without a sponson is the only one which can be compared, as can be seen in figure 4.1.

The computational fluid dynamics (CFD) calculation is done by Van Oossanen [30]. The CFD calculations are done with a full scale model of the hull with appendages, such as the rudders. The solver uses the (Unsteady) Reynolds Averaged Navier-Stokes (U)RANS equations to describe the flow. The resistance from the

CFD calculation is divided into a viscous resistance and a pressure resistance. The roughness effects, which contains imperfections of and marine growth on the hull, is also a separate factor.

The results of the calculation of the Fairplayer on a draft of 6.5 meter with the Holtrop-Mennen method can be found in table 4.1. The calculation can be found in appendix C.1. As described in paragraph 2.4 the total resistance is split into six different components. The source of the six resistance components is different, but the resistance components are grouped in order to compare the results with CFD and RAPID. The frictional resistance and the appendage resistance are both of viscous origin. The wave-making resistance, bulbous bow resistance and resistance of the immersed transom all contribute to the total wave-making resistance. The model-ship correlation resistance is the same as the roughness correction, because it is a correction factor to apply for the difference in roughness of the model ship and full scale ship. The combined resistance as calculated with the Holtrop-Mennen method can be found in table 4.2.

Table 4.1: The Holtrop-Mennen resistance calculation of the Fairplayer at a draft of 6.5 meter.

Holtrop-Mennen method		[kN]
Frictional resistance	R_v	336.7
Appendage resistance	R_{app}	22.1
Wave-making resistance	R_w	197.9
Bulbous bow resistance	R_b	70.8
Additional resistance of the immersed transom	R_{tr}	0.0
Model-ship correlation resistance	R_a	81.2
Total resistance	R	708.6

The calculation done with RAPID calculates the wave-making resistance, based on inviscid flow theory. The friction resistance is obtained from the ITTC-57 flat plate friction line with a standard form factor of 1.2, which is not a quite accurate form factor. The calculation with RAPID correct for the model-ship correlation.

The results of the CFD, RAPID and the Holtrop-Mennen calculation can be found in table 4.2. All calculations are performed with a model of the Fairplayer without sponson at a draft of 6.5 meter and a speed of 17 knots.

Table 4.2: Results of the CFD calculation, the RAPID calculation and the Holtrop-Mennen method.

Resistance component		CFD calculation	RAPID calculation	Holtrop-Mennen method
Viscous resistance [kN]	R_v	301.4	262.2	358.8
Wave-making resistance [kN]	R_w	289.4	225.4	268.7
Roughness correction [kN]	R_r	71.1	-	81.2
Total resistance [kN]	R_t	661.8	487.6	708.6

The percentage difference of the three calculation methods can be found in table 4.3. The CFD calculation is taken as the base case in the comparison.

Table 4.3: The total resistance of the three methods.

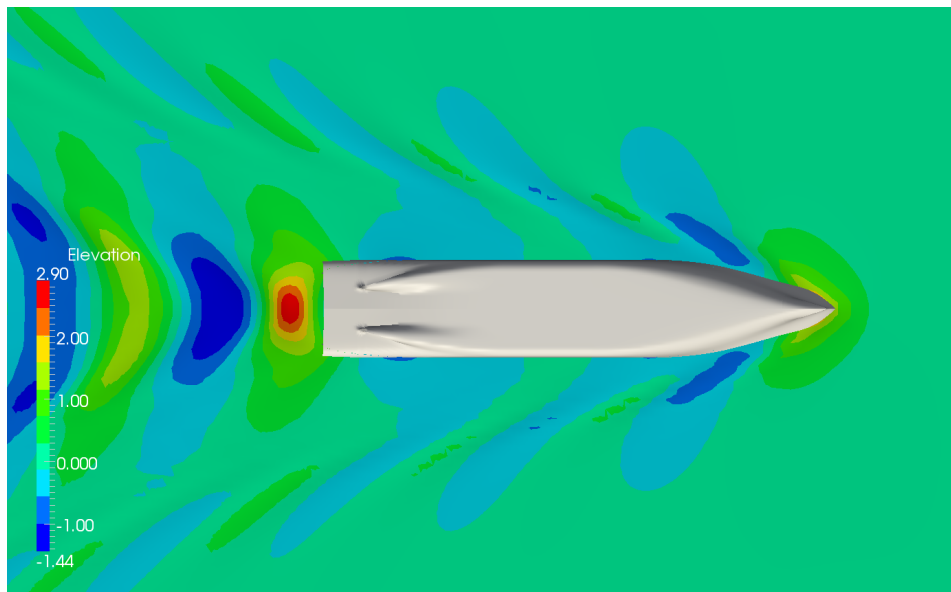
	Total resistance [kN]	Difference [%]
CFD calculation	661.8	-
RAPID calculation	487.6	-26.3
Holtrop-Mennen calculation	708.6	7.1

The difference between the CFD and Holtrop-Mennen method does not differ much. The total resistance of the two methods only differs 7%, which makes it a reasonable assumption to use the Holtrop-Mennen method as a starting point of adjusted Holtrop-Mennen method.

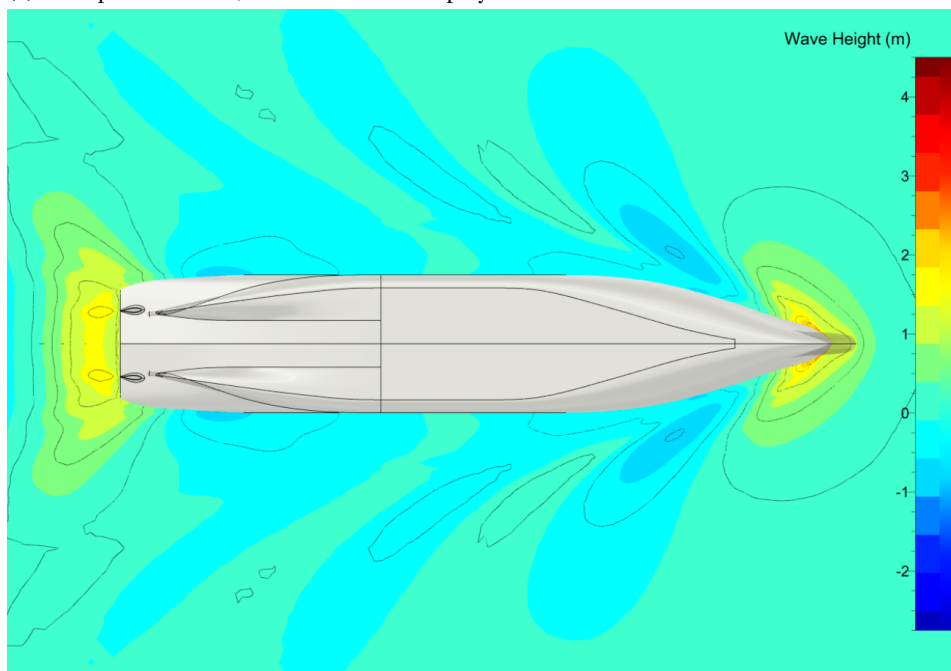
The difference between the CFD and RAPID calculation is 26.3%, which is significant. The difference can be explained by three factors. The first one is underprediction of the friction resistance in RAPID. The assumption to calculate the resistance of the vessel in RAPID without appendages leads to a lower frictional resistance. The standard form factor taken in RAPID is also lower than the actual form factor, which also leads to a lower frictional resistance. The second factor that explains the difference between the calculations

is the fact that resistance in RAPID is not done with an actuator disk. The actuator disk is a method to model a propeller and leads to an increase of velocity of the flow at the position of the propeller. This increase in velocity results in a lower pressure at the aft of the vessel, so the integrated pressure over the hull in longitudinal direction (as calculated in equation 2.27) will increase. The CFD calculations done at Van Oossanen [30] are done with and without actuator disk. The calculation with an actuator disk results in an increase of the resistance with about 100 kN. The third factor is the roughness correction, which is not taken into account in the RAPID calculation. This factor is about 75 kN, as can be seen in table 4.2. These three factors result in an underestimation of the resistance with RAPID of about 175 kN, which is about the difference with the other two calculation methods as can be seen in table 4.3.

The wave pattern from the CFD calculation and the calculation with RAPID are compared and can be seen in figure 4.2b and 4.2a. The shape of the wave pattern of the two calculation methods is comparable and also the sinkage and trim are similar. The maximum wave height at the stern in the RAPID calculation is around the 3.0 meter and with the CFD calculation around the 1.8 meter. This can be explained by the non-viscous potential flow, which is used in the RAPID calculation. The non-viscous effects in the RAPID result in a wave system behind the stern that is overestimated. This can be explained by the fact that the flow in the aft of the vessel is mainly dominated by viscous effects, such as separation of and vorticity in the flow. These viscous effects result in a decrease of the energy in the wave pattern and therefore lower wave heights.



(a) Wave pattern of the J-class vessel the Fairplayer calculated with RAPID.



(b) Wave pattern of the J-class vessel the Fairplayer calculated with CFD by Van Oossanen.

Figure 4.2: Comparison of the wave pattern from the CFD and RAPID calculation ($T = 6.5$ meter).

4.2. Input options in RAPID

The main calculation is described in appendix D.3, but there are input options within RAPID that need to be further explained. In RAPID it is possible to place panels behind the transom to calculate the transom flow, but there are limitations to this option. It is also possible to perform an asymmetrical hull calculation. The amount of panels on the surfaces need to be determined to give an appropriate result. These three options are explained in this paragraph.

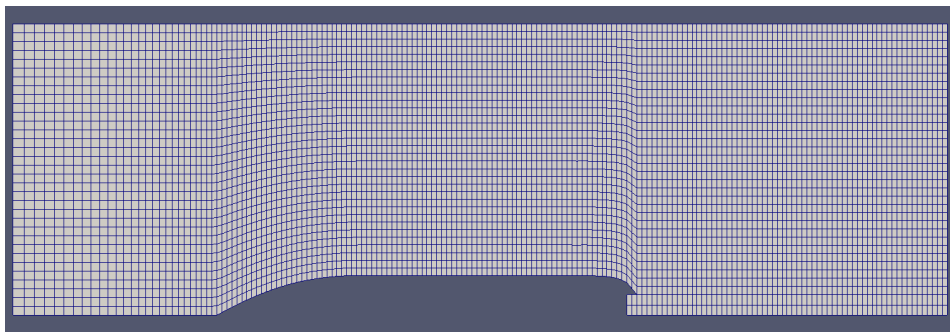
4.2.1. Calculation of the transom flow

The flow behind the transom contains viscous effects, which are not included in RAPID. The flow can be calculated with a non-viscous flow when the hull comes together in one point or when the transom is cleared.

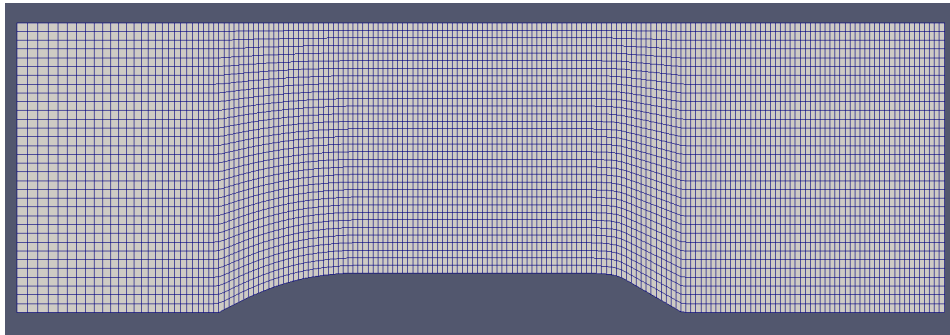
In this case panels are placed behind the transom to calculate this flow. In the case that the transom is not cleared and a dead-water region is present behind the transom, a potential flow solution does not exist anymore. The calculations should be done with the non-transom mode of RAPID, which leaves a triangular gap in the free surface behind the transom. Whether or not the calculations should be dealt with as transom flow depends both on hull form and on speed. This is done with the transom depth Froude number as calculated with equation 4.1 [20].

$$Fn_{tr} = \frac{V}{\sqrt{-g \cdot \eta_{tr}}} \quad (4.1)$$

where η_{tr} is the depth of the transom, taking into account the dynamic trim and sinkage. This Froude number gives an indication of the calculation of the transom flow. If this Froude number is above 5, it is most likely that the transom will be cleared and the transom flow calculation is appropriate and accurate. It is probable that some amount of dead water will be behind the transom if this Froude number is between the 2.2 and 4. In this case it is expected that the stern wave system is significantly overestimated. This is not a problem if the analysis is used as a comparison between different concepts instead of obtaining absolute resistance values. In case of the transom Froude number below 2.2, the calculations can better be done in the non-transom mode of RAPID. Otherwise the calculation rarely gives a converged result, because the potential flow solution does not exist anymore. The non-transom calculation leaves a triangular gap in the free-surface panelling, which can be seen in figure 4.3b. An example of the free surface with panels on the transom and the free surface without a transom can be found in figure 4.3.



(a) Free surface with panels behind the transom.



(b) Free surface without panels behind the transom.

Figure 4.3: Different configurations of the free surface.

The Froude number of the transom can be plotted against the submerged depth of the transom. This is done in figure 4.4 at a speed of 17 knots. As can be seen from the figure, the Froude number is higher than 5 only if the submerged depth is lower than 0.35 meter. The Froude number is lower than 2.2 if the submerged depth is more than 1.8 meter.

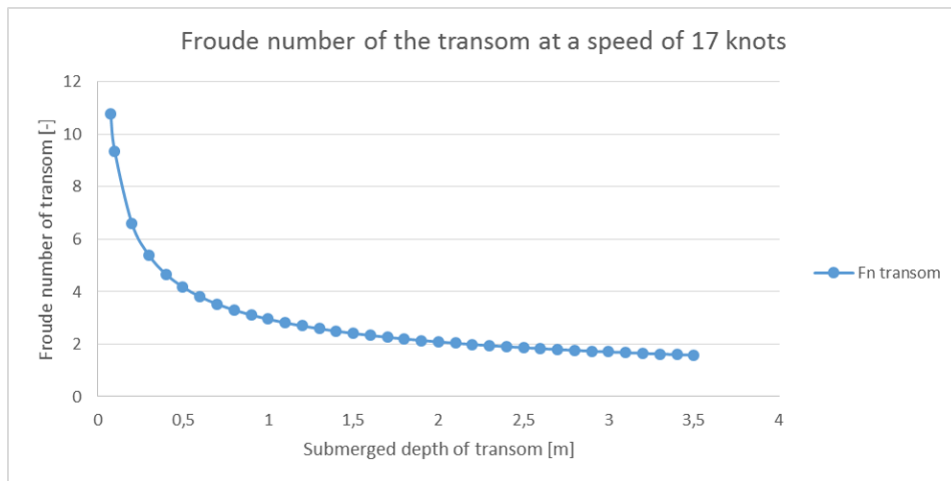
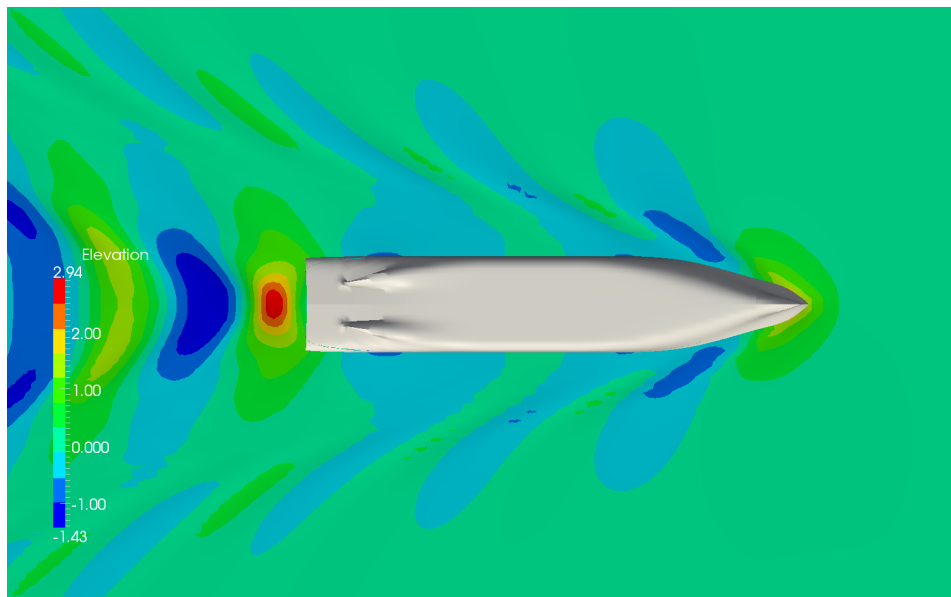


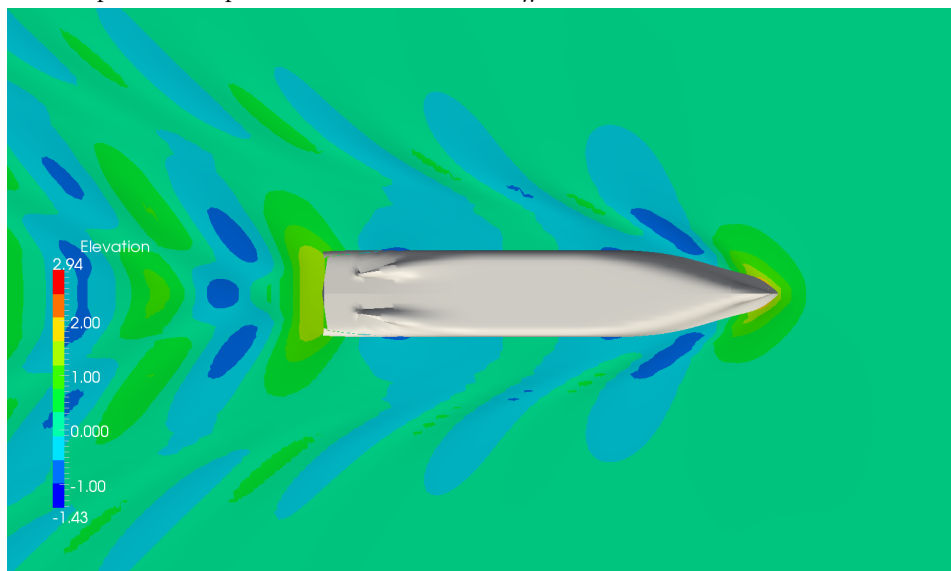
Figure 4.4: Froude number of the transom at a speed of 17 knots.

For the Fairplayer at a draft of 6.5 meter the depth of the transom is about 0.2 meter, when taking into account the dynamic trim and sinkage. If the draft is increased to 7.5 meter, the depth of the transom is 1.2 meter. This means that the calculations with panels on the transom can be only be done at a draft of 6.5 meter and not at the draft of 7.5 meter.

A significant difference in outcome can be seen, when calculating the Fairplayer at a draft of 6.5 meter with and without panels on the transom. The wave making resistance of the two cases are 104 kN and 225 kN for the case without panels on the transom and with panels on the transom respectively. This difference can also be found in the wave pattern of both calculations, as can be seen in figure 4.5. The main difference in the two cases is the wave pattern behind the transom. In the case with panels behind the transom, the wave height is more than one meter higher. A higher wave system results in a higher wave-making resistance, as explained in paragraph 2.5.2.



(a) Wave pattern with panels behind the transom ($R_W = 225$ kN).



(b) Wave pattern without panels behind the transom ($R_W = 104$ kN).

Figure 4.5: Wave pattern comparison for panels behind the transom.

The calculations at a draft of 7.5 meter cannot be done with panels at the transom, because it is expected that there is a dead-water region behind the transom. The results from RAPID without panels on the transom are lower than the calculation with panels on the transom. This makes the difference for the wave-making resistance between RAPID and the other two methods described in paragraph 4.1.1 even larger. The absolute value for the wave-making resistance is therefore not taken into account. Only the relative increase of wave-making resistance is used in the adjusted Holtrop-Mennen method. If there is a dead-water region behind the transom, the R_{w1} value (which is the integrated pressure over the hull) cannot be calculated and only the R_{w3} value can be used.

4.2.2. Asymmetrical calculation

In RAPID it is possible to perform an asymmetrical calculation. For this, the panel file (.pan) need to contain the information of both halves of the vessel. When importing the panel file in the version used in this research, the displacement is given as a negative value. This indicates an error in the part of the code where the normal direction of the panels are defined. The calculation can be done with an asymmetric hull, but has two large

issues. The computational time is twice the time of a symmetric calculation and the wave pattern that is created looks unrealistic as can be seen in figure 4.6. At the starboard side of the vessel, the wave surface will intersect the hull and will be placed inside the vessel. For these reasons it is chosen not to use the asymmetric calculations in RAPID.

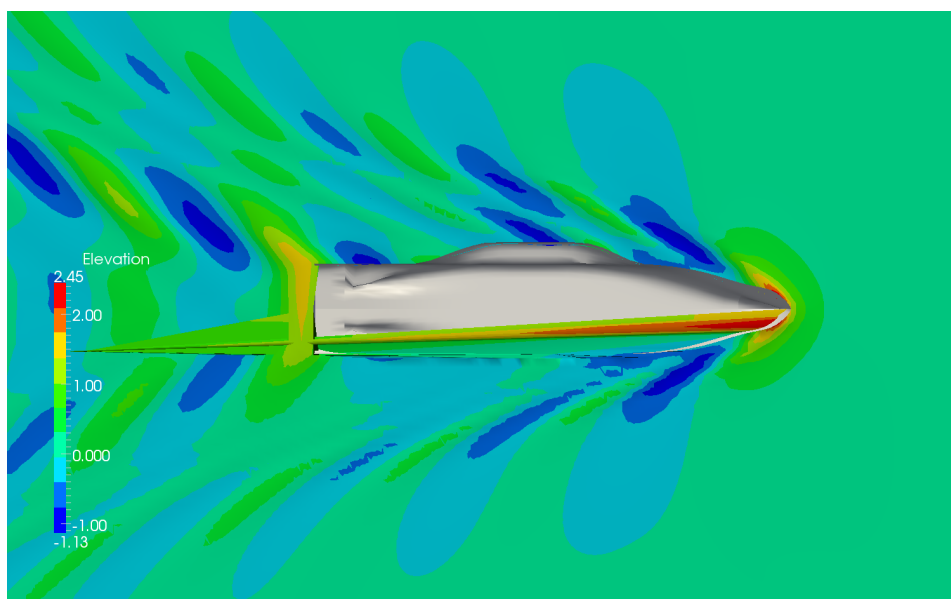


Figure 4.6: Wave pattern of a calculation with an asymmetric hull in RAPID.

4.2.3. Grid study

In paragraph 2.6 it is explained that the input in RAPID are panels which are placed on the hull and the wave surface. It is known that the amount and size of the panels on the surfaces has a significant influence on the output of the RAPID calculation. A coarse grid on the hull decreases the computational time, but gives a less accurate outcome. A fine grid on the other hand results in a unnecessarily long computation time, so a trade-off need to be found. This is found by performing a grid study, which is a systematic increase of the amount of panels on the hull as well as on the free surface. In order to see if the coarseness of the grid needs to be changed if the hull significantly changes, the grid study is carried out with the base hull of the Fairplayer and with the Fairplayer with a sponson.

Grid study of the Fairplayer

The grid study on the base hull of the Fairplayer is performed at a draft of 6.5 meter. During this study the aspect-ratio of the panels is kept constant as well as the size of panels over the hull. In table 4.4 the amount of panels in the eight cases can be seen.

Table 4.4: Amount of panels on the hull surface in the grid study.

Case:	Amount of row x columns	Amount of panels
1	6x36	216
2	9x54	486
3	12x72	864
4	18x108	1944
5	24x144	3456
6	30x180	5400
7	36x216	7776
8	48x288	13824

The results of the grid study can be seen in figure 4.7. In this figure the two different resistance (R_{w1} and R_{w3}) values are plotted. In paragraph 2.6 the different methods of calculating the R_{w1} and R_{w3} value are explained. One thing that can be seen immediately is the big differences in the R_{w1} values. The resistance

value fluctuates a lot when the amount of panels changes, which can be explained by the orientation of the panels on the hull. When the grid is coarse, the panels cannot follow the curvature of the hull exactly, which results in panels that have a different orientation than the hull surface. By integrating the pressure over these panels, taking into account the orientation, the result could differ much. On the other hand the resistance values of R_{w3} only change a bit when the amount of panels is relatively low.

It can be concluded that the R_{w3} value is less sensitive for variations in the amount of panels on the hull and from about 2000 panels the resistance is constant. The computation time increases, therefore it is chosen to work with the hull grid in case 5 (which corresponds to 3456 panels) to investigate the influence of the amount of panels on the wave surface.

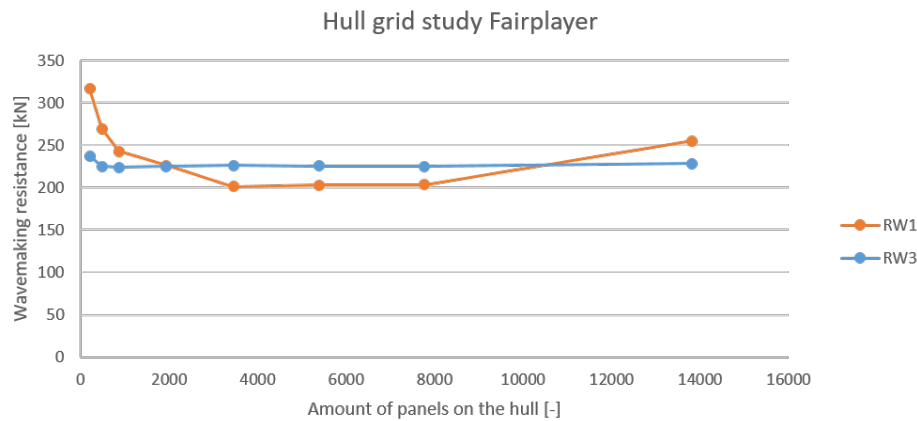


Figure 4.7: Hull surface grid study of the Fairplayer.

A similar study can be performed with the amount of panels on the free surface. The amount of panels on the free surface can be changed by changing the amount of panels in one wavelength. The grid study to the influence of the amount of free surface panels on the outcome of the calculation can be seen in figure 4.8.

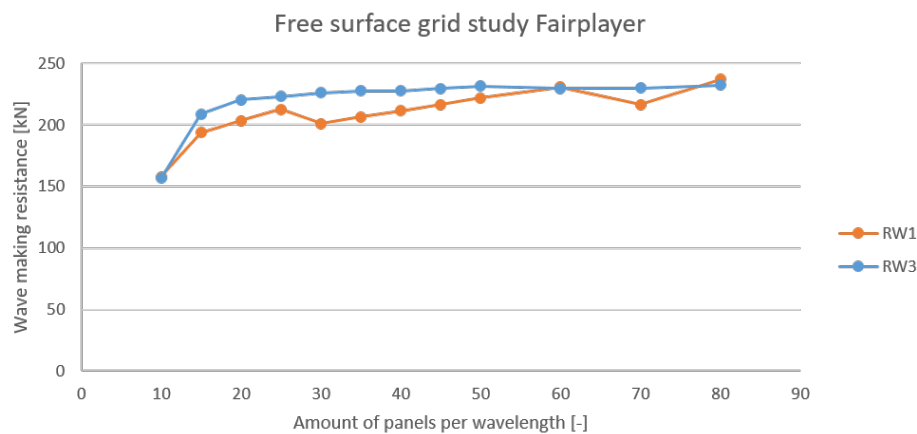


Figure 4.8: Free surface grid study of the Fairplayer.

The default amount of panels per wavelength from RAPID is set to 30. The analysis starts at a lower number of panels. The first thing that can be noticed is that the R_{w3} value converges faster to the final result. Also can be seen that the R_{w3} value is less sensitive for small changes in panel size. Also during the calculations done with the variation of the amount of panels per wavelength it was found that the calculation time increases significantly when the amount of panels increases. So the default value of 30 panels per wavelength is the minimum value that should be taken.

Grid study of the Fairplayer with a sponson

The grid study for the Fairplayer with a sponson is performed in the same way. Because the draft is increased to 7.5 meter, the transom flow cannot be calculated as accurate due to an amount of dead water behind the transom as described in paragraph 4.2.1. The calculations are done with the same amount of panels on the hull as described in table 4.4 and the results can be found in figure 4.9. The amount of panels on the free surface is also performed in a similar way and can be found in figure 4.10. From this grid study it can be concluded that the convergence is reached with a finer grid. This is a result of the more curved hull due to the sponson. The amount of panels at the hull should be at least 7776, as in case 7 of table 4.4 and the amount of panels at the free surface should be at least 45 per wavelength to exclude the influence from the panels on the result.

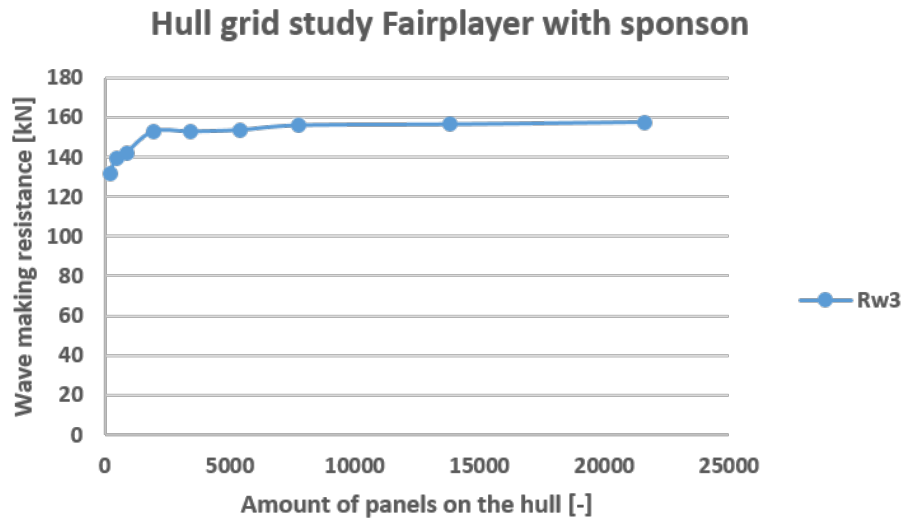


Figure 4.9: Hull surface grid study of the Fairplayer with a sponson.

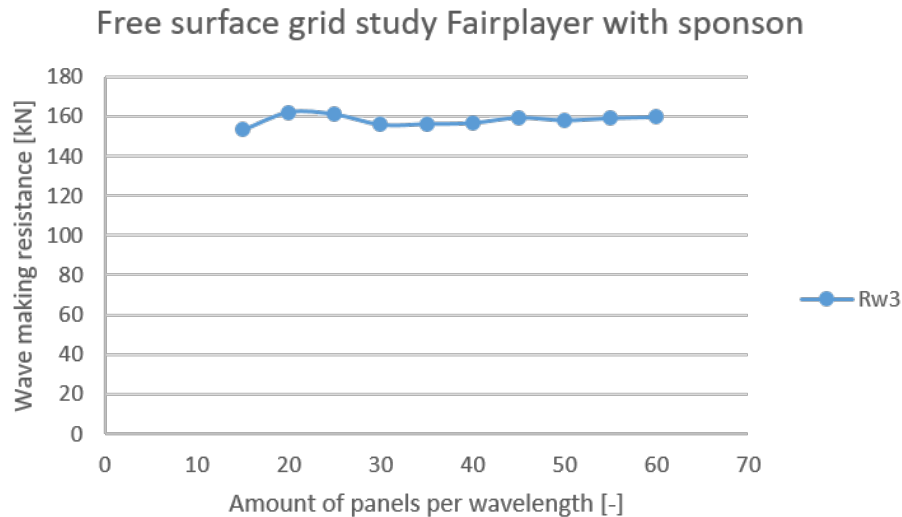


Figure 4.10: Free surface grid study of the Fairplayer with a sponson.

4.3. Adjusted Holtrop-Mennen method for the resistance calculation

In order to find the influence of a sponson on the resistance of the vessel, an adjusted Holtrop-Mennen method is developed in this research. This method is a result from the analysis of the different calculation methods as described in paragraph 4.1 and is a combination of the Holtrop-Mennen resistance prediction method and the potential flow theory program RAPID. The starting point of this method is the Holtrop-Mennen resistance calculation of current J-Class vessel Fairplayer.

The method that is followed can be explained in five steps:

1. Holtrop-Mennen method to find the resistance of the Fairplayer.
2. Calculate the wave-making resistance of the concept of the Fairplayer with a sponson.
3. Calculate the frictional resistance and the form factor ($1 + k$) of the Fairplayer with a sponson.
4. Calculate the other resistance components of the Fairplayer with a sponson.
5. Express the total resistance of the Fairplayer with a sponson as a percentage of the current Fairplayer.

Step 1: Holtrop-Mennen method to find the resistance of the Fairplayer

The resistance of the J-Class vessel Fairplayer can be calculated with the Holtrop-Mennen method as described in paragraph 2.4. The analysis is done at a draft of 7.5 meter and can be found in table 4.5. This resistance calculation is done with the current design of the Fairplayer and is used as starting point for the analysis of the Fairplayer with a sponson.

Table 4.5: The Holtrop-Mennen resistance calculation of the Fairplayer at a draft of 7.5 meter.

Holtrop-Mennen method		[kN]	Percentage of total [%]
Frictional resistance	R_v	366.8	48.5
Appendage resistance	R_{app}	22.1	2.9
Wave-making resistance	R_w	262.4	34.7
Bulbous bow resistance	R_b	18.8	2.5
Additional resistance of the immersed transom	R_{tr}	0.0	0.0
Model-ship correlation resistance	R_a	87.0	11.5
Total resistance	R	757.2	100.0

The resistance calculation at a draft of 7.5 meter from table 4.5 can be compared with the calculations at a draft of 6.5 meter in table 4.1 to see how the individual components change due to the change in draft. The frictional resistance of the vessel is increased, due to the increase of the wetted surface. The appendage resistance remains the same, because the appendages are the same and no appendages are added or deleted. The wave-making resistance increases significantly, because of the larger draft and therefore larger displacement of the vessel. The bulbous bow resistance is decreased significantly, due to the larger draft of the vessel. The larger submersion of the bulbous bow results in a smaller pressure disturbance at the free surface. The additional resistance due to the immersed transom is in both situations zero. The last resistance component is the correlation between the model and ship, which is mainly dependent on the wetted surface of the vessel, which also explains the increase in the resistance at the draft of 7.5 meter. The total resistance is increased as can be seen in table 4.5.

Step 2: Calculate the wave-making resistance of the concept of the Fairplayer with a sponson

The total wave-making resistance of the Fairplayer with a sponson cannot simply be calculated with the formulas stated by Holtrop-Mennen, due to the difference in the hull shape compared to conventional hull shapes as described in paragraph 4.1. The total wave-making resistance in the Holtrop-Mennen method is split up into three components: the wave-making resistance, the bulbous bow resistance and the resistance due to the immersed transom. The wave-making resistance calculated with the potential flow theory program RAPID is a combination of these three components. The increase of the wave-making resistance is calculated as a percentage of the wave-making resistance of the vessel without sponson. This is due to the limitations of the program for vessels with a dead-water region behind the transom as explained in paragraph 4.2.1. This

results in a significant lower absolute resistance value and only comparisons between the concepts can be made [20]. The basic hull of the Fairplayer without sponson, propeller and rudders is analysed on the wave-making resistance. This wave-making resistance is 83.8 kN. The wave pattern can be found in figure 4.11. Due to the version of RAPID, the calculations cannot be done with an asymmetric hull shape, so it need to be calculated with a symmetric vessel with sponsons on both sides of the vessel as described in paragraph 4.2.2. The results of the symmetrical calculation need to be corrected to estimate the wave-making resistance of the asymmetrical vessel, which is explained in step 5.

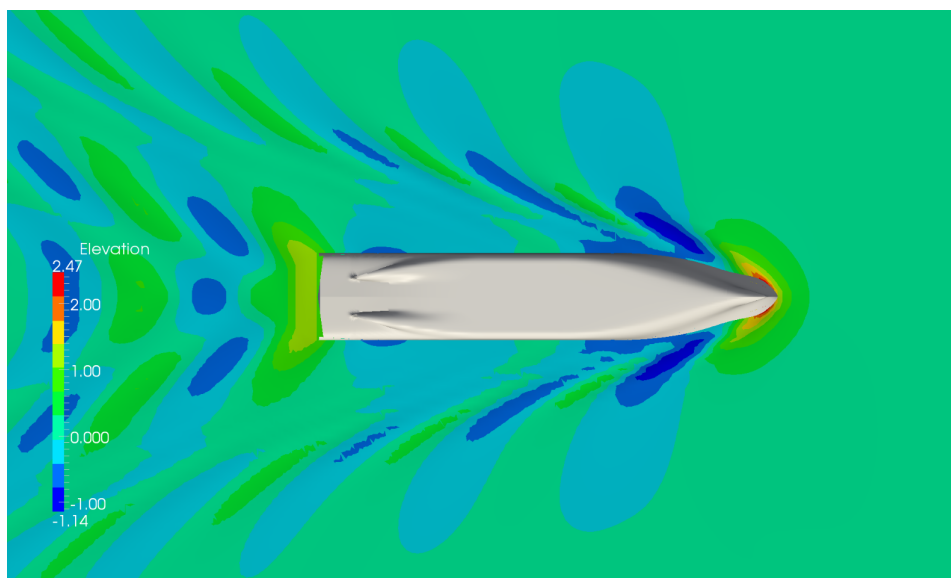


Figure 4.11: The wave pattern of the Fairplayer at a draft of 7.5 meter.

Step 3: Calculate the frictional resistance and the form factor $(1 + k)$ of the Fairplayer with a sponson

The frictional resistance of the Fairplayer with a sponson cannot be calculated in RAPID, because RAPID uses a non-viscous flow to calculate the flow lines. In order to find the total influence of a sponson also the viscous resistance need to be taken into account. This is calculated with equation 2.7. The addition of a sponson results in a change of two different components in the formula. Namely the wetted surface and the form factor $(1 + k)$. The change in wetted surface comes from the 3D model, but the form factor need to be calculated.

The form factor represents the ratio of the frictional resistance and the resistance of the equivalent flat plate [17]. It incorporates the effect from the form on the frictional resistance. This form effect results in an increased flow speed along the hull and the change in boundary layer at the aft results in a decrease of the pressure in the aftship. The most used flat plate friction formula is the ITTC-57 formula [17], which is also described in equation 2.8. There are multiple ways of determining the form factor, the two main ways are empirical formulas or model testing. In model tests the form factor can be determined, by running the model at low speed (e.g. $Fn < 0.15$), because the wave resistance is then negligible. This method is not applicable in this research, because no model tests are performed. The second method is the use of empirical formulas. There are two formulas which are commonly used, namely the formula of Watanabe as can be seen in equation 4.2 [17] and the formula by Holtrop-Mennen as can be found in equation 2.9.

$$k = -0.095 + 25.6 \cdot \frac{C_B}{\left(\frac{L^2}{B}\right) \cdot \sqrt{\frac{B}{T}}} \quad (4.2)$$

Both of these two formulas can only be used in combination with the ITTC-57 formula, because the empirical formula is also based on this flat plate friction line. The formula from Watanabe and Holtrop-Mennen are both dependent on the main dimensions of the underwater part of the vessel. The shape of the vessel

is not a conventional hull shape, due to the sponson, which can be seen in figure 4.12. The $\frac{L}{B}$ ratio of the concepts with a sponson is in the order of 3.5, which does not make it plausible that the method of Holtrop-Mennen can be used, given the range in figure 2.5. The formula from Watanabe is dependent on the block coefficient, which is in the order of 0.5 to 0.55 for the concepts with a sponson. Block coefficients in this range are fast vessels, such as frigates. The Fairplayer with a sponson is therefore not suitable to use the formula from Watanabe.

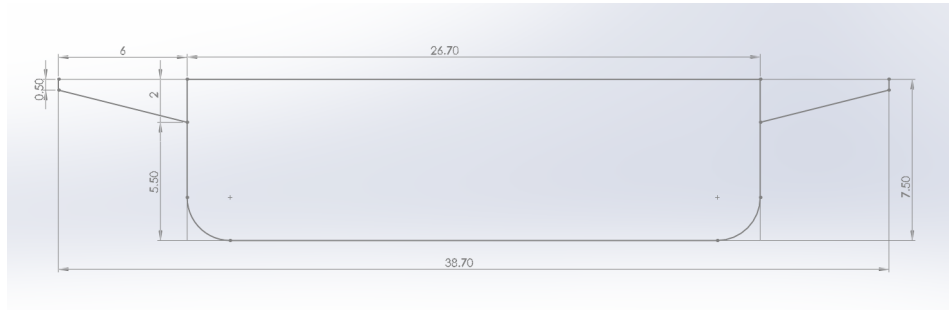


Figure 4.12: The underwater ship of the symmetric Fairplayer with sponsons.

In order to give a first estimation of the form factor, an assumption is made. The sponsons are rotated 90 degrees as can be seen in figure 4.13. The sponsons are rotated in such way that the wetted surface is equal, causing the draft to increase. The vessel will now have a V-shaped hull, which gets closer to the conventional hull shapes. The form factor is calculated both with the method of Watanabe as well as with the Holtrop-Mennen method. With the method of Watanabe, the form factor from the concepts was more spread than when the method of Holtrop-Mennen was used. With the method of Watanabe, the form factor varied between the 1.4 and 1.5, whereas with the Holtrop-Mennen method this was between 1.34 and 1.37.

In literature the form factor is often linked to the block coefficient of the vessel. The form factor $(1 + k)$ increases when the block coefficient increases from 1.11 at a C_b of 0.55 until 1.35 at a C_b of 0.88 [28]. In [13] the same relation was found. The form factor calculated with the method of Holtrop-Mennen is more in the range which are seen in literature. The form factor are less spread with this method, which is more likely, because the shape of the sponson in the different concepts does not change significantly. It is therefore chosen to use the method of Holtrop-Mennen in this analysis.

The form factor for the concepts of the Fairplayer with sponson are in the range of 1.34 to 1.37 and the form factor for the Fairplayer, calculated with equation 2.9, is 1.29. This means that the concept with two sponsons gives an increase of about 6% on the form factor and therefore on the frictional resistance. This need to be corrected to go to one sponson, which means that influence of form factor of one sponson leads to an increase of about 3% of the frictional resistance. The frictional resistance is about 50% of the total resistance, as can be seen in table 4.5, so the effect of the increased form factor on the total resistance is about 1.5%.

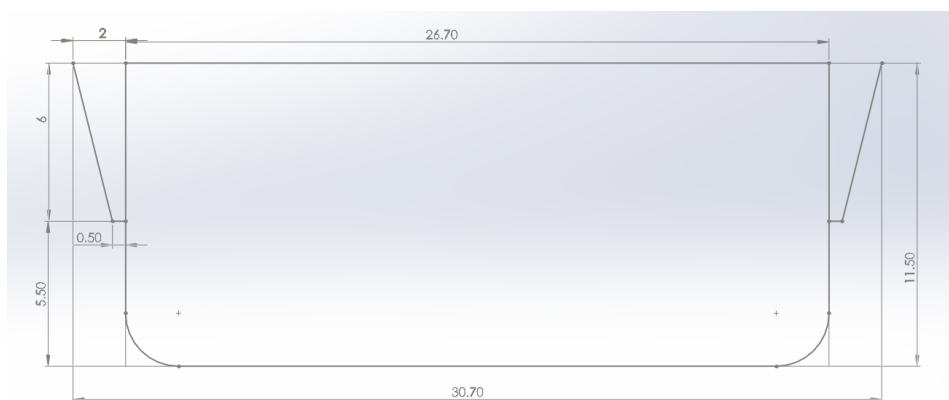


Figure 4.13: The underwater ship of the adjusted hull with sponsons.

The method that is used to calculate the form factor is only a first estimation in the concept phase of the design process. If one or two concepts are chosen, the form factor should be determined more accurate with a model test.

Step 4: Calculate the other resistance components of the Fairplayer with a sponson

In step 2 and 3 the influence of the sponson on the total wave-making and frictional resistance are explained respectively. The method of Holtrop-Mennen makes a subdivision in more components as can be seen in table 4.5 and equation 2.6. The appendage resistance does not change, because the appendages of the vessel will not change and no appendages are added or removed when applying a sponson.

The model-ship correlation resistance changes, because of the change in wetted surface of the vessel, as can be seen in equation 2.15. The model-ship correlation resistance is calculated with the wetted surface of the concept with one sponson.

Step 5: Express the total resistance of the Fairplayer with a sponson as a percentage of the current Fairplayer.

In the previous steps the different resistance components of the Fairplayer with a sponson are calculated. In order to combine these resistance components, some of the components need to be corrected.

The wave-making resistance is calculated as an increase in percentage compared to the base hull as described in step 2. This percentage is the increase of a vessel with a sponson at both sides of the vessel and therefore need to be converted to a vessel with a sponson at one side. This is done by dividing the percentage by two. With this assumption the interaction of the wave pattern at the two sides of the vessel is neglected. The line of symmetry is far away from the sponson and therefore it is assumed that the interference of the sponson on the line of symmetry is reduced to a minimum. The frictional resistance is calculated with a symmetric vessel with two sponsons. The frictional resistance needs to be divided by two to get the resistance of the side with a sponson. The frictional resistance of the base hull is calculated in step 1 and half of this needs to be added to the frictional resistance of the vessel with a sponson. This results in the sum of the half frictional resistance of the bare hull and half of the frictional resistance of the symmetric hull with two sponsons. As described in step 4, the appendage resistance and the model-ship correlation resistance can be replaced without further assumptions. The total resistance of the concepts of the Fairplayer with a sponson is written as a percentage of the Fairplayer as calculated in step 1.

5

Results of the adjusted Holtrop-Mennen method

The adjusted Holtrop-Mennen method uses the five step plan for the calculation of the resistance as described in paragraph 4.3. This method is used to see the influence of a sponson on the resistance of the Fairplayer.

There are three variations in main dimensions done, which are explained in paragraph 5.1. The outcome of this concept variation is shown and discussed in paragraph 5.2. In paragraph 5.3 the conclusions from this concept variation will be drawn and discussed. Also the final design is shown. In paragraph 5.4 the decrease in maximum speed of the Fairplayer with a sponson is calculated.

5.1. Systematic concept variation

The influence of the main dimensions of the sponson on the resistance is systematically examined. There are three different dimensions that are varied. These three are: the longitudinal position of the sponson, the length over width $\left(\frac{L}{B}\right)$ ratio and the vertical position of the sponson.

For each of these three variables, five different designs are made so influence of one design variable on the total resistance can be determined. In table 5.1 the main dimensions of the 15 concepts are given. The sponson can be described by using six dimensions: the length of the sponson, the width of the sponson, the vertical starting point of the sponson, the height of the vertical transition, the length of the longitudinal transition and the longitudinal starting point. These six dimensions are shown in figure 5.1.

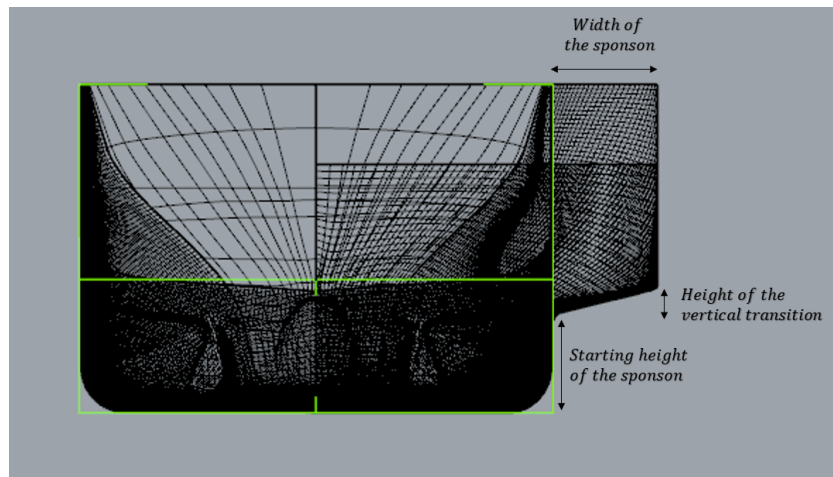
The three variables that are systematically varied, are labelled with an a, b or c as can be found below:

a = The longitudinal starting position of the sponson.

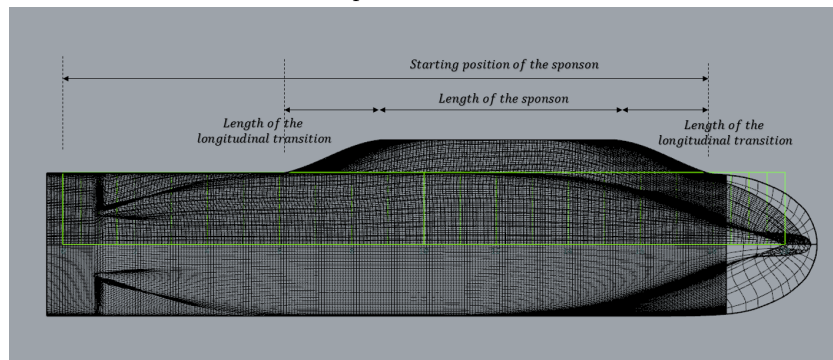
b = The length over width ratio of the sponson.

c = The vertical starting position of the sponson.

The number in table 5.1 distinguishes the different concepts, which can be compared to each other to see the influence of the variable on the resistance.



(a) Front view of the vessel with a sponson.



(b) Top view of the vessel with a sponson.

Figure 5.1: Definitions of the six variables which define the dimensions of the sponson.

Table 5.1: Main variables of the fifteen concepts of the sponson.

Variation concept	Length of the sponson [m]	Width of the sponson [m]	Vertical starting point [m]	Longitudinal starting point [m]	Height of the vertical transition [m]	Length of the longitudinal transition [m]
a1	43	6	5.5	120	1.5	18
a2	43	6	5.5	110	1.5	18
a3	43	6	5.5	100	1.5	18
a4	43	6	5.5	90	1.5	18
a5	43	6	5.5	80	1.5	18
b1	30	7	5.3	100	1.8	21
b2	40	6.2	5.5	100	1.6	18.6
b3	50	5.5	5.6	100	1.4	16.5
b4	60	5	5.8	100	1.3	15
b5	70	4.6	5.9	100	1.2	13.8
c1	55	5.3	5.5	110	1.3	15.9
c2	55	5.4	4.5	110	1.4	16.2
c3	55	5.5	3.5	110	1.4	16.5
c4	55	5.7	2.5	110	1.4	17.1
c5	55	5.9	1.5	110	1.5	17.7

In appendix E the 15 different concepts can be found. Each of these concepts is visualised from the side, top, front and in a perspective view. Also the wave pattern for each of the concepts can be found in appendix E.

The contours of the different sponsons are all the same to reduce the influence of the contour on the result. The transition at the front and aft of the sponson have the same angle for all concepts, the same counts for the vertical transition. The concepts are all designed to have enough static stability at a draft of 8.5 meter to perform a lift operation of 1800 ton. The concepts are all analysed at a draft of 7.5 meter. The amount of panels are chosen on the basis of the grid study performed in paragraph 4.2.3. The amount of panels is 7776 (36 x 216) panels on one side of the hull and 45 panels per wavelength on the free water surface.

5.2. Results of the adjusted Holtrop-Mennen method

The five step plan for the resistance calculation is done as described in paragraph 4.3. The results are divided into three different components: the frictional resistance, the wave-making resistance and the model-ship correlation resistance. The frictional resistance contains the components of the Holtrop-Mennen method which have a viscous origin, namely the frictional resistance and the appendage resistance. The wave-making resistance contains all components which have an influence on the wave-making resistance, namely the wave-making resistance, the bulbous bow resistance and the resistance due to the immersion of the transom. The percentage increase of the individual components can be found in table E.1 and are also discussed in this paragraph. Since there are three variables that are systematically varied, these three are also analysed separately.

The longitudinal starting position of the sponson

The influence of the longitudinal starting position of the sponson is analysed with five different concepts. The starting position of concept a1 is the most to the bow and consecutive concepts are each ten meter more to the back.

The increase of the individual resistance components compared with the base case as described in paragraph 4.3 can be found in figure 5.2. As can be seen, the frictional resistance and the model-ship correlation resistance are almost equal to all five concepts. The only component that varied significantly is the wave-making resistance. From this it can be concluded that the position of the sponson in the longitudinal direction has a significant influence on the total resistance of the Fairplayer with a sponson.

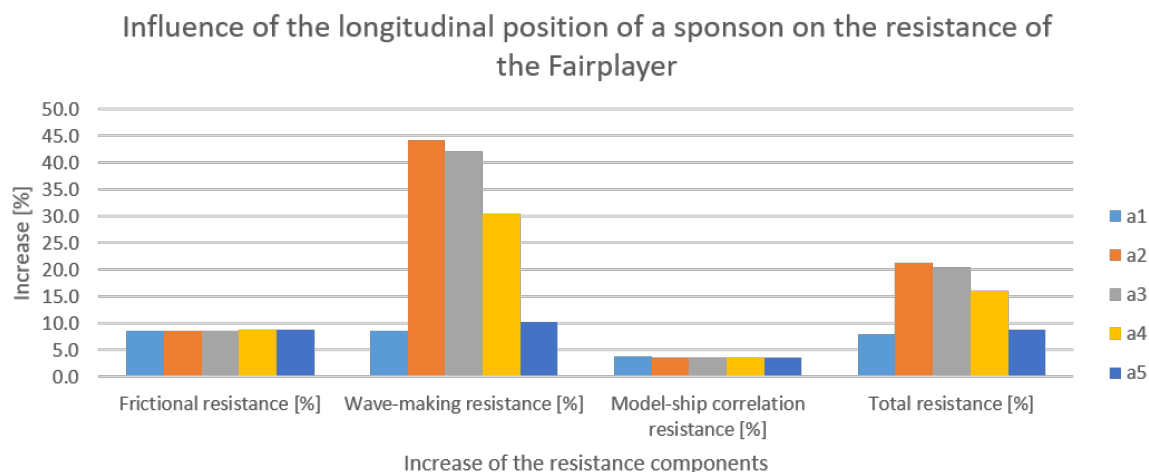


Figure 5.2: Increase of the individual resistance components w.r.t. the Fairplayer, when the longitudinal position of the sponson is varied.

As can be seen in figure 5.2, the longitudinal position has a significant influence on the wave-making resistance, which can be explained with the wave pattern of the different concepts. The sponson creates wave systems which interacts with the wave systems from the vessel. The wave system consists of crests and troughs, if the crests of the bow wave system coincide with a trough of the sponson wave system, they cancel. If the crests of bow system coincide with a crest of the sponson wave system, this results in even higher waves.

The wave pattern for the five concepts and the Fairplayer can be found in figure 5.3. The scale of the wave patterns of the five concepts is adjusted for the comparison and is therefore only shown in figure 5.3b. The maximum wave height for the different concepts changes a bit and can be found in appendix E. Concept

a1 (5.3c) and concept a5 (5.3g) have the smallest resistance and these two positions are therefore optimal in longitudinal direction. Concept a5 has the starting position of the sponson most aft, causing an influence on the flow field of the propeller. This interaction of the sponson and the propeller is not analysed in this research and needs to be done with a CFD calculation, because of the viscous effects which play a role in the aft part of the vessel.

The wavelength of the wave system can be calculated with equation 2.25. For the Fairplayer at the design speed of 17 knots, the wavelength is about 50 meter. De difference in starting position between concept a1 and concept a5 is 50 meter, which explains why the wave-making resistance is almost the same.

Concluded can be said that a relatively small variation of the longitudinal position of the sponson could lead to a large increase or decrease in the wave-making resistance. This longitudinal position is therefore an important factor for the performance of the Fairplayer with a sponson.

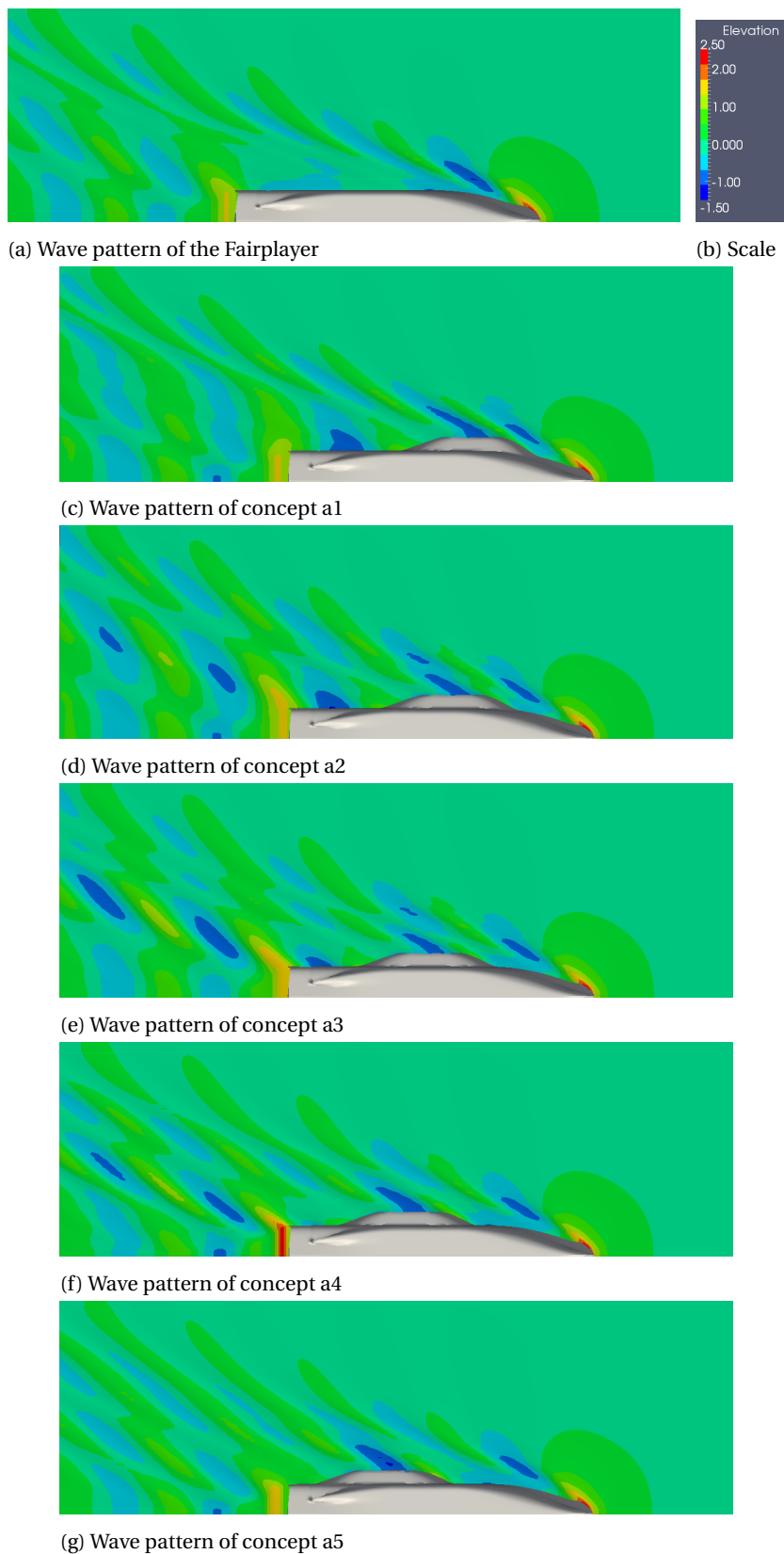


Figure 5.3: Wave pattern comparison of the variation in longitudinal position of the sponson.

The length over width ratio of the sponson

The influence of the length over width ratio of the sponson is analysed with five different concepts. Concept b1 has the smallest $\frac{L}{B}$ ratio, which means that the sponson is shorter, but wider. The consecutive concepts have a larger $\frac{L}{B}$ ratio, and therefore increase in length and decrease in width.

The increase of the individual resistance components compared with the base case as described in paragraph 4.3 can be found in figure 5.4. The frictional resistance is increase slightly equal for the five concepts, because of the increase in wetted surface. The same can be noticed for the model-ship correlation resistance. The wave-making resistance again has a significant influence on the increase of the total resistance.

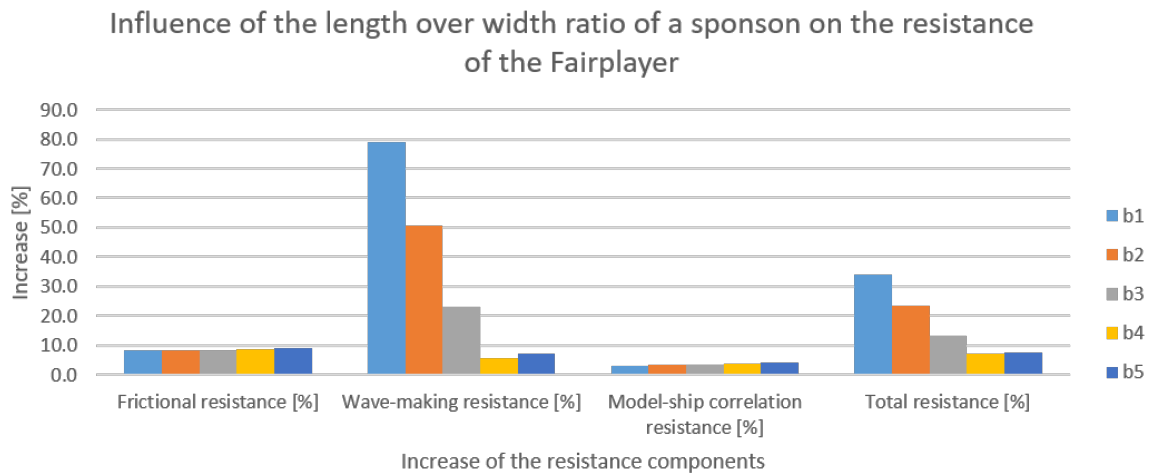


Figure 5.4: Increase of the individual resistance components w.r.t. the Fairplayer, when the length over width ratio of the sponson is varied.

As can be seen in figure 5.4, the resistance of a vessel is in general lower when the sponson becomes smaller and longer. This can be explained by the pressure disturbance around the shoulder of the vessel. A wider sponson leads to a larger acceleration of the flow around the sponson, which results in a larger pressure disturbance. The waves generated by this larger pressure disturbance contain more energy and are higher. This is not the case for the step between concepts b4 and b5. This can be explained by analysing the wave patterns. The aft of the sponson also generates a wave system, which interacts with the wave systems of the bow and the sponson. If this interference leads to a higher waves, the total resistance is higher as described in paragraph 2.5.2.

The increase in the total resistance varies from 7 to 35%, which indicates that the length over width ratio has a more negative effect than the longitudinal position of the sponson, as described above.

The wave pattern for the five concepts and the Fairplayer can be found in figure 5.5. The scale of the wave patterns of the five concepts is adjusted for the comparison and is therefore only shown in figure 5.5b. The maximum wave height for the different concepts changes a bit and can be found in appendix E.

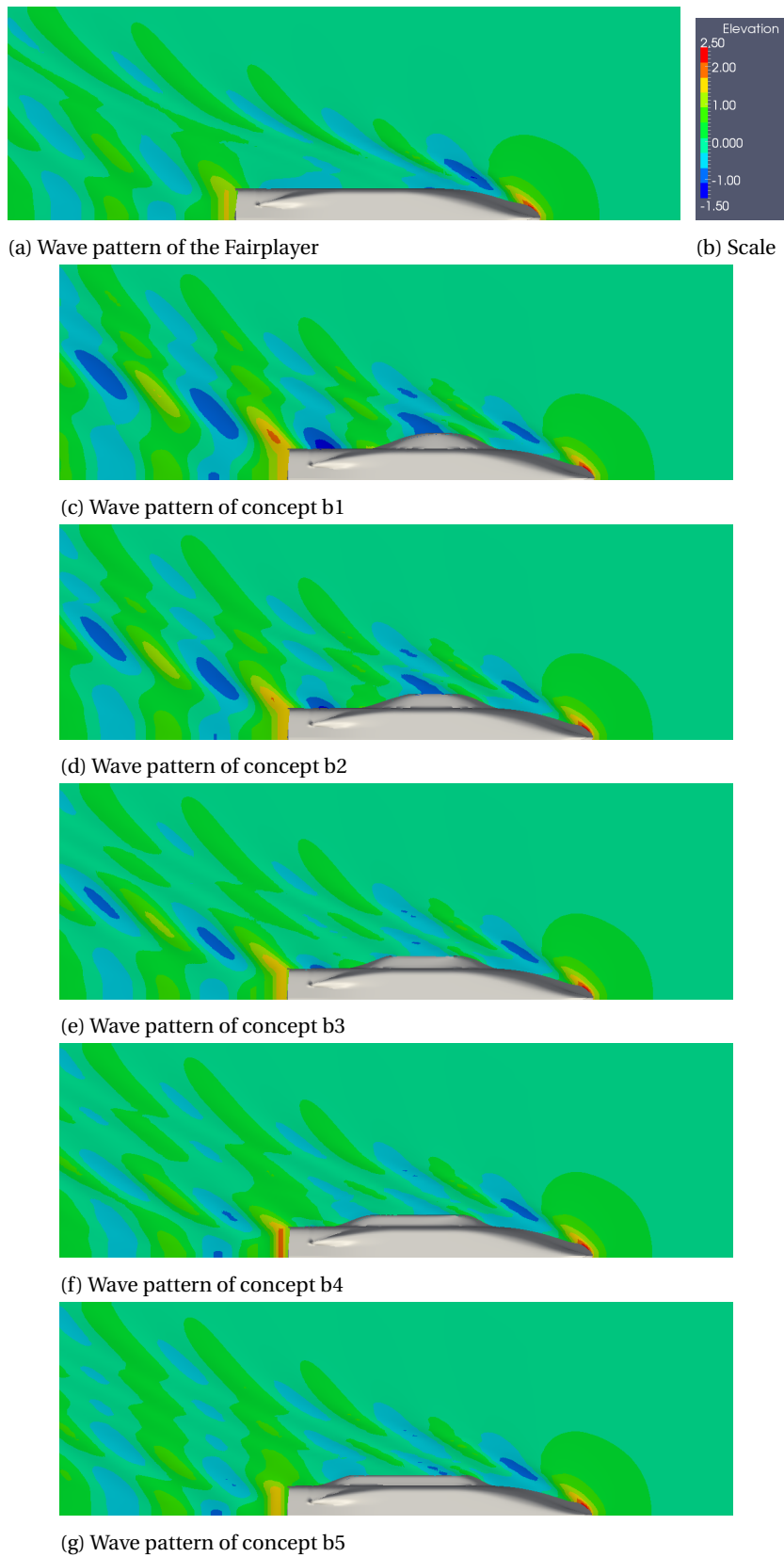


Figure 5.5: Wave pattern comparison of the variation in length over width ratio of the sponson.

The vertical starting position of the sponson

The influence of the vertical starting position of the sponson is also analysed with five different concepts. Concept c1 has the starting position of the sponson at a height of 5.5 meter from the base line and the consecutive concept have a starting position which each starting one meter lower.

The increase of the individual resistance components compared with the base case as described in paragraph 4.3 can be found in figure 5.6. The frictional resistance and the model-ship correlation resistance are both almost equal for all five concepts and again the wave-making resistance increases significantly. The results of concept c5 are shown, but the calculation with RAPID did not give a convergent solution. Therefore the results of concept c5 are not taken into account in the analysis. The wave-making resistance increases when the starting position of the sponson is lower. This is a result of the increased displacement of the vessel. The velocity of the flow increases, because the flow needs to go around the sponson. The increase in velocity of the flow results in a higher pressure disturbance, which generates a wave system. The increase in the total resistance can be up to 75%, which becomes significant. The increase in resistance and therefore the decrease in speed is not favourable for Jumbo Maritime, which uses a relatively high transit speed as strength for their market position. The low starting position of the sponson also results that the vessel cannot be converted into a dual draft vessel, which means that it always have to sail with this increased resistance.

The wave patterns of the five concepts cannot be compared into one figure as done in figure 5.3 and figure 5.5, because the scale of the wave pattern differs to much. Nevertheless it can be concluded that the wave-making resistance increases when the sponson starts at a lower vertical position.

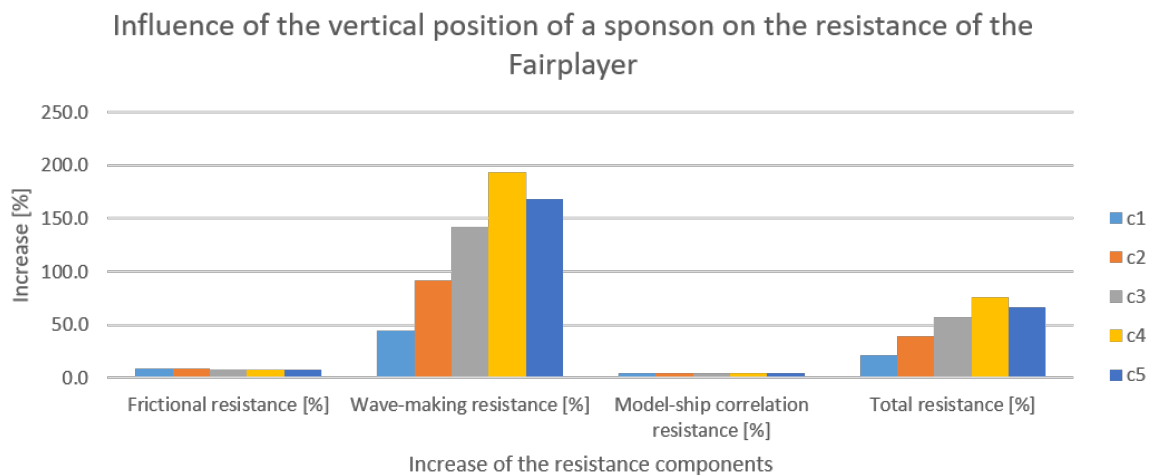


Figure 5.6: Increase of the individual resistance components w.r.t. the Fairplayer, when the vertical position of the sponson is varied.

5.3. Conclusions of the adjusted Holtrop-Mennen method

The influence of a sponson at the Fairplayer is analysed with the five step method as described in paragraph 4.3. The results of this analysis are discussed in paragraph 5.2. From these results some interesting conclusions can be drawn. As can be seen in the results, the total increase of resistance can change from 7 to 35%, when only changing the longitudinal position or the length over width ratio. The longitudinal position chosen 10 meter more to the aft results in an resistance increase of 12%, as can be seen between concept a1 and a2. This means that the position and shape need to be chosen correctly, to avoid an unnecessary increase in resistance. The frictional resistance of all the concepts with a sponson increases with about the same percentage (7.5 to 9.0%). From this it can be concluded that the frictional resistance does not significantly change if the shape and position of the sponson are varied. The frictional resistance is 50% of the total resistance as can be seen in paragraph 4.3. This means that the frictional resistance has a large contribution of the total resistance, but due to the limited variation it is not the dominant factor for the different concepts. The wave-making resistance on the other hand has a significant influence. As can be seen in table F1 and in paragraph 5.2 the increase of wave-making resistance can be from 5.9 up until 193.1%. As described in paragraph 2.5.2 the interference between the different wave systems can have a significant influence on the wave-making resistance. The wave-making resistance is about a third of the total resistance as can be seen in table 4.5, which make the large variations in the increase of the wave-making component of significant influence on the total

resistance. The model-ship correlation resistance is also quite constant over the different concepts (between 3.5 and 5%) and is only one tenth of the total resistance.

Coming back to the conclusions of the concept study in paragraph 3.4.1, the increased resistance can be an important factor. In the concept study of chapter 3 concept 1 is the Fairplayer with a sponson starting at a vertical height of 5.5 meter, which can be compared to the concept variations a and b in this chapter. The longitudinal position and the length over width ratio result in an increase of the resistance in the range between 7 to 35%. The concepts which have an increase of 7% are very feasible, because the decrease in speed is not significant. The weighting of the resistance of concept 1 in paragraph 3.4 is therefore a good estimation, which makes concept 1 still a good possibility for the adjustment of the Fairplayer. Concept 3 as described in chapter 3 can be compared to concept c3, c4 and c5, for which the increase of the total resistance is more than 55%. This increase gives a significant reduction of the maximum speed and is the concept would therefore be not feasible for Jumbo Maritime. For this reason the weighting of concept 3 in the concept study of paragraph 3.4 is too high and concept 3 is dropped as a possible concept for a sponson on the Fairplayer.

From the three different variations there are three trends that can be noticed. The influence of the longitudinal position is of importance for the interference with the wave systems of the Fairplayer. There are two positions (concept a1 and a5) which both have about the same interference because the starting position is about one wave length apart. The length over width ratio also has a large influence and generally the larger this ratio, the lower the resistance will be. From the variation of the position in height direction it could be concluded that the higher (a smaller part of the sponson in the water) the sponson, the lower the resistance.

Extra iteration for the Fairplayer with a sponson

From these three trends it would be a logical step to combine this into one optimized concept. This concept has the longitudinal position of concept a1, the vertical position of concept c1 and the length over width ratio of b4. This concept is called concept d1 and can be found in appendix E. The total resistance of this concept turned out to be an increase of 18%, as can be seen in table E3. This is twice as high as concept b4. This concludes that the wave interference as described in paragraph 2.5.2 cannot be predicted easily, due to the interaction of the seven wave systems. The seven wave systems are the five described in paragraph 2.5.2 and two wave systems generated by the forward and aft shoulder of the sponson. This example shows that this interaction cannot be predicted based on the results of the three variations. Therefore it is chosen to continue with the current concepts as described in paragraph 5.1.

There are four concepts which have an increase of resistance in the range between 7 and 9%. The concepts are: a1, a5, b4 and b5. The different concepts all have a different shape and position on the Fairplayer, which can be an advantage or disadvantage. Concept a1 has the sponson positioned as far as possible to the front of the vessel. This gives an advantage when optimizing the aft of the sponson to optimize the inflow of the propeller. But the construction of the sponson is more difficult, because the position is at a strongly curved hull of the Fairplayer. Concept a5 and b5 are both positioned as far aft as possible, which has an impact on the inflow of the propeller. Concept b4 has the smallest resistance of all the concepts and is positioned in the parallel section of the hull. This means that connection to the hull of the Fairplayer is relatively the easiest. Therefore it is chosen investigate this concept further.

Final concept of the Fairplayer with a sponson

The final concept of the Fairplayer with a sponson is concept b4 and can be found in figure 5.7.

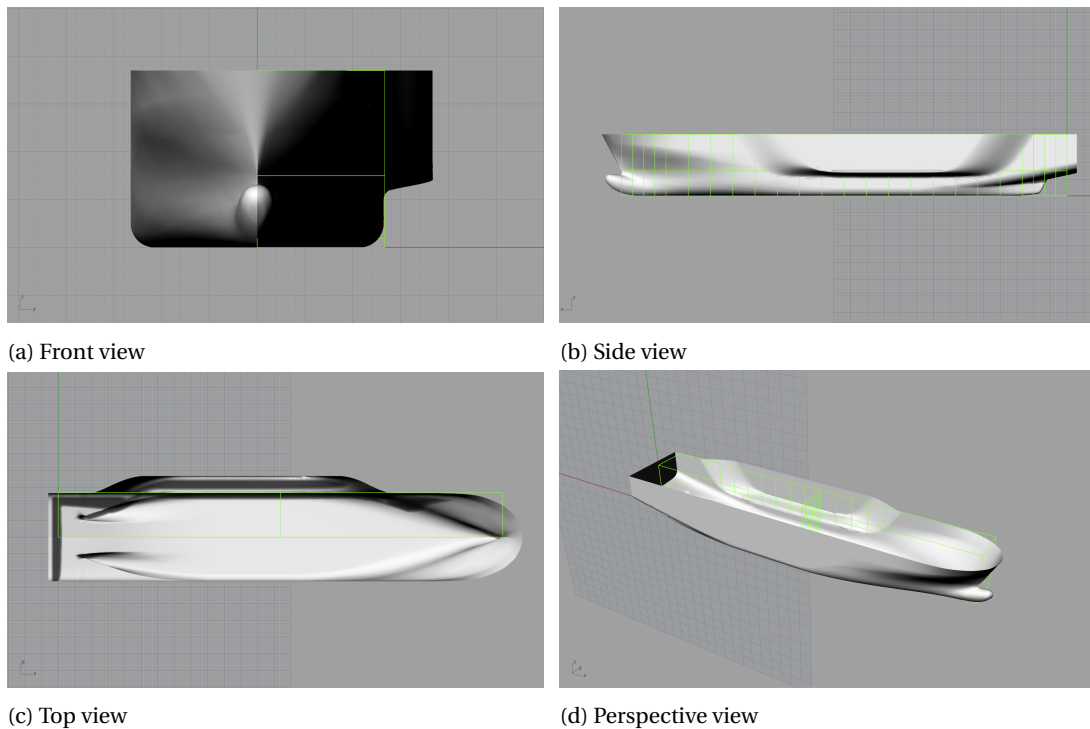


Figure 5.7: Rhinoceros 3D model of concept b4.

The operational profile of the Fairplayer with a sponson differs from the current profile of the Fairplayer. The vessel with sponson has become a dual draft vessel. When the vessel does not have cargo on board, it can sail a draft of 5.5 meter. The resistance is the same as for the current vessel. During transit with cargo stored on board, the draft needs to be increased until 7.5 meter. The lifting operations will be performed at a draft of 8.5 meter, to create vertical sides around the lifting draft. The static stability (GM) of the Fairplayer at a draft of 8.5 meter increases from 2.3 meter to 5.7 meter for the Fairplayer with a sponson. The dimensions of the sponson can be found in table 5.2. The mass of the sponson is estimated based on the mass density of the pontoons which are currently used for the Fairplayer.

Table 5.2: Main characteristics of the sponson on the Fairplayer

Main characteristics of the sponson	
Length [m]	60
Width [m]	5
Vertical starting point [m]	5.8
Longitudinal starting point [m]	100
Weight [T]	500
Volume [m^3]	2850

An additional advantage of the sponson is the increased ballast capacity in the sponson. The sponson has a volume of $2850 m^3$, which can be used as an additional ballast tank. During lifting operations these ballast tanks create a compensating moment at the 'crane out' phase. The compensating moment from the ballast water need to be larger than the moment created by the load in the crane. The moment created by the load can be fully compensated by the ballast water in the sponson if the cargo is maximum 8 meter outside of the hull. An even larger outreach of the cranes can be reached if the ballast tanks in the hull also provide a compensating moment.

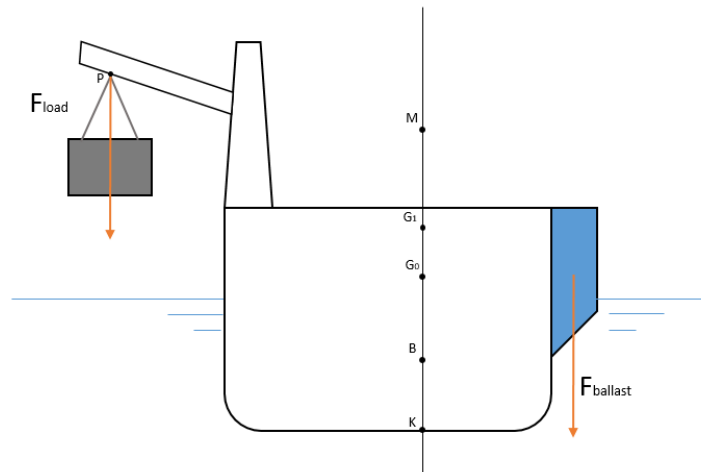


Figure 5.8: 'Crane out' phase during the lifting operation of the Fairplayer with a sponson.

The increase of the total resistance of the Fairplayer with a sponson is 7%, but the maximum speed of the vessel needs to be calculated. This is done in paragraph 5.4.

5.4. Speed of the Fairplayer with a sponson

The final concept of the Fairplayer with a sponson has an increase in the total resistance of 7%. The increase of resistance results in a decrease of the maximum speed of the vessel. It is often acceptable to assume that the ship's resistance is roughly proportional to the square of the ship speed [29], which is applicable for low speeds. For medium-sized and medium speed ships, the resistance increases with a power 3.5 [4]. The relation between the resistance and the speed can be found in equation 5.1.

$$R = C1 \cdot V^{3.5}, \quad (5.1)$$

in which R is the resistance, $C1$ is a constant and V is the ship speed. This is the resistance curve if the ship does not change. With a sponson on the Fairplayer, the resistance curve shifts a little upwards. A better method to find the new speed of the vessel is to calculate the new resistance curve of the Fairplayer with a sponson.

The resistance curve of the Fairplayer with and without a sponson can be found in figure 5.9. As can be seen, the resistance curve for the Fairplayer with sponson is above the resistance curve for the Fairplayer. The increased resistance due to the sponson leads to a change in the operating point of the propeller and the engine. The current propulsion system consists of two 4500 kW main engines each connected to a controllable pitch propeller (CPP) by means of a gearbox. The design speed of the Fairplayer is 17.0 knots at 90% MCR. The operating point of the Fairplayer without a sponson is drawn in red in figure 5.9. The two resistance curves are close together, especially around the operating point of the Fairplayer. It is assumed that the operating point of the propeller and the engine will not change significantly in a small range around the design speed. The pitch of the CPP can be adjusted that the thrust generated at a slightly lower speed stays equal. This requires a larger torque from the engine. With this assumption, a horizontal orange line is drawn in figure 5.9. The intersection with the new resistance curve defines the new ship speed, which is about 16.5 knots.

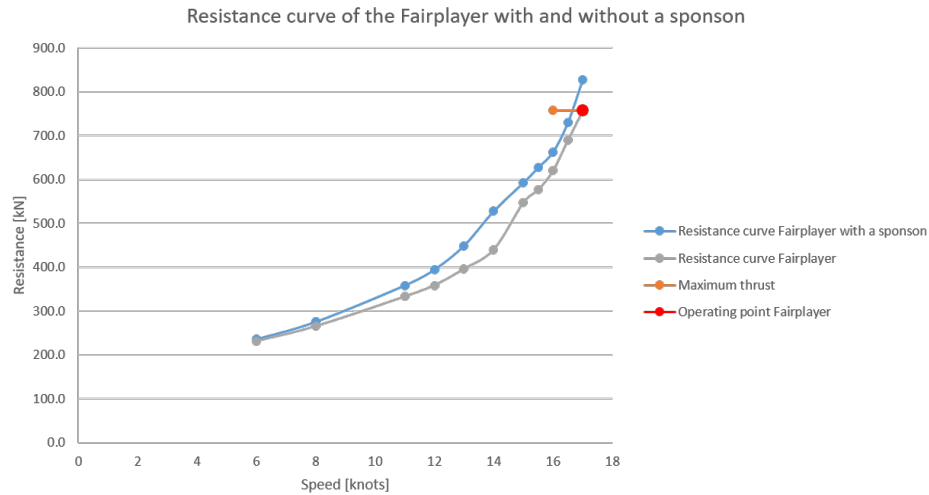


Figure 5.9: The resistance of the Fairplayer with a sponson as function of the speed.

For the calculation of the resistance curve the asymmetric hull shape of the Fairplayer with a sponson is not taken into account. The placement of a sponson on the vessel leads to an asymmetric resistance distribution over the hull. Due to the sponson, a moment is created, which needs to be compensated to sail in a straight line. The rudders of the vessel can create a counter moment, but this results in a drag of the rudders. The moment created by the asymmetric hull is assumed to be the increased resistance acting on the sponson, so the lever arm of this is half the width of the vessel and sponson. The rudders are positioned at a distance of 66 meter from the COG, so the force needed from each of the rudders is 6.5 kN. The lift force and induced drag force of the rudders can be calculated with equation 5.2 and 5.3 [17].

$$L = 0.5 \cdot \rho_w \cdot V^2 \cdot S_{rudder} \cdot C_L, \quad (5.2)$$

$$D_i = 0.5 \cdot \rho_w \cdot V^2 \cdot S_{rudder} \cdot C_{Di}, \quad (5.3)$$

where S_{rudder} is the projected area of the rudder and the lift coefficient C_L and the induced drag coefficient C_{Di} are calculated with equation 5.4 and 5.5 respectively.

$$C_L = \frac{2\pi}{1 + \frac{2}{AR}} \alpha, \quad (5.4)$$

$$C_{Di} = \frac{C_L^2}{\pi \cdot AR}, \quad (5.5)$$

where AR is the aspect ratio of the rudder, as calculated with equation 5.6 and α is the angle of the rudder.

$$AR = \frac{b^2}{S_{rudder}}, \quad (5.6)$$

where b is the span of the rudder. From this, the angle of the rudders needs to be 3 degrees to generate a lift force of 6.5 kN. The induced drag at 3 degrees is 2 kN, so the two rudders generate a resistance of 4 kN. This increase in resistance of the propellers is small relative to the resistance of the sponson, so the reduction of this will be neglected. At the speed of 16.5 knots, on which this calculation is done, the rudders do not need

a large angle to generate a lift force. When sailing at a lower speed, the rudders generate less drag. At a lower speed the moment created by the sponson could also be counteracted by a difference in thrust generation of the two propellers. If the portside propeller (the same side as the sponson) generates more thrust than the starboard propeller, a turning moment is generated. This can be a better solution at a low speed, due to the reduced effectiveness of the rudders at low speed.

Jumbo Maritime needs to decide if this reduction in the maximum speed is desired. This reduction in speed results in longer trip times and therefore less operations that can be done per year. If a reduction of the speed is not desired an extra generator can be installed. This generator can deliver power to the propeller through a power take in, which needs to be installed on the propeller shaft. This generator and power take in results in an increase of the power, but results in a higher fuel consumption and an extra investment. This decision can be taken into account when performing a financial analysis to the applicability of a sponson on the Fairplayer.

6

Conclusions and recommendations

The maximum lifting capacity of the Fairplayer is limited to 1000 ton in offshore conditions, due to the insufficient static stability. The Fairplayer is a heavy lift and offshore installation vessel with two 900 ton cranes, which can lift up to 1800 ton combined. The limited lifting capacity in offshore conditions is a missed opportunity to make use of the Fairplayer in a wider segment of the offshore installation market. The conversion of the Fairplayer in a dual draft vessel by applying a sponson leads to an increased static stability during lifting operations. This chapter provides the conclusions and interpretation of the results of the research to the optimized position of a sponson on the Fairplayer. Also the recommendations arising from this research are described in this chapter.

6.1. Conclusions

- **Concept study to operational profile**

The concept study to the different vertical positions of the sponson showed that the Fairplayer with a sponson partly submerged is the most feasible solution. The Fairplayer with a sponson starting at 5.5 meter and a lifting draft of 8.5 meter has large vertical sides, which results in safe lifting operations without the chance of a submersion of the deck. This concept does not perform well on the resistance, which is estimated with an adjusted Holtrop-Mennen method. The vessel can sail at a draft of 5.5 meter without an increase resistance, which is an important strength for Jumbo Maritime.

- **Adjusted Holtrop-Mennen method**

The current prediction methods all have limitations and could not be applied in this research, so an adjusted Holtrop-Mennen method is set up. CFD calculations and model testing are too expensive and time consuming, when taking into account the amount of concepts that are evaluated for this research. The potential flow theory program RAPID only calculates the wave-making resistance of a vessel and does not take the frictional resistance into account. The prediction method of Holtrop & Mennen is an empirical method based on a large number of different hull shapes and the Fairplayer with a sponson is different compared to conventional hull shapes. The strengths of the Holtrop-Mennen method and RAPID are combined into an adjusted Holtrop-Mennen method. This method uses the calculation with Holtrop-Mennen for the Fairplayer as a starting point. The increase in wave-making resistance is calculated with RAPID and the increase in frictional resistance is calculated with the ITTC flat plate friction formula. The remaining resistance components in the Holtrop-Mennen method are also calculated for the Fairplayer with a sponson. The total resistance of the Fairplayer with a sponson is expressed as a percentage of the base case of the Fairplayer.

- **Resistance components**

The three different resistance components all have a different influence on the increase of the total resistance. The increase in frictional resistance is in the range between 7.5 and 9% for all 15 concepts of the Fairplayer with a sponson. This is mainly due to the wetted surface increase that is almost equal and the form factor which does not change significantly for the different concepts. The frictional resistance is, with 50% of the total resistance, a large component, but due to the small variations not important in the comparison between the different concepts. The model-ship correlation resistance gave the same

results as the frictional resistance and give an increase between the 3 and 5%, but is only 15% of the total resistance. The wave-making resistance gives the most variation and gives an increase between the 6 and 190%. Since the wave-making resistance is 35% of the total resistance of the vessel, this large variation also has a large effect on the total resistance.

- **Longitudinal starting position of the sponson**

The longitudinal starting position of the sponson has a significant influence on the total resistance. The total resistance can vary between an increase of 8 and 20% for different longitudinal positions of the sponson. The wave system generated by the vessel and sponson interferes in such a way that the crests of the one coincide with the troughs of the other wave system. This results in a significantly smaller amount of wave-making resistance. The interference of the wave systems, and therefore the low increase of resistance, is obtained with a starting position of the sponson around the shoulder of the vessel and also with a starting position 50 meter more to the aft. This is about one wave length difference, so the wave systems have the same interference, but starts one wave length more to the back.

- **Length over width ratio of the sponson**

The length over width ratio of the sponson also gave a clear dependency. A smaller and longer sponson results in a lower wave-making resistance in general. This dependency can be explained by the fact that the water is accelerated faster to flow around the sponson if this becomes wider. This creates a larger pressure disturbance which generates a larger wave system. A side note needs to be made, because the position of front and aft of the sponson also have an influence on the resistance. If wave systems generated by the front and aft shoulder negatively interfere with the wave system from the vessel, the resistance is higher than a wider sponson with a better interference. The increase in the total resistance varies from 7 to 35%, which indicates that the length over width ratio has a more negative effect than the longitudinal position of the sponson.

- **Vertical starting position**

The last systematic variation is the vertical starting position of the sponson. The wave-making resistance increases rapidly when the vertical starting position is lower. The increase in the total resistance can be up to 75%. The low vertical starting position of the sponson also affects the operational profile of the vessel, because it can not be used as a dual draft vessel.

- **Final concept**

The concept with the smallest resistance is concept b4, which can be seen in figure 6.1. The resistance increases with 7% compared to the Fairplayer without a sponson. This results in a decrease of the maximum speed with 3% to a speed of 16.5 knots. Due to the asymmetric shape of the vessel, the resistance creates a turning moment. This needs to be compensated by an angle of the rudders of 3 degrees. The induced drag of the rudders is 4 kN and the decrease in speed because of this can be neglected.

The operational profile of the Fairplayer changes due to the addition of a sponson. The vessel is converted into a dual draft vessel, which means that the vessel has two different drafts at which it can operate. At a draft of 5.5 meter, the underwater part of the vessel is not changed, which means that the resistance is not increased during transit. When in transit with cargo on board, the vessel sails at a larger draft of 7.5 meter, because the static stability is not sufficient at 5.5 meter. The resistance of the vessel leads to a decrease of speed. There are multiple ways to handle with this increase in resistance. Jumbo Maritime could decide to count more time for their trips. The second solution would be to install an extra generator on the propeller axis. This generator delivers power to the propeller through a power take in, which results in an increase of propulsion power, but also an increase of the fuel consumption and requires an initial investment.

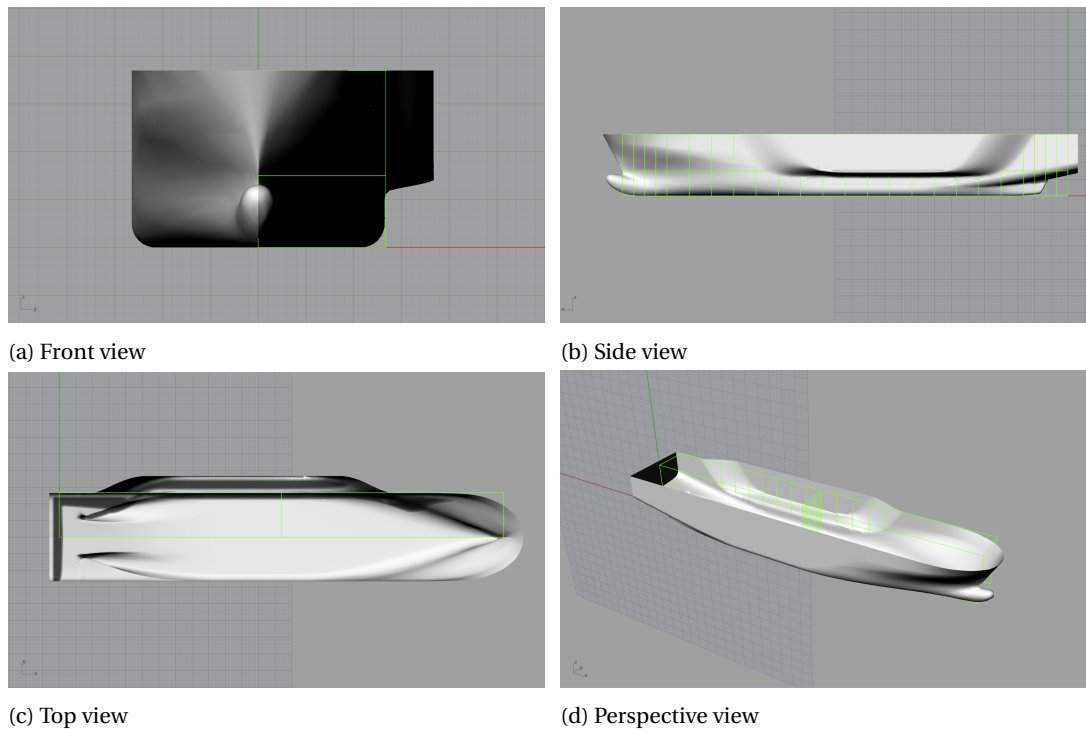


Figure 6.1: Rhinoceros 3D model of the final concept (concept b4) of the Fairplayer with a sponson.

6.2. Recommendation

Based on this research there are recommendations for further research to the Fairplayer with a sponson.

- **Validation of the method**

The adjusted Holtrop-Mennen method that has been set up in this research, uses a combination of the potential flow program RAPID and the Holtrop-Mennen calculation for the resistance of the Fairplayer with a sponson. The results of this study need to be validated, either with model tests or a CFD calculation. The form factor calculated in this research is only a first estimation. In order to improve the adjusted Holtrop-Mennen method the form factor needs to be determined, for example with a model test.

- **Optimization of the aft of the sponson**

The potential flow program RAPID calculates the wave pattern of a vessel and does not take the viscosity of the fluid into account. This means that in the aft of the vessel and behind the sponson, where separation of the flow and viscosity has a significant influence, the calculation could be wrong. For the optimization of the aft part of the sponson a CFD calculation needs to be done to investigate the streamlines of the flow and to optimize the water inflow of the propeller.

- **Analyse the workability of the Fairplayer with a sponson**

The workability of the vessel during offshore operations is assumed to have about the same characteristics as the concepts of P. Harenberg [6]. A workability study needs to be performed in order to see whether this assumption is justified and to find the workability of the Fairplayer with a sponson.

- **Analyse the ship's performance in waves**

The still water resistance of the Fairplayer with a sponson is calculated in this research, but the resistance in wave conditions will be higher. This is not taken into account in this research but could be of importance due to the change in width just above the still waterline. The motion behaviour of the vessel with a sponson during transit and the amount of slamming which occurs during sailing at a draft of 5.5 meter could be of interest to investigate. Slamming is mainly of a constructional problem, but could also significantly reduce the comfort on board. A solution to prevent the problems of slamming on the sponson, the draft of the vessel could be increased, which lead to an submersion of the sponson under

the waterline. The high static stability at a draft of 7.5 meter while sailing with cargo on board could result in large accelerations of the vessel. This high static stability could probably be reduced by filling the ballast tanks in a higher part of the hull, but an analysis of this motion behaviour is recommended.

- **Financial analysis of the Fairplayer with a sponson**

The increase in lifting capacity leads to a wider segment to perform the offshore installation work, which provides a higher turnover. The reduced speed of the Fairplayer leads to larger transit times and the initial investment of the sponson, both results in higher expenses. A financial analysis should be done to see if the increase in revenues due to the larger crane capacity weighs up the initial investment and the reduced speed.

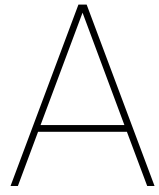
- **Patent of a dual draft vessel**

GustoMSC and Seaway Heavy Lifting own a patent on the concept of a dual draft vessel. This patent could give conflicts with the concept of a sponson on the Fairplayer and needs therefore be compared from a juristic point of view.

Bibliography

- [1] 4c offshore. <http://www.4coffshore.com/windfarms/vessels.aspx?catid=3>. Accessed: Februari 6th, 2017.
- [2] B. Abeil. L-class heavy lift vessel (162 m); seakeeping tests, volume 1 - summary, discussion and conclusions. Technical report, MARIN Wageningen, 2015.
- [3] *DNV-RP-C205 Environmental Conditions and Environmental Loads*. Det Norske Veritas (DNV), April 2014. Recommended practice).
- [4] MAN Diesel and Turbo. Basic principles of ship propulsion. Technical report, Man Diesel and Turbo, 2011.
- [5] Odd M. Faltinsen. Slamming, whipping, and springing. In *Hydrodynamics of High-Speed Marine Vehicles*; pages 286–341. Cambridge University Press, 2006.
- [6] P. Harenberg. Developing the optimal design solution for jumbo to increase the offshore stability of a heavy crane lift vessel. Master's thesis, Delft University of Technology & Jumbo Maritime, The Netherlands, 2016.
- [7] R.C. Hibbeler. *Engineering Mechanics: Statics*. Prentice Hall, 12 edition, 2009.
- [8] J. Holtrop. A statistical analysis of performance test results. *International shipbuilding progress*, 24(270), 1977.
- [9] J. Holtrop. A statistical re-analysis of resistance and propulsion data, 1984.
- [10] J. Holtrop and G.G.J. Mennen. A statistical power prediction method. *International shipbuilding progress*, 25(290), 1978.
- [11] J. Holtrop and G.G.J. Mennen. An approximate power prediction method, 1982.
- [12] *2008 SPS Code - Code of Safety for Special Purpose Ships*. International Maritime Organization (IMO), 2008. Resolution MSC.266(84).
- [13] J.M.J. Journée and W.W. Massie. *Offshore Hydromechanics*. Delft University of Technology, 1 edition, 2001.
- [14] *Kahn Rule 2*. Jumbo Maritime, 2009. Internal document, Jumbo Maritime.
- [15] *Investigation SPS conversion J-type, Improved damage stability*. Jumbo Maritime, November 2015. Internal document, Jumbo Maritime.
- [16] *Vessel stability information*. Jumbo Maritime, 2016. Internal document from Jumbo Management System, Jumbo Maritime.
- [17] L. Larsson and H. C. Raven. *The Principles of Naval Architecture Series: Ship Resistance and Flow*. The Society of Naval Architects and Marine Engineers, 2010.
- [18] I. Lukas. Metocean data to support motion analysis. Technical report, BMT ARGOSS, September 2015.
- [19] *Grid Plug-Ins for Rhino*. MARIN, 2015.
- [20] *RAPID User's Guide*. MARIN, 2015.
- [21] Jumbo Maritime. Offshore installation contracting. URL <https://www.jumbomaritime.nl/en/offshore/>.

- [22] J. Pinkster and C.J. Bom. *Hydromechanica 2, Deel 2 Geometrie en Stabiliteit*. Delft University of Technology, 2006.
- [23] Vuyk Engineering Rotterdam. Final stability booklet heavy lift vessel 'm/v fairplayer'. Technical report, Vuyk Engineering Rotterdam, January 2009.
- [24] L.T. Saaty and L.G. Vargas. *Models, Methods, Concepts and Applications of the Analytic Hierarchy Process*. Springer, 2012.
- [25] T. Van Schalkwijk. Increasing the workability for offshore lifting operations by reducing the roll motion. Master's thesis, Delft University of Technology & Jumbo Maritime, The Netherlands, 2015.
- [26] CIG Maritime Technology. J-series feasibility study changes. Technical report, CIG Maritime Technology, November 2015.
- [27] W.J. van der Velde, W.J.A. Wassink, J.A. Commandeur (GustoMSC Resources B.V., and Seaway Heavy Lifting Engineering B.V.). *DUAL DRAFT CRANE VESSEL*, 02 2015. United States Patent: US 8960116 B2.
- [28] D.G.M. Watson. *Practical Ship Design*, volume 1. Elsevier, 1998.
- [29] H. Klein Woud and D. Stapersma. *Design of propulsion and electric power generation systems*. IMarEST, 2008.
- [30] S. Zaaijer. Computational fluid dynamics (cfd) calculations for the j-class heavy lift ship - results. Technical report, Van Oossanen Naval Architects, June 2014.



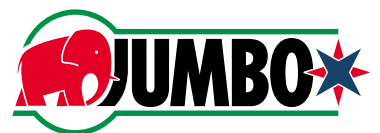
Factsheet Fairplayer



DP2 Heavy Lift Crane Vessel **FAIRPLAYER**

A multi-functional dynamic positioned Heavy Lift Crane Vessel (HLCV) well suited to the offshore requirements of the Energy Industry worldwide.

Length	144.1 m
Breadth	26.7 m
Depth	14.1 m
Accommodation	80 POB
Helideck	Sikorsky S-92
Transit Speed	17 Knots
Mast Cranes	2 x 900 Te
Depth rating	3,000 m



CAPABILITIES



Quayside-to-Seabed

Offering versatility, high transit speed, stability and the ability to work in deep-water and harsh offshore environments, the Fairplayer provides cost effective transport and installation solutions. An exceptionally large, flush working deck and a multi-level cargo hold enables the Fairplayer to add modular components to suit specific project requirements and to integrate all offshore activities from “Quayside-to-Seabed”. This unique method saves multiple resources, critical time, complex logistics and offshore interfaces.

Fast Economical Transit and High Workability

The Fairplayer is a large vessel with motion characteristics that allows safe working in the harshest offshore environments. The high freeboard and dock walls protect crew and cargo in harsh weather conditions. A key attribute of Fairplayer is its fast and economical transit speed, saving time and cost to operate in remote logistically challenging locations. On location, its method to lift all components from its own deck ensures maximum safety, installation control and workability.

Dual- Crane Deepwater Heavy Lifting

Fairplayer is equipped with two mast cranes with a Safe Working Load (SWL) of 900Te each. The dual cranes provide tandem heavy lift capacity, dual crane upending capability as well as deep-water lowering capability.

The integrated deep-water deployment systems allow direct lowering and accurate positioning of subsea structures in water depths up to 3,000 m.

Large Main Deck and adjustable Cargo Hold

The main deck has an exceptionally large working area of 3,100 m² and offers a loading capacity of 12 Te/m². The adjustable tween deck has an area of 1,700 m² and offers a loading capacity of 7 Te/m² and the lower hold area of 1,400 m² has a loading capacity of 12 Te/m².

Dynamic Positioning (DP) System

The Fairplayer is fitted with a fully redundant Kongsberg SDP 21 Dynamic Positioning System with six independent reference systems, enabling her to maintain its position during all offshore installation activities.

ROV and LARS

During subsea operations the Fairplayer is fitted with two (2) Work Class ROV systems (150HP), launched over the side (starboard and/or portside) with a Launch And Recovery System (LARS) rated to 3,000m depth.

Accommodation/Helideck

The modern living quarters are equipped to accommodate up to 80 persons. All quarters have heating and air-conditioning facilities. The life-saving and fire-fighting equipment are according to the latest class and SOLAS requirements. The helicopter deck is certified for 12,8 Te take-off weight (Sikorsky S-92 Class - CAP 437)

SPECIFICATIONS

General

Call sign	PHPU
IMO no.	9371579
Built	2008
Flag	The Netherlands
Port of Registry	Rotterdam
Classification	Lloyd's Register+ 100A1, Strengthened for Heavy Cargos LMC, UMS, CG, LI, DP (AA), IWS

Principal Dimensions/Tonnage

Length o.a.	144.1 m
Length b.p.p	133.8 m
Breadth moulded	26.7 m
Depth to Main Deck	14.1 m
Draft (bottom keel)	6.0 m / 8.1 m
Displacement (at 7.5m)	20,120 Te
Deadweight (at 7.5m)	10,700 Te
GRT	15,027 Te
NRT	5,244 Te

Main Deck/Cargo Hold Area Strength

Main Deck/Cargo Hold	Area	Strength
Main Deck	3,100 m ²	9-12 Te/m ²
Tween Deck	1,700 m ²	7 Te/m ²
Lower Hold/Tank top	1,400 m ²	12 Te/m ²

Power Plant

Main Engines	2 x MAK 9M 32C 4,500 kW
Auxiliary Engines	2 x Caterpillar 3516B 1,824 kW/ea
Shaft Generators	2 x AEM SE 630 M4 3,000 kW/ea
Emergency Generator	1 x 465 kW

Propulsion Plant

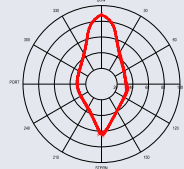
Stern Main Thrusters	2 x Wartsila CPP
Bow Tunnel Thrusters	2 x Wartsila 1,500 kW
Retractable Azimuth Thrusters	1 x Wartsila 1,700 kW

Service Speed

Transit average	17 Knots
Economical	14 Knots

Dynamic Positioning System

DP System	Kongsberg SDP 21
Reference Systems	2 x Seatex 116cm DGPS



1 x Veripos Verify DGPS
1 x HiPAP 501
1 x LTW (tautwire system)
RADius/Fanbeam

Cranage

Cranes/Type	Huisman Mast Cranes
	2 x 900 Te Revolving
Heavy Lift Capacity	1,000 Te (Offshore)
	1,800 Te (Calm Water/Harbor)
Subsea Lift Capacity	1,000 Te at 1,000 m water depth
	660 Te at 1,500 m water depth
	280 Te at 2,000 m water depth
	200 Te at 3,000 m water depth
Heave Compensation	Passive Heave Compensators
	project specific/tailor made
Ancillary Lifting	Auxiliary Hoists: 2 x 37,5 Te
	Travel Trolley
	Sling Handling Hoists: 2 x 10 Te
	Tugger Winches: 2 x 25 Te / crane
	(constant tension)
	1 x 700 Te Fly-Jib

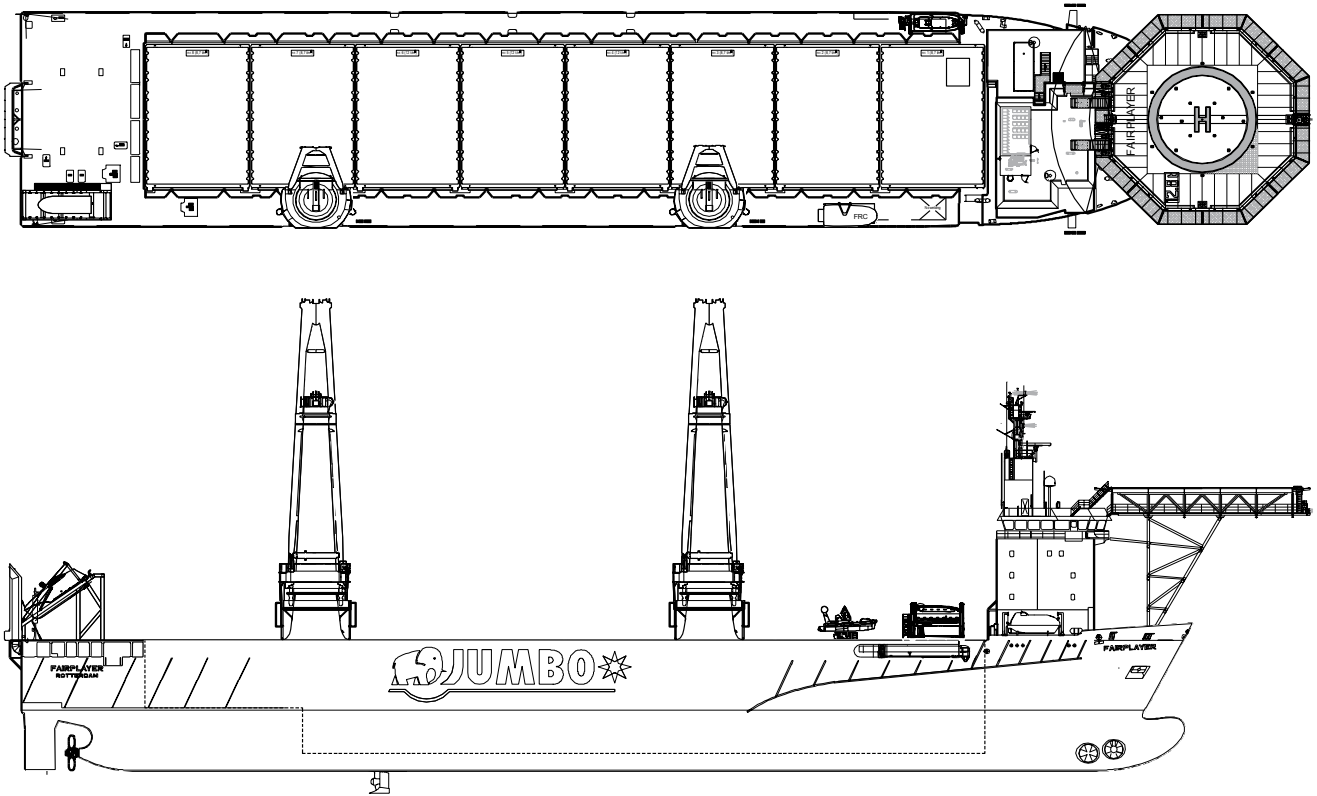
Capacities

Fuel Oil	1,340 Te I.F.O/290 Te M.G.O
Fresh water	200 Te

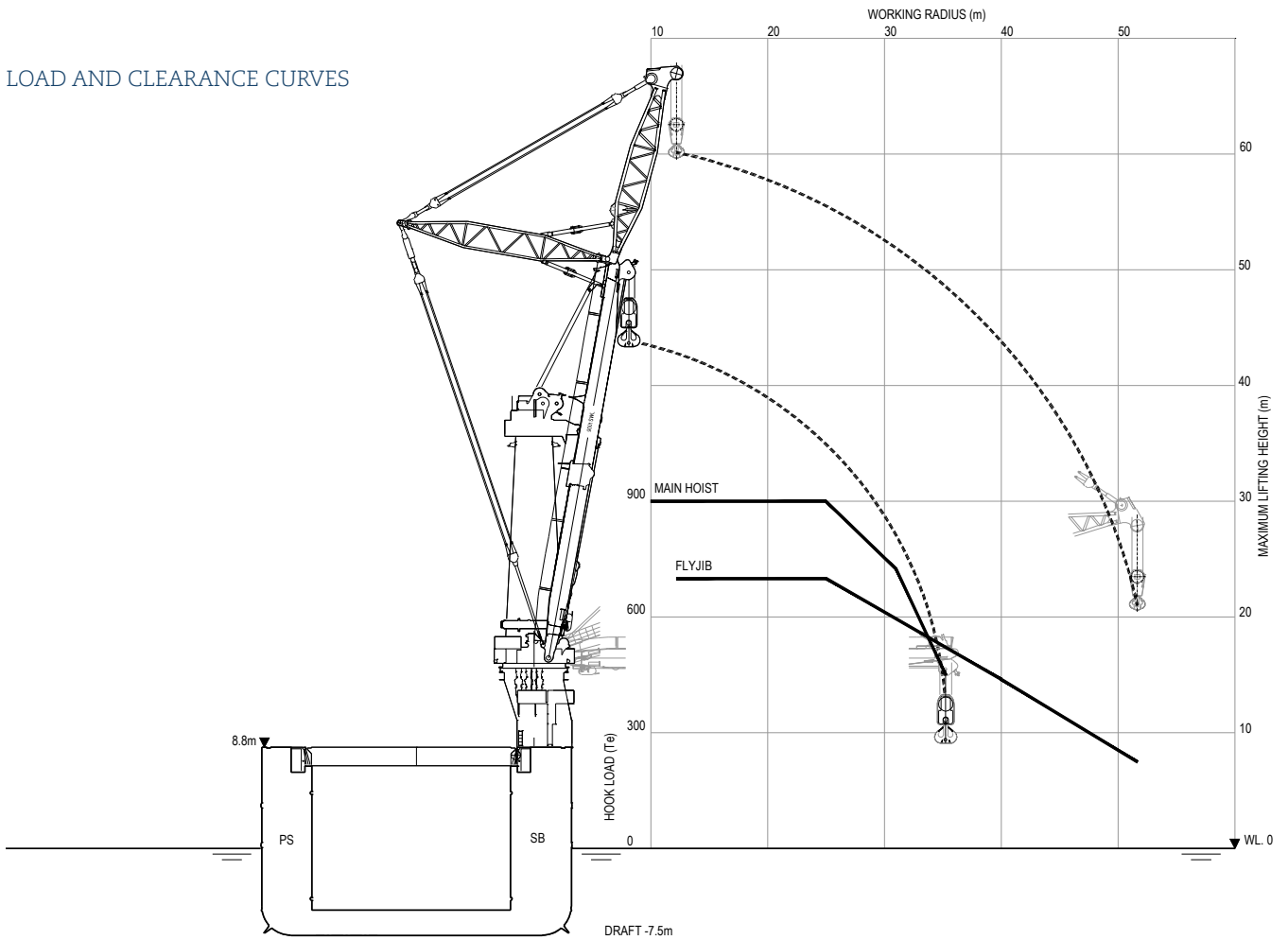
Accommodation/Helideck

Accommodation	up to 80 persons (incl. hospital)
	13 x single cabins,
	33 x double cabins
Helideck	12.8 Te (Sikorsky S-92-CAP437)

GENERAL ARRANGEMENT



LOAD AND CLEARANCE CURVES



HAVENSTRAAT 23
 3115 HC SCHIEDAM
 THE NETHERLANDS
 PHONE +31 10 79 00 300
 INFO@JUMBOMARITIME.NL



B

Previous research

In this appendix the four concepts which are analysed in the research of P. Harenberg are shown [6]. The four concepts can be found in figure B.1. Concept 1 is a pontoon attached next to the hull. Concept 2 is a pontoon, positioned at a distance from the hull. Concept 3 are hull extensions at both sides of the hull, which are almost all the way to the bottom of the hull. Concept 4 are two pontoons, positioned at one side of the vessel each.

A workability study is performed, from which the results can be found in paragraph 3.2.4. Concept 3 and 4 are analysed further and the conclusion of the research turned out that these concepts will lead to an increase of lifting capacity, but will also have negative side effects. Concept 3 has as drawback that the resistance significantly increases and therefore the speed decreases. Concept 4 has as drawback that the connection to the hull cannot be done in offshore conditions. The connection cannot be done offshore and therefore the solution would be to sail with the pontoons from the harbour, what also results in a higher resistance.

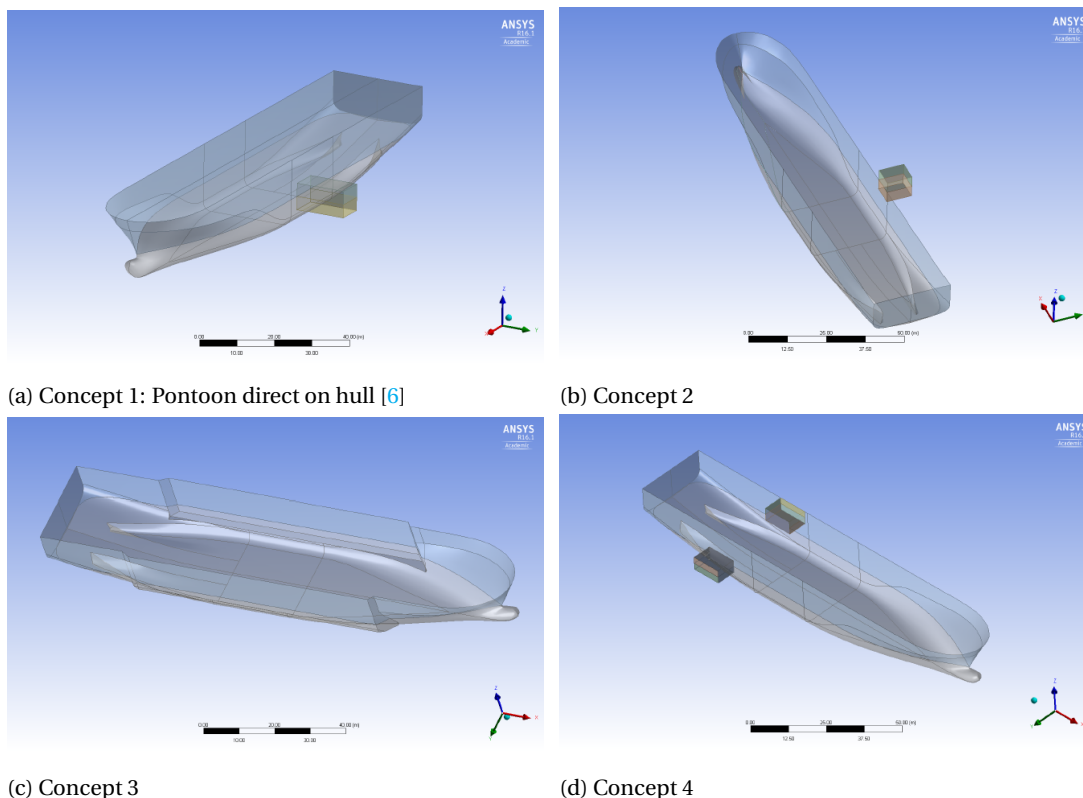


Figure B.1: Four concepts defined by P. Harenberg [6].

C

Resistance prediction method by Holtrop & Mennen

In this appendix the resistance method developed by Holtrop & Mennen is described [8], [10], [11] and [9]. The total resistance can be calculated as given in equation C.1.

$$R_{total} = R_F + R_{APP} + R_W + R_B + R_{TR} + R_A \quad (C.1)$$

where:

R_F	=	frictional resistance according to the ITTC-57 formula
R_{APP}	=	appendage resistance
R_W	=	wave-making resistance and wave breaking resistance
R_B	=	additional pressure resistance of bulbous bow
R_{TR}	=	additional pressure resistance due to transom immersion
R_A	=	model-ship correlation resistance

The frictional resistance R_F is determined from the flat plate friction formula, which is corrected for the ship form and can be calculated with equation C.2.

$$R_F = \frac{1}{2} \cdot \rho \cdot V^2 \cdot C_F \cdot (1 + k) \cdot S \quad (C.2)$$

where ρ is the water density, V the speed, C_F the coefficient of frictional resistance and S the total wetted surface. The flat plate friction coefficient C_F is calculated from the ITTC-57 formula with equation C.3.

$$C_F = \frac{0.075}{(\log R_n - 2)^2} \quad (C.3)$$

The form factor $(1 + k)$ can be calculated with equation C.4.

$$1 + k = 0.93 + 0.487118 \cdot c_{14} \cdot \left(\frac{B}{L}\right)^{1.06806} \cdot \left(\frac{T}{L}\right)^{0.46106} \cdot \left(\frac{L}{L_R}\right)^{0.121563} \cdot \left(\frac{L^3}{\nabla}\right)^{0.36486} \cdot (1 - C_p)^{-0.604247} \quad (C.4)$$

In this formula B and T are the moulded breadth and draught, respectively. L is the length on the waterline and ∇ is the displacement volume. C_p is the prismatic coefficient and L_R is defined as shown in equation C.5.

$$L_R = L \left(1 - C_P + 0.06 \cdot C_P \cdot \frac{LCB}{(4 \cdot C_P - 1)} \right) \quad (C.5)$$

where LCB is the longitudinal position of the center of buoyancy forward of $0.5L$ as percentage of L . The coefficient C_{14} (C.6) takes into account the stern shape of the vessel and is dependent on the aftbody form as can be seen in figure C.1.

Afterbody form	C_{stern}
Pram with gondola	-25
V-shaped sections	-10
Normal section shape	0
U-shaped sections with Hogner stern	10

Figure C.1: Stern shape coefficient C_{stern} .

$$c_{14} = 1 + 0.011 \cdot C_{stern} \quad (C.6)$$

The wave-making resistance for low and moderate speeds can be calculated with equation C.7. The other speed ranges are not described here, but can be found in the paper [9].

$$R_W = c_1 \cdot c_2 \cdot c_5 \cdot \nabla \cdot \rho \cdot g \cdot e^{(m_1 \cdot F_n^d + m_4 \cdot \cos(\lambda \cdot F_n^{-2}))} \quad (C.7)$$

where:

$$\begin{aligned} c_1 &= 2223105 \cdot c_7^{3.78613} \cdot \left(\frac{T}{B} \right)^{1.07961} \cdot (90 - i_E)^{-1.37565} \\ c_2 &= e^{-1.89 \cdot \sqrt{c_3}} \\ c_3 &= 0.56 \cdot A_{BT}^{1.5} / (B \cdot T \cdot (0.31 \cdot \sqrt{A_{BT}} + T_F - h_B)) \\ c_5 &= 1 - 0.8 \cdot A_T / (B \cdot T \cdot C_M) \\ c_7 &= 0.229577 \cdot \left(\frac{B}{L} \right)^{0.33333} \quad \text{when } \frac{B}{L} < 0.11 \\ c_7 &= \frac{B}{L} \quad \text{when } 0.11 < \frac{B}{L} < 0.25 \\ c_7 &= 0.5 - 0.0625 \cdot \frac{B}{L} \quad \text{when } \frac{B}{L} > 0.25 \\ c_{15} &= -1.69385 \quad \text{when } L^3 / \nabla < 512 \quad \text{or} \\ c_{15} &= -1.69385 + (L / \nabla^{1/3} - 8) / 2.36 \quad \text{when } 512 < L^3 / \nabla < 1726.91 \quad \text{or} \\ c_{15} &= 0 \quad \text{when } L^3 / \nabla > 1726.91 \quad \text{or} \\ c_{16} &= 8.07981 \cdot C_P - 13.8673 \cdot C_P^2 + 6.984388 \cdot C_P^3 \quad \text{when } C_P < 0.8 \\ c_{16} &= 1.73014 - 0.7067 \cdot C_P \quad \text{when } C_P > 0.8 \\ \lambda &= 1.446 \cdot C_P - 0.03 \frac{L}{B} \quad \text{when } \frac{L}{B} < 12 \quad \text{or} \\ \lambda &= 1.446 \cdot C_P - 0.36 \quad \text{when } \frac{L}{B} > 12 \\ d &= -0.9 \\ m_1 &= 0.0140407 \cdot \frac{L}{T} - 1.75254 \cdot \nabla^{1/3} / L - 4.79323 \cdot \frac{B}{L} - c_{16} \\ m_4 &= c_{15} \cdot 0.4 \cdot e^{(-0.034 \cdot F_n^{-3.29})} \end{aligned}$$

where i_E is the half angle of entrance of the waterline at the bow in degrees. C_M is the midship section coefficient and the immersed transom at rest is defined as A_T . The transverse area of the bulbous bow A_{BT}

measured at the position where the still waterline intersects the bow. The position of the center of this transverse area above the base is h_B .

The appendage resistance can be determined with equation C.8.

$$R_{APP} = 0.5 \cdot \rho \cdot V^2 \cdot S_{APP} \cdot (1 + k_2)_{eq} \cdot C_F \quad (C.8)$$

In this formula is S_{APP} the wetted area of the appendages. The form factors $(1 + k_2)$ change between different appendages and need to be estimated with the values in figure C.2.

Approximate $1 + k_2$ values	
rudder behind skeg	1.5 – 2.0
rudder behind stern	1.3 – 1.5
twin-screw balance rudders	2.8
shaft brackets	3.0
skeg	1.5 – 2.0
strut bossings	3.0
hull bossings	2.0
shafts	2.0 – 4.0
stabilizer fins	2.8
dome	2.7
bilge keels	1.4

Figure C.2: Approximate $1 + k_2$ values.

The equivalent $1 + k_2$ value for multiple appendages can be calculated with equation C.9.

$$(1 + k_2)_{eq} = \frac{\sum(1 + k_2) \cdot S_{APP}}{\sum S_{APP}} \quad (C.9)$$

The resistance of bow thruster tunnel openings need to be added by the appendage resistance and can be calculated with equation C.10.

$$R_{Bow\ thruster\ tunnel} = \rho \cdot V^2 \cdot \pi \cdot d^2 \cdot C_{BTO} \quad (C.10)$$

where d is the tunnel diameter and C_{BTO} ranges from 0.003 to 0.012.

The additional resistance due to the bulbous bow near the water surface can be calculated with equation C.11.

$$R_B = 0.11 \cdot e^{(-3 \cdot P_B^2)} \cdot F_{ni}^3 \cdot A_{BT}^{1.5} \cdot \frac{\rho \cdot g}{(1 + F_{ni}^2)} \quad (C.11)$$

where P_B is a coefficient which is dependent on the emergence of the bow and can be calculated with equation C.12. F_{ni} is the Froude number based on the immersions of the bow and can be calculated with equation C.13.

$$P_B = 0.56 \cdot \sqrt{A_{BT}} / (T_F - 1.5 \cdot h_B) \quad (C.12)$$

$$F_{ni} = V / \sqrt{g \cdot (T_F - h_B - 0.25 \cdot \sqrt{A_{BT}}) + 0.15 \cdot V^2} \quad (\text{C.13})$$

The additional pressure resistance due to the immersed transom can be determined with equation C.14.

$$R_{TR} = 0.5 \cdot \rho \cdot V^2 \cdot A_T \cdot c_6 \quad (\text{C.14})$$

where c_6 is related to the Froude number based on the transom immersion, which can be calculated with equation C.15. In this equation C_{WP} is the waterplane area coefficient.

$$\begin{aligned} c_6 &= 0.2 \cdot (1 - 0.2 \cdot F_{nT}) \text{ when } F_{nT} < 5 \text{ or} \\ c_6 &= 0 \text{ when } F_{nT} \geq 5 \end{aligned}$$

$$F_{nT} = V / \sqrt{2 \cdot g \cdot A_T / (B + B \cdot C_{WP})} \quad (\text{C.15})$$

The last resistance component defined by Holtrop & Mennen [9] is the model-ship correlation resistance R_A , which can be calculated with equation C.16.

$$R_A = \frac{1}{2} \cdot \rho \cdot V^2 \cdot S \cdot C_A \quad (\text{C.16})$$

where C_A can be calculated with equation C.17.

$$C_A = 0.006 \cdot (L + 100)^{-0.16} - 0.00205 + 0.003 \cdot \sqrt{L/7.5} \cdot C_B^4 \cdot c_2 \cdot (0.04 - c_4) \quad (\text{C.17})$$

$$\begin{aligned} c_4 &= \frac{T_F}{L} \text{ when } \frac{T_F}{L} \leq 0.04 \text{ or} \\ c_4 &= 0.04 \text{ when } \frac{T_F}{L} > 0.04 \end{aligned}$$

C.1. Raw data from the Holtrop-Mennen method

Table C.1 contains the raw data of the calculations of the Holtrop-Mennen method as described above. The calculations are done at a draft of 6.5 meter and 7.5 meter.

Table C.1: Raw data from the Holtrop-Mennen method of 1984.

Holtrop-Mennen method			
	Draft 7.5 meter	Remarks (T=7.5m T=6.5m)	Draft 6.5 meter
Ship dimensions:			
Loa [m]	144.1		144.1
Lpp [m]	133.8		133.8
B [m]	26.7		26.7
Depth [m]	14.1		14.1
Draft [m]	7.5		6.5
V (17 knots) [m/s]	8.75		8.75
Displacement (at 7.5 m) [Te]	20120		17117
Wetted surface area bare hull [m ²]	4740		4412
Wetted surface area with appendages [m ²]	4860		4532
C _b	0.741		0.719
C _m	0.985		0.977
C _p	0.752		0.736
L/B ratio	5.011		5.011
B/D ratio	3.533		4.108
L _r	40.60		42.82
l _{cb}	2.47		2.47
rho [kg / m ³]	1025		1025
Displacement volume	19629.27		16699.26
Fn	0.2414		0.2414
Frictional resistance:			
R _f [kN]	366.82		336.71
vorm factor 1+k	1.29		1.27
c ₁₂	0.53	T/L=0.056 T/L=0.049	0.51
c ₁₄	1	Normal section shape	1
C _f	1.53E-03		1.53E-03
R _n	9.85E+08		9.85E+08
Kinematic viscosity	1.19E-06	Seawater at 15 degree	1.19E-06
Appendage resistance:			
R _{app} [kN]	22.13		22.13
vorm factor 1+k ₂	2.22		2.22
C _f	1.53E-03		1.53E-03
Bow thruster tunnel openings resistance [kN]	6.14		6.14
Diameter thruster opening	2.04	Document MARIN	2.04
C _{BTO}	0.006	Ranges from 0.003 to 0.012	0.006
Wave-making resistance:			
R _w [kN]	262.35		197.85
labda	0.94		0.91
d	-0.90		-0.90
c ₁	6.42		5.29
c ₂	0.71		0.66
c ₅	0.97		0.97
c ₇	0.20	0.11 <B/L <0.25	0.20
m ₁	-2.26		-2.22
m ₄	-1.76E-02	c ₁₅ : L ³ /displacement = 512	-1.76E-02

0.5*alpha of i_E	43.49		42.14
c3	0.03		0.05
Abt	13.88	Calculated met rhinoceros	13.88
hB	4.15	Calculated met rhinoceros	4.15
A_T (area of the transom)	6.30	See noteblock	6.30
Bulbous bow resistance:			
Rb [kN]	18.83		70.75
pB	1.64		7.59
Fni	1.47		1.74
i	2.42		1.42
Pressure resistance due to the immersed transom:			
Rtr [kN]	0		0
c6	0		0
F_nT	5.59		5.59
C_WP	0.89		0.89
Model-ship correlation resistance:			
Ra [kN]	87.04		81.17
Ca	4.57E-04		4.57E-04
c4	0.04	T/L > 0.04	0.04
OR Ca	-8.31E-09		-8.31E-09
ks	1.50E-04		1.50E-04

C.2. Evolution of the Holtrop-Mennen method from 1977 to 1984

In table C.2 the resistance method developed by Holtrop & Mennen for the Fairplayer is shown for the years 1977 [8], 1978 [10], 1982[11] and 1984 [9]. The calculations are also done for the Fairplayer with a sponson and shown in the bottom of table C.2. There are a few remarks that can be made. The method is improved over the years with an increase in the amount of resistance components. The frictional resistance and the model-ship correlation resistance are not changed much over the years. This cannot be said from the wave-making resistance which is significantly changed in 1982. The wave-making resistance component of the Fairplayer with a sponson is decreased significantly compared to the Fairplayer without a sponson. The empirical formulas are based on a series of hull shapes and the Fairplayer with a sponson will differ significantly from these hull shapes, which can explain the large difference.

Table C.2: Evolution of the Holtrop-Mennen method.

Holtrop-Mennen method		Draft 7.5 meter		Draft of 6.5 meter	
1977					
		[kN]	%	[kN]	%
Frictional resistance	Rv	378.23	78.23	344.50	78.80
Wave-making resistance	Rw	33.95	7.02	26.18	5.99
Model-ship correlation resistance	Ra	71.31	14.75	66.50	15.21
Total	R	483.49	100.00	437.17	100.00
1978					
		[kN]	%	[kN]	%
Frictional resistance	Rv	376.66	74.16	343.35	66.78
Wave-making resistance	Rw	25.36	4.99	18.91	3.68
Bulbous bow resistance	Rb	18.83	3.71	70.75	13.76
Model-ship correlation resistance	Ra	87.04	17.14	81.17	15.79
Total	R	507.89	100.00	514.18	100.00
1982					
		[kN]	%	[kN]	%
Frictional resistance	Rv	368.89	46.12	335.40	45.40
Appendage resistance	Rapp	22.13	2.77	22.13	3.00
Wave-making resistance	Rw	302.97	37.88	229.25	31.03
Bulbous bow resistance	Rb	18.83	2.35	70.75	9.58
Additional resistance of stern	Rtr	0.00	0.00	0.00	0.00
Model-ship correlation resistance	Ra	87.04	10.88	81.17	10.99
Total	R	799.86	100.00	738.69	100.00
1984					
		[kN]	%	[kN]	%
Frictional resistance	Rv	366.82	48.45	336.71	47.52
Appendage resistance	Rapp	22.13	2.92	22.13	3.12
Wave-making resistance	Rw	262.35	34.65	197.85	27.92
Bulbous bow resistance	Rb	18.83	2.49	70.75	9.98
Additional resistance of stern	Rtr	0.00	0.00	0.00	0.00
Model-ship correlation resistance	Ra	87.04	11.50	81.17	11.45
Total	R	757.18	100.00	708.60	100.00
1984, Fairplayer with a sponson					
		[kN]	%		
Frictional resistance	Rv	414.75	61.45		
Appendage resistance	Rapp	22.13	3.28		
Wave-making resistance	Rw	125.73	18.63		
Bulbous bow resistance	Rb	18.83	2.79		
Additional resistance of stern	Rtr	0.00	0.00		
Model-ship correlation resistance	Ra	93.49	13.85		
Total	R	674.93	100.00		

D

RAPID calculation

The adjusted Holtrop-Mennen method to calculate the resistance of the Fairplayer uses the program RAPID to calculate the wave-making resistance. The software RAPID is developed at MARIN and solves the exact, fully non-linear potential flow problem by an iterative procedure, based on a raised-panel method [20]. The steps that are followed to create a 3D model of the Fairplayer and to create the concepts with a sponson are described in this appendix.

In paragraph D.1 the adjustment of the 3D model, to make it suitable for calculations with RAPID, is described. RAPID is a panel method, so a grid of the concepts need to be generated in Rhinoceros, which is explained in paragraph D.2. The calculation with RAPID is described in paragraph D.3. Finally the symmetric calculations are done with RAPID, which are described in paragraph D.4.

D.1. Adjustment of the 3D model

The 3D model of the J-class vessel, which is available for the analysis can be found in figure D.1. The adjustments and generation of the concepts are done with Rhinoceros.

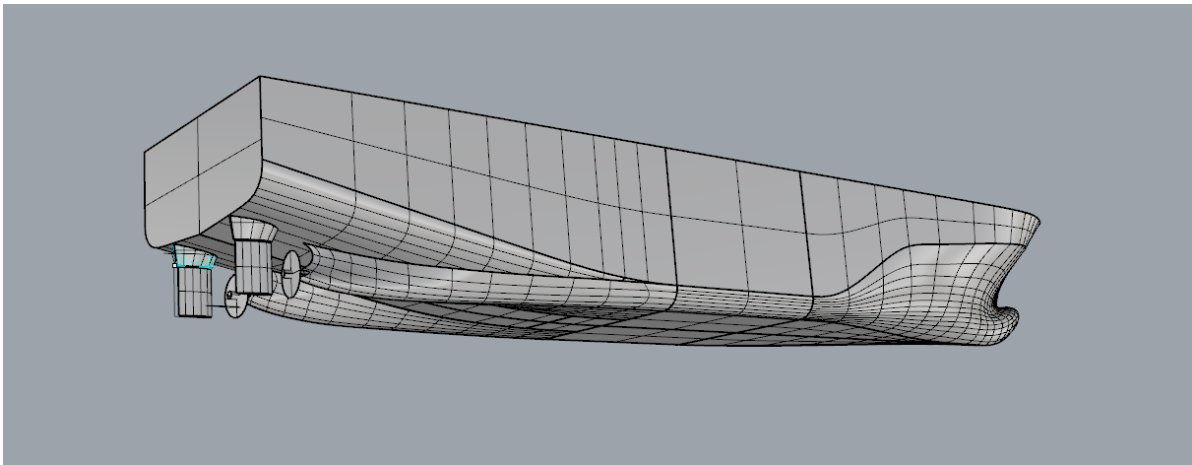


Figure D.1: 3D model of the J-class vessel the Fairplayer.

The 3D model contains details such as the rudders and the propellers. The rudders and propellers does not change when the sponson is applied to the vessel, so it is chosen to leave them out from the analysis. The modified hull form without rudders and propellers can be seen in figure D.2.

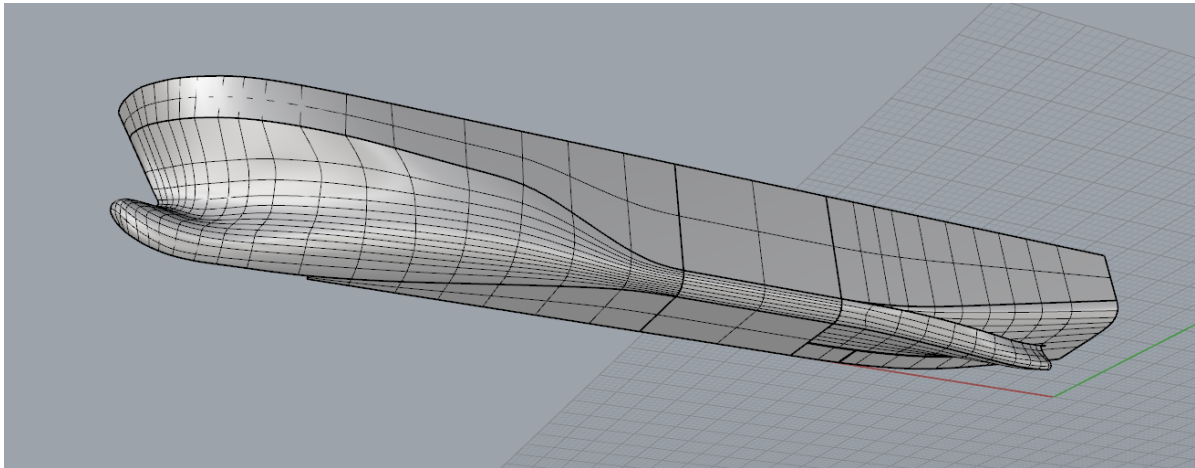


Figure D.2: 3D model of the J-class vessel the Fairplayer without rudders and propeller.

A separate plug-in for Rhinoceros comes with the software of RAPID, which can be used to generate a grid in Rhinoceros. It turned out that this hull file could not simply be used to generate a grid for the calculations in RAPID. The plug-in can generate a grid on a surface of the 3D model, but the original hull file consists of eleven surfaces, which are separated by the thick black lines in figure D.2. The program RAPID can calculate the wave pattern of a hull shape which has multiple surfaces. The program is unable to cope with a panel file where the free surface changes from one to another surface in height direction. This is seen in the fore- and aftship of the vessel, so the vessel needs to be adjusted.

The bow of the vessel is merged into one surface, which extends over the whole height of the vessel. The aft of the vessel could not be merged (with the *'merge'* function in Rhinoceros), because the surfaces lay too much apart. Therefore it is chosen to create contour lines over the aft of the vessel with the *'contour'* function in Rhinoceros. This function creates line elements over the height of the vessel, which can be connected to create a smooth surface. In order to use this method, the point on the hull where the propeller shaft comes out of the hull needs to be adjusted. The hull model which is used for the calculations can be found in figure D.3.

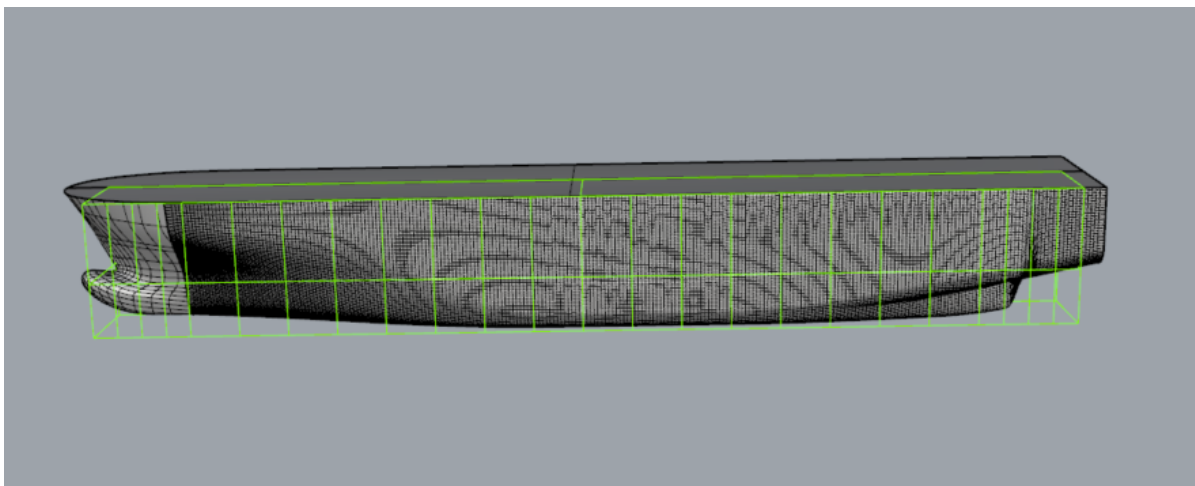


Figure D.3: 3D model of the J-class vessel the Fairplayer, which is used to create a grid for RAPID.

The green frame in figure D.3 marks the main dimensions of the vessel, which are filled in. From this 3D model with only two surfaces at one side of the vessel, the generation of a grid is only a small step.

D.2. Grid generation

The program RAPID uses panels on the hull and on the free surface around the hull. The input of RAPID needs to be done as a .pan file, which can be seen as a text file. It contains coordinates of the corner points of the

hull panels, arranged in a fixed order. This panel file can be created with a plug-in for Rhinoceros [19].

With the plug-in in Rhinoceros the grid can be generated, where the number of rows and columns for each surface need to be filled in. An example of a grid on this hull can be found in figure D.4. For a symmetric vessel only on the portside of the hull panels needs to be defined. If an asymmetric vessel is analysed, the starboard side of the hull needs to be defined as well.

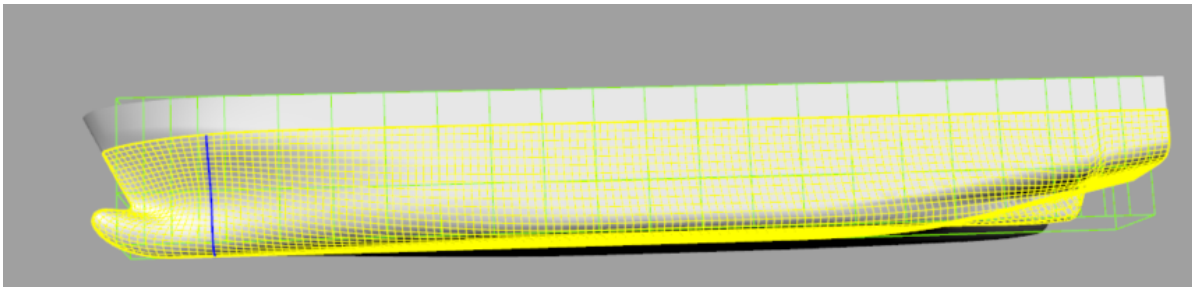


Figure D.4: 3D model of the J-class vessel the Fairplayer with a grid for RAPID.

Besides the input for the amount of columns and rows for each of the surfaces the grid contractions can also be adjusted. The grid contractions results in panels that are large or smaller at the sides of the surface. This can be useful to use when a part of the surface has a very complex or curved shape, such as a bulbous bow.

Before saving the grid in a panel file, the grid needs to be oriented for RAPID, which is one of the functions of the plug-in. After this the file can be saved as a panel file (.pan) and can be imported in RAPID to perform a calculation.

D.3. Calculation

The calculation in RAPID starts with importing a panel file. This panel file contains the coordinates of the corner points of the panels on the hull in an organized way. The panel file is read by the program and the wetted surface, the displacement and the LCB are shown. These can be checked in order to see if the panel file is created and imported correctly, which can be seen in figure D.5.

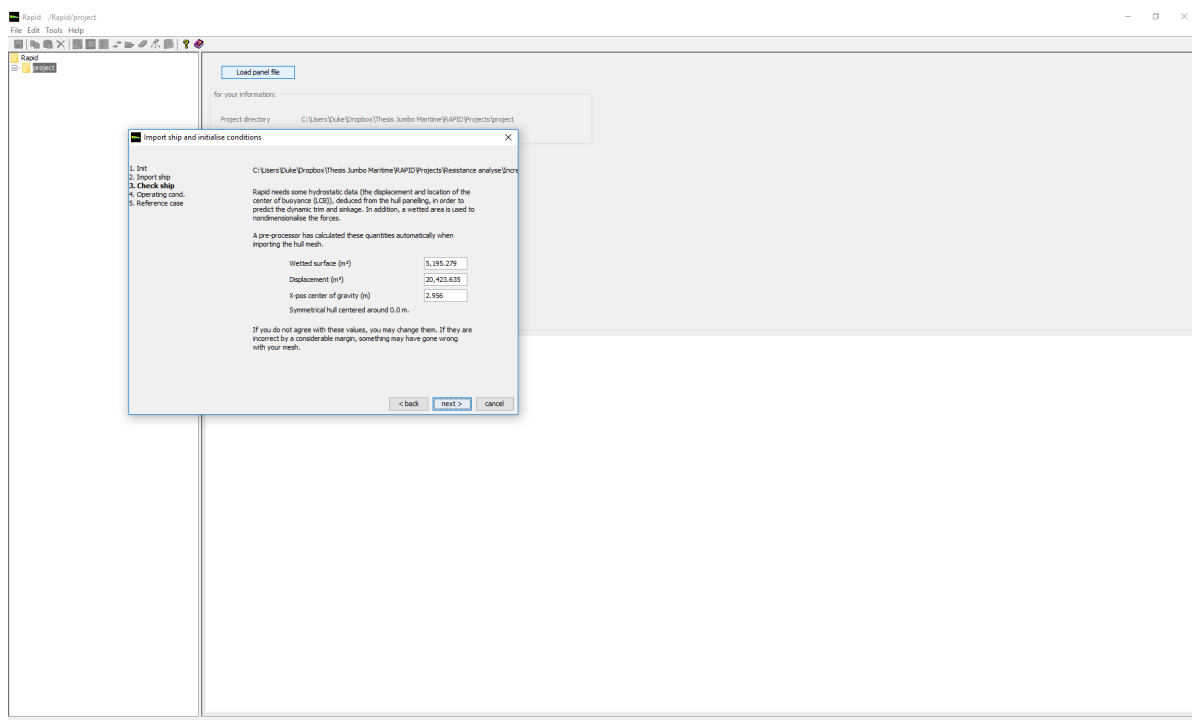


Figure D.5: Window with the dimensions of the imported panel file of the hull.

After this the input variables such as the speed of the vessel and the water depth can be chosen. For the calculations the water depth is set at infinite and the speed of the vessel at 17 knots, which can be seen in figure D.6.

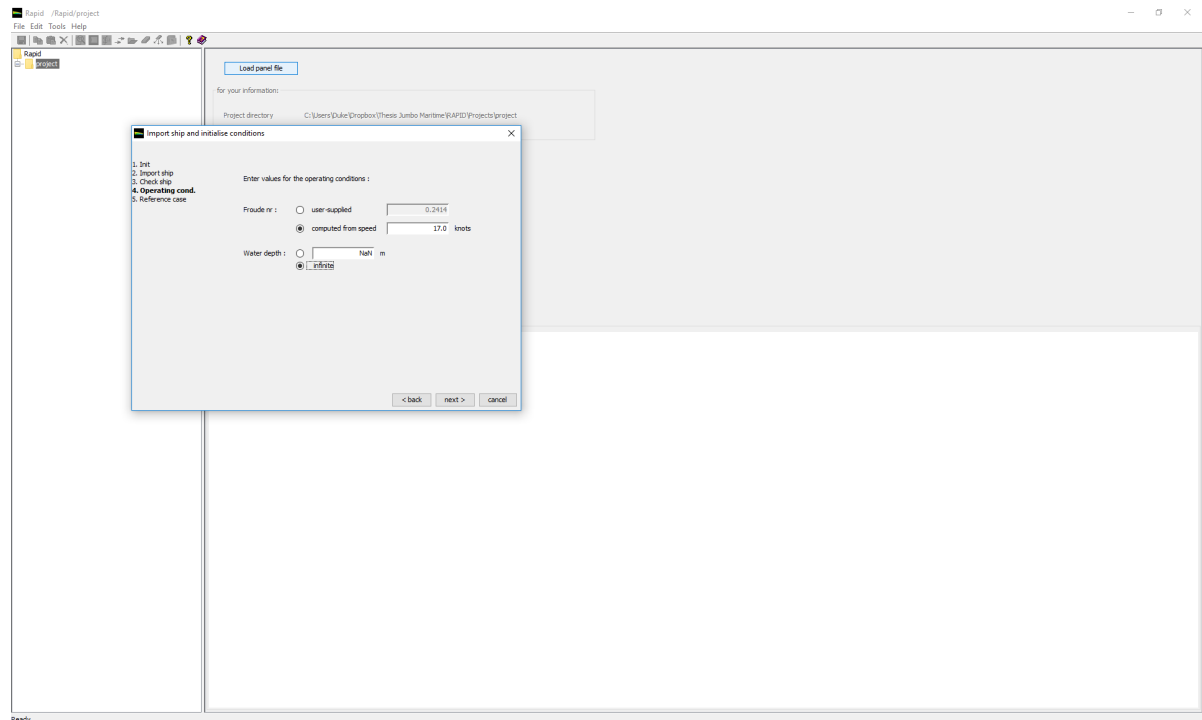


Figure D.6: Window with the speed of the vessel and the water depth can be seen.

The generation of the grid can be viewed in ParaView, which can read the panel file from RAPID. This gives a check if the panel file is generated correctly and if the panels represent the hull surface in a proper way. An example of the hull shape described by the panels can be found in figure D.7.

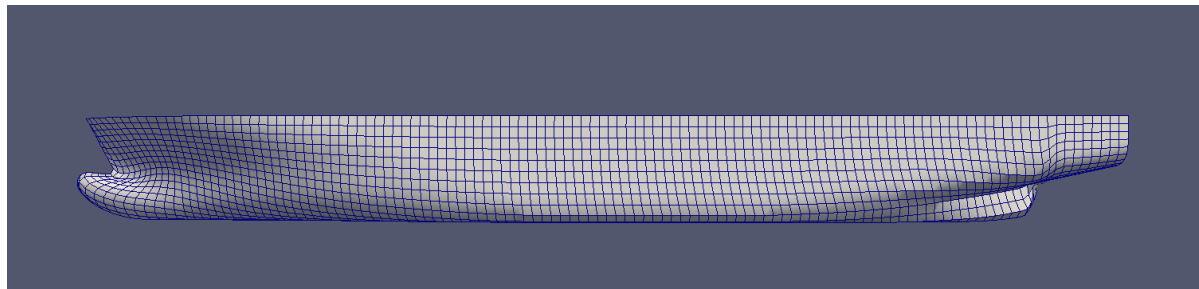


Figure D.7: Panel file of the J-class vessel the Fairplayer in ParaView.

The next step after importing the panel file is to generate a free surface around the vessel. For this free surface the number of panels per wavelength needs to be specified, the default value is 30 panels. Besides the amount of panels in front and aft of the hull can be adjusted, as well as the amount of strips. The calculations can be done with and without panels at the transom of the hull, this is explained in detail in paragraph 4.2.1. The input window can be found in figure D.8.

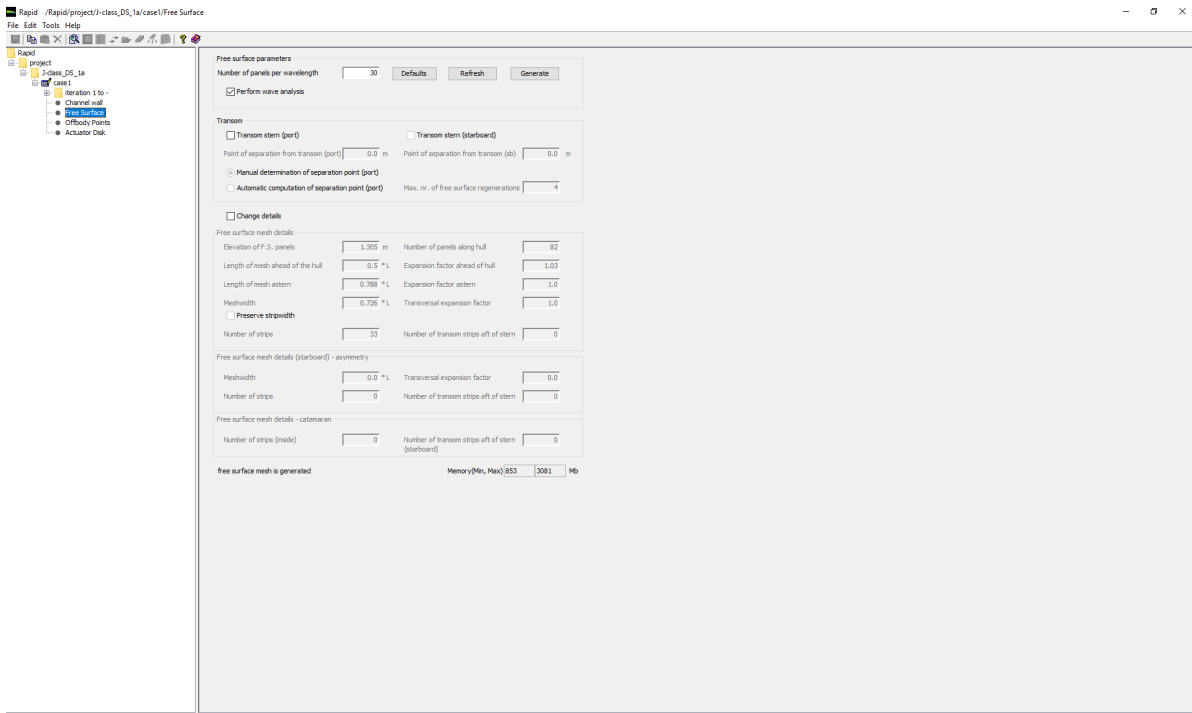


Figure D.8: Input window for the generation of the free surface in RAPID.

After generation of the free surface, the calculation can be started. The input window can be found in figure D.9. In order to increase the speed and to help the calculation to reach convergence faster, the sinkage and trim of the vessel can be entered. There are also other methods to help convergence of the solution, which are not discussed here but can be found in the user guide [20].

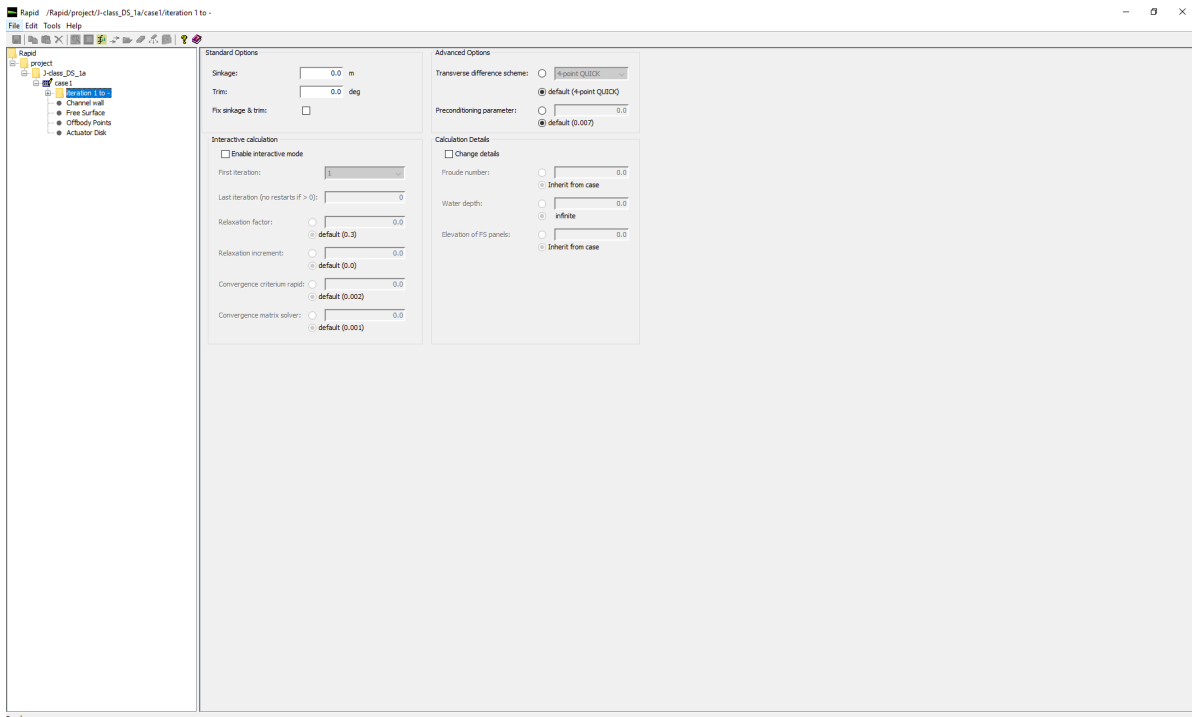


Figure D.9: Input window for the start of the calculation in RAPID.

When starting the calculation RAPID automatically opens a new window which contains the information

about the current run as can be seen in figure D.10.

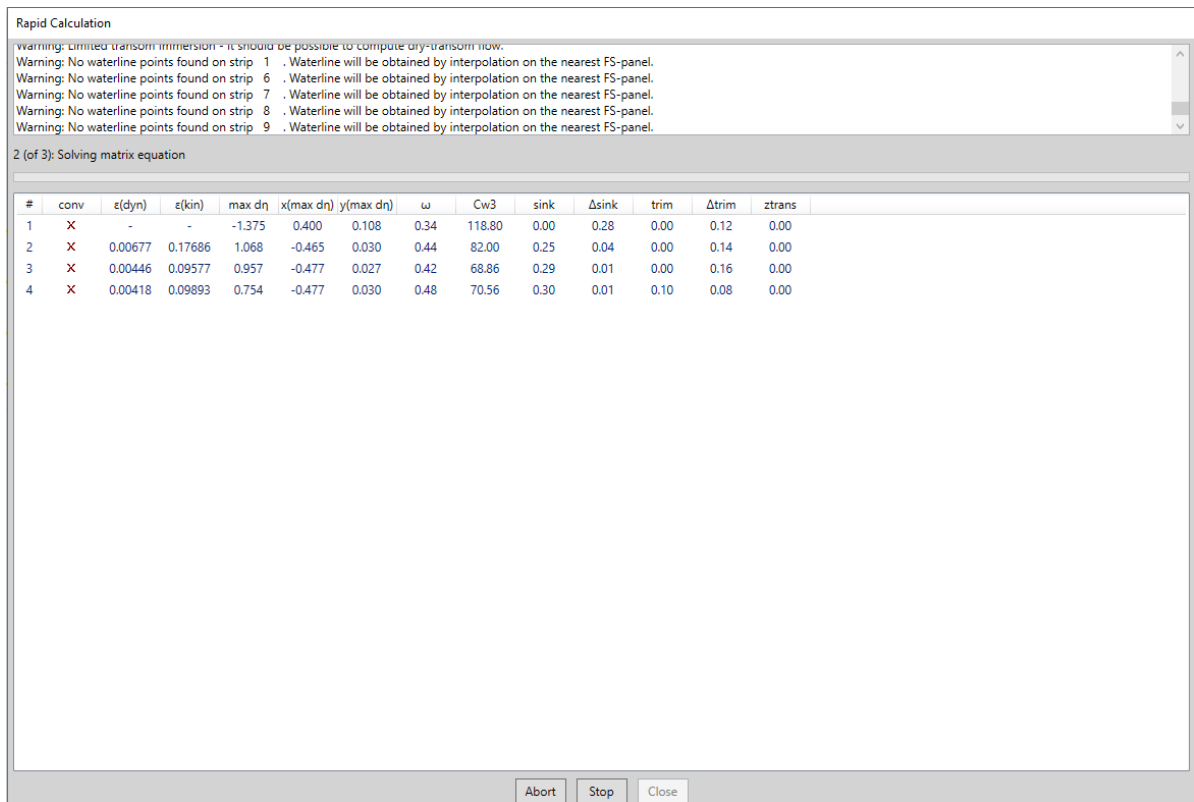


Figure D.10: Window with all the information about the calculation in RAPID.

When the calculation is performed the information about all iterations can be found in the output window, as well as all the warnings which occurred. This output window can be seen in figure D.11.

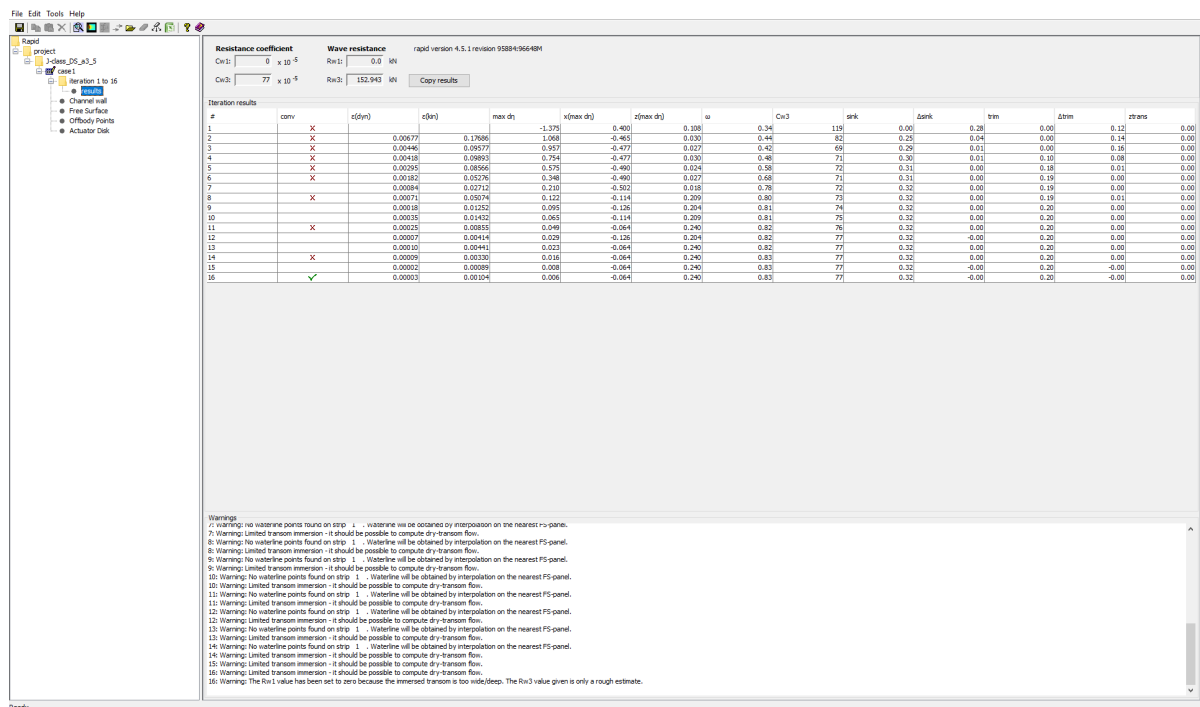


Figure D.11: Output window with all the information about the iterations of the calculation in RAPID.

Next to the resistance values and all the information about the iterations, RAPID generates also other output files. These output files contain information, such as velocities and pressures at the panels on the hull, velocities and wave heights at panels of the free surface, but also on the hull. Information about the sinkage and trim of the vessel and the forces and moments on the panels of the hull can also be found. This can be visualized with ParaView and an example of the wave pattern can be found in figure 4.2a.

D.4. Calculation with a sponson

The calculations are described in paragraph D.3 for the base hull of the Fairplayer. The calculations of the Fairplayer with a sponson are quite similar, but the creation of a concepts need to be done. The generation of the concepts in Rhinoceros starts with the base hull as can be seen in figure D.3. The contours of the sponson are drawn yellow in the side view in figure D.12.

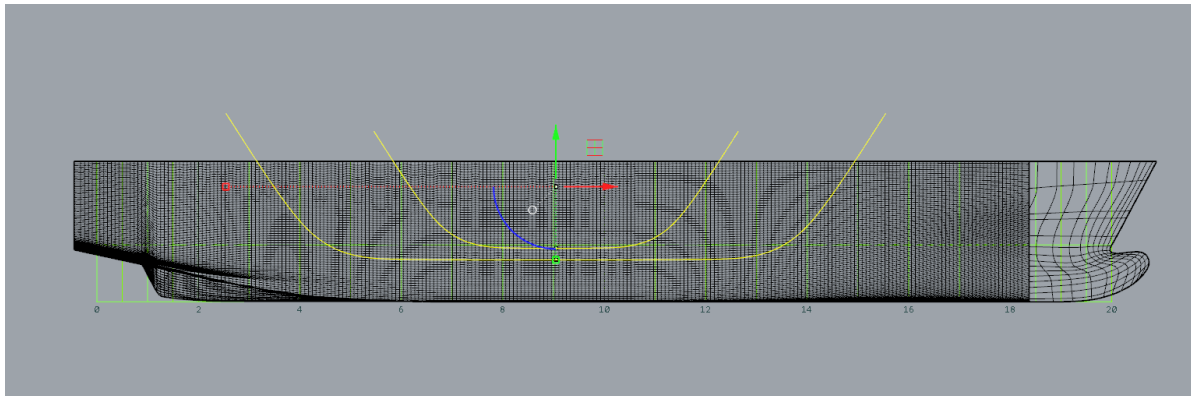


Figure D.12: Contours of the sponson in the hull of the Fairplayer in Rhinoceros.

The contours are extended to create an intersection with the surface of the hull. The intersections are used to split the hull surface into three parts, which can be seen in figure D.13. The bottom part is kept untouched, the middle part is deleted to create the transition and the top part is used as side of the sponson.

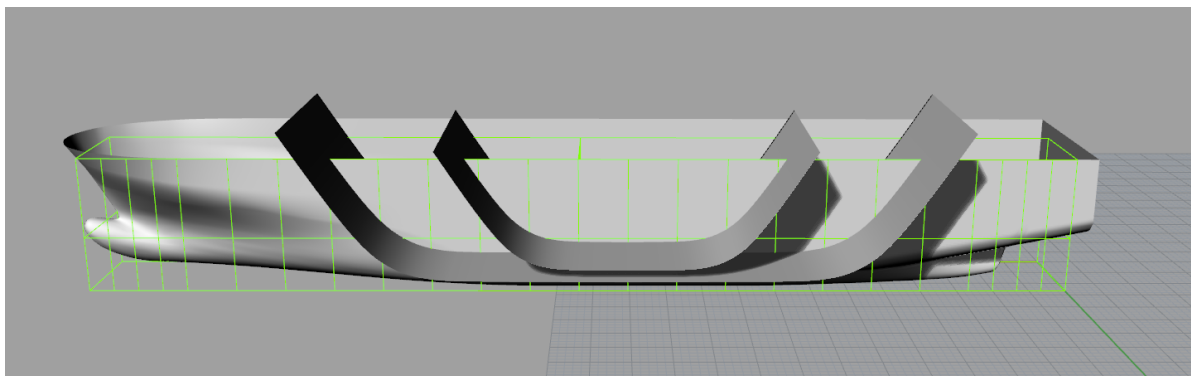


Figure D.13: Intersection of the contours with the hull of the Fairplayer in Rhinoceros.

As described, the side of the sponson is moved to the desired width. In order to create the transition between the sponson and the vessel, a contour line is drawn. This contour line is shown in yellow in figure D.14.

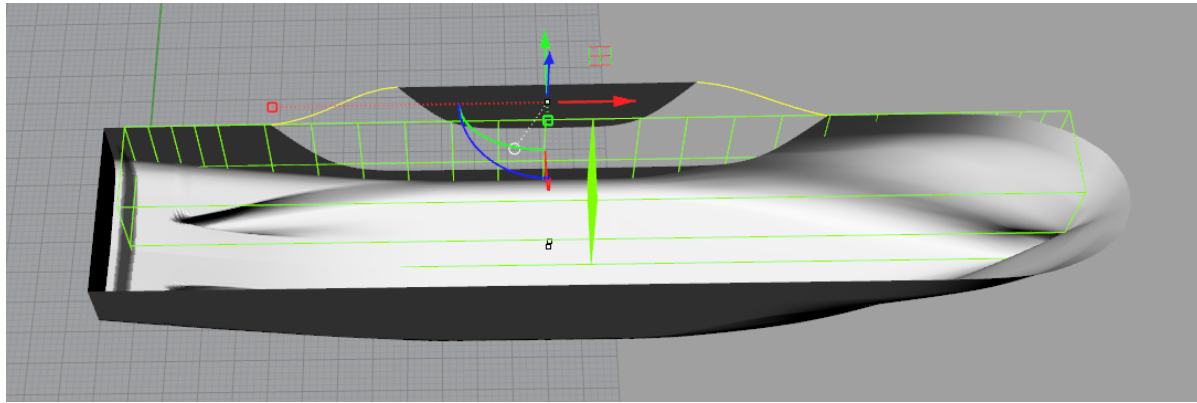


Figure D.14: Transition of the sponson to the hull of the Fairplayer in Rhinoceros.

From these contours the transition of the sponson is generated. As described in paragraph D.1 the model should not have different surfaces in height direction around the waterline. The sponson now consists of three surfaces in height direction. In order to create one surface from this, contour lines in height direction are drawn and are connected. The contour lines can be found in figure D.15.

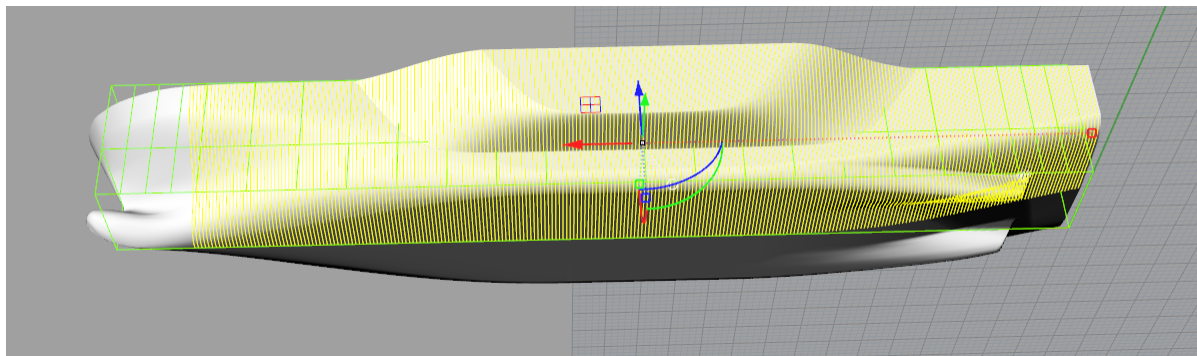


Figure D.15: Contour lines to create one surface at the side of the sponson in Rhinoceros.

Now the model is created, the generation of the grid in Rhinoceros is done the same as described in paragraph D.2 and the calculation is the same as described in paragraph D.3. The panels on the free surface will be slightly different, due to the sponson at the side of the hull. The free surface of the Fairplayer with a sponson can be found in figure D.16.

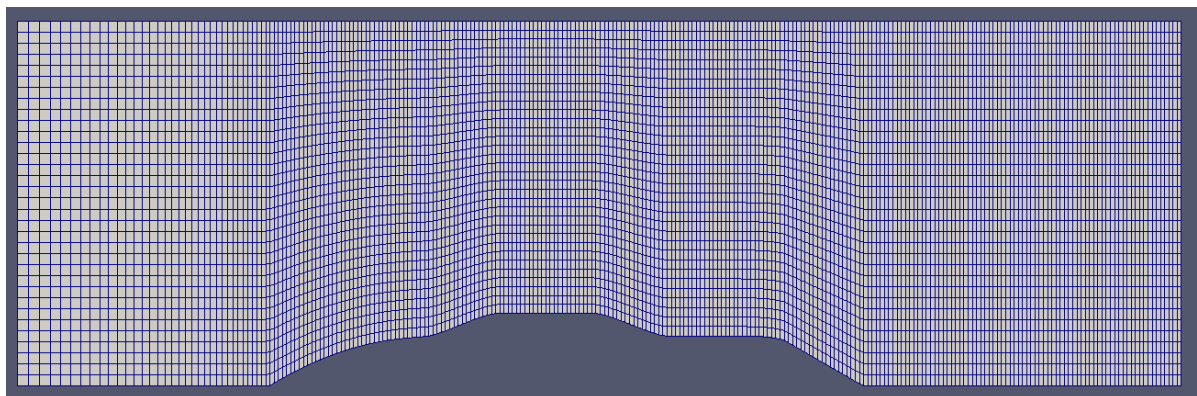


Figure D.16: Panels of the free surface for the Fairplayer with a sponson.

The wave pattern for the Fairplayer with a sponson is a symmetrical calculation and an example can be seen in figure D.17.

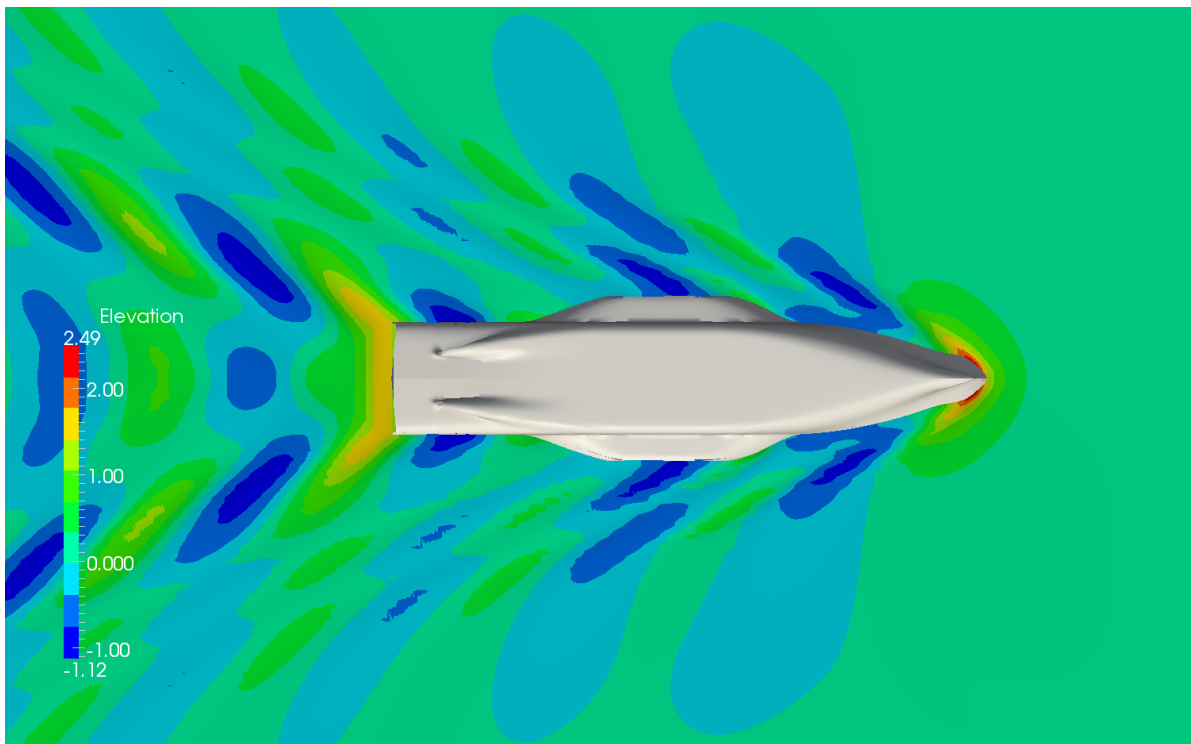


Figure D.17: Wave pattern of the Fairplayer with a sponson calculated with RAPID.

D.5. First calculations of a sponson with RAPID

The first calculations of a concept with a sponson in RAPID had a sponson which had a short transition at the front and aft. This concept can be seen in figure D.18. This concept turned out not to give a convergent solution. The non-viscous flow calculation in RAPID resulted in wave height which becomes larger than twice the stagnation wave height and the calculation aborted. This can be seen in figure D.19. Behind the sponson the non-viscous flow resulted in wave crests and troughs which became significantly. With a viscous fluid, this would result in a separation of the flow, so in practice this concept would not be feasible.

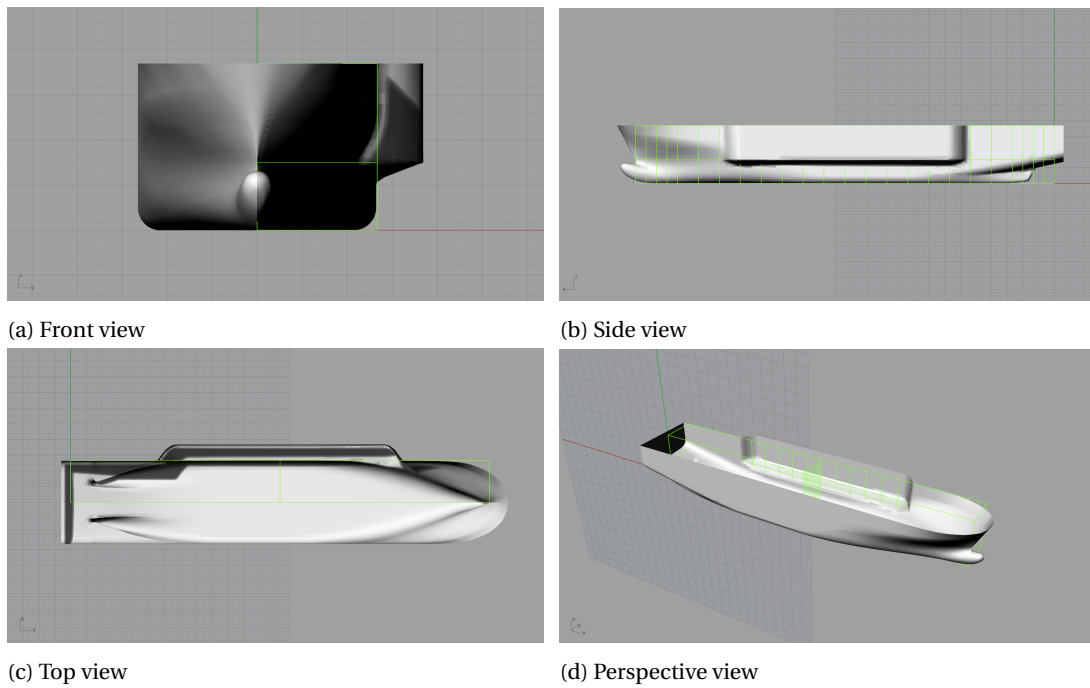


Figure D.18: Rhinoceros 3D model of the first test concept.

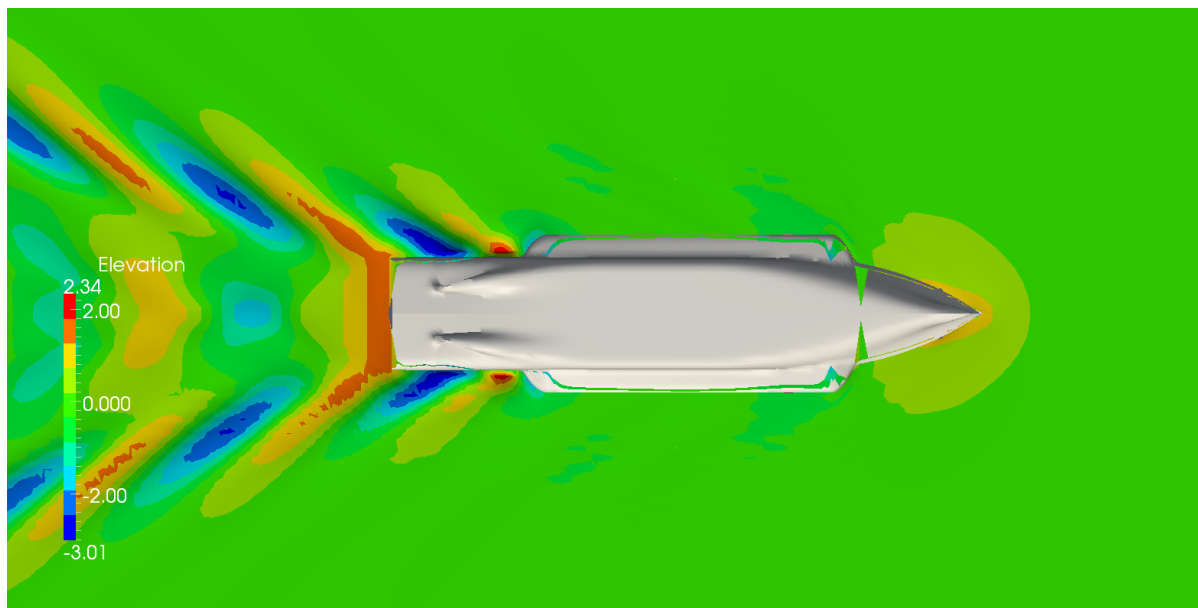


Figure D.19: Wave pattern of the first concept with a sponson calculated with RAPID.

By suggestion, the next series of concepts is made with a larger transition at the front and an open aft of the sponson. With this open aft it was planned to avoid large waves behind the sponson, so the position and shape of the front of the sponson could be optimized. This concept is seen in figure D.20. The wave pattern of this concept is seen in figure D.21.

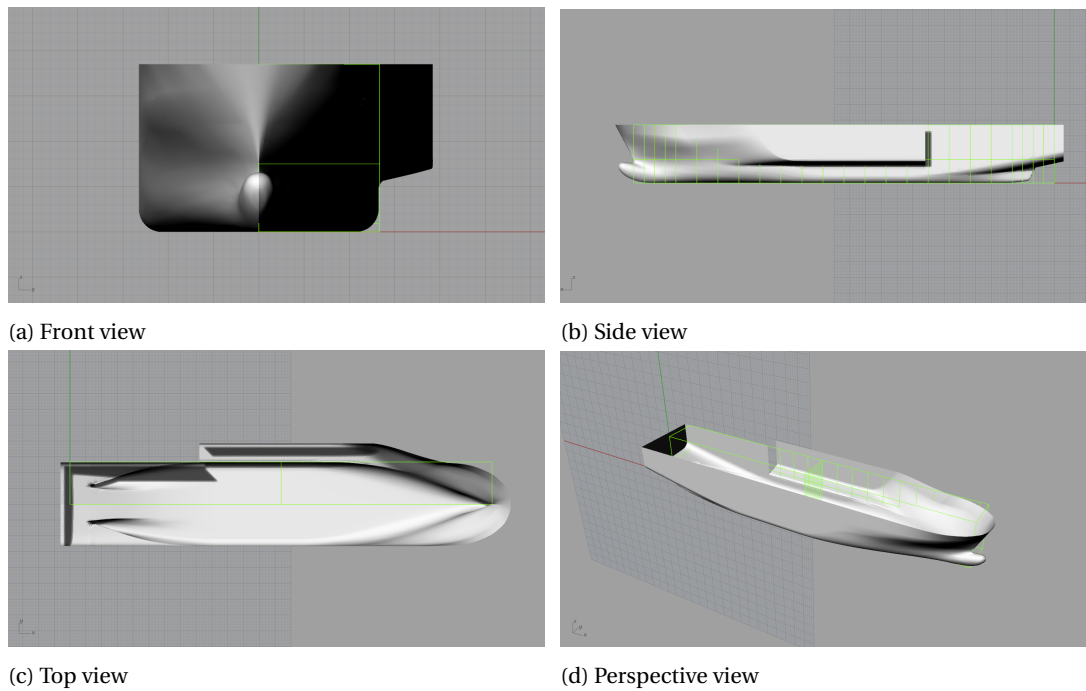


Figure D.20: Rhinoceros 3D model of the test concept with an open aft of the sponson.

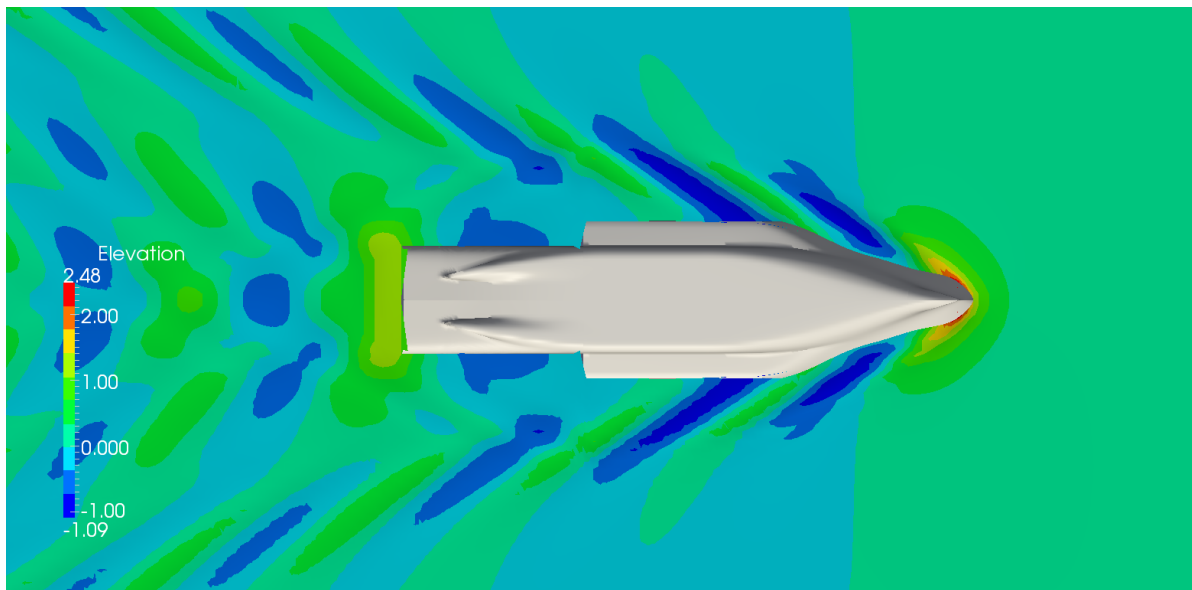


Figure D.21: Wave pattern of the concept with an open aft of the sponson calculated with RAPID.

This open aft of the sponson resulted in an unpredictable RAPID calculation. The free surface grid study for a concept with a sponson with an open aft resulted in 40% of the calculations with an error:

Error in RAPID: Divergence of the iteration process!

This is checked in the RAPID manual where the following instructions are given:

Remedy: The calculated change of the wave height becomes larger than twice the stagnation wave height. Check your meshes and your input. Are they according to the rules given in Chapter 8? If so, see Chapter 10 for other remedies.

The other calculations of the grid study gave such diverse results that this concept with an open aft of the sponson have been questioned. This can be seen in figure D.22. The free surface changes resulted in wave-making resistance differences of 70%, by only a small change of the free surface.

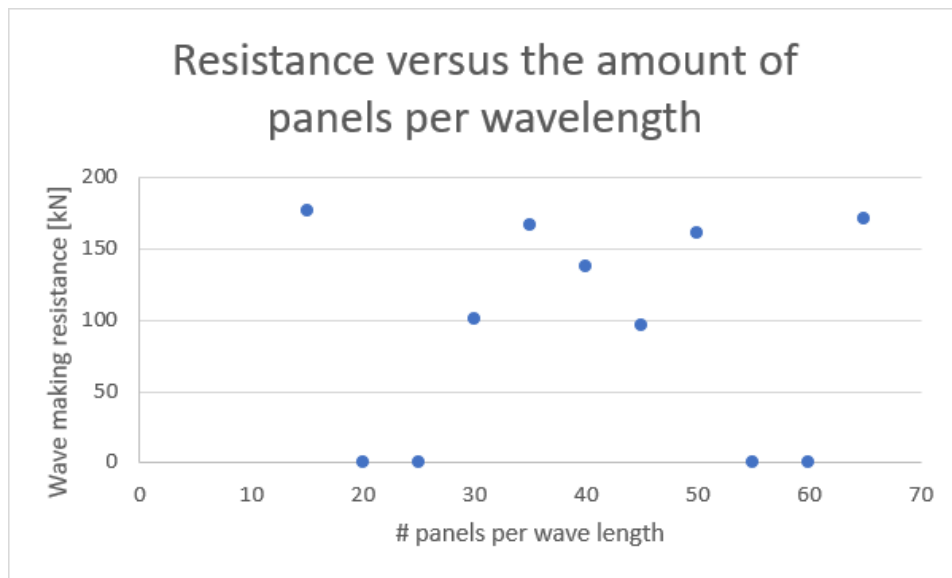


Figure D.22: Free surface grid study for the concept with a sponson with an open aft.

If looking at the free surface critically, it can be seen that there is large jump in the free surface grid at the aft of the sponson. This can be seen in figure D.23. It is expected that this jump leads to discretization errors in the calculation, which explains the errors and the unpredictable results.

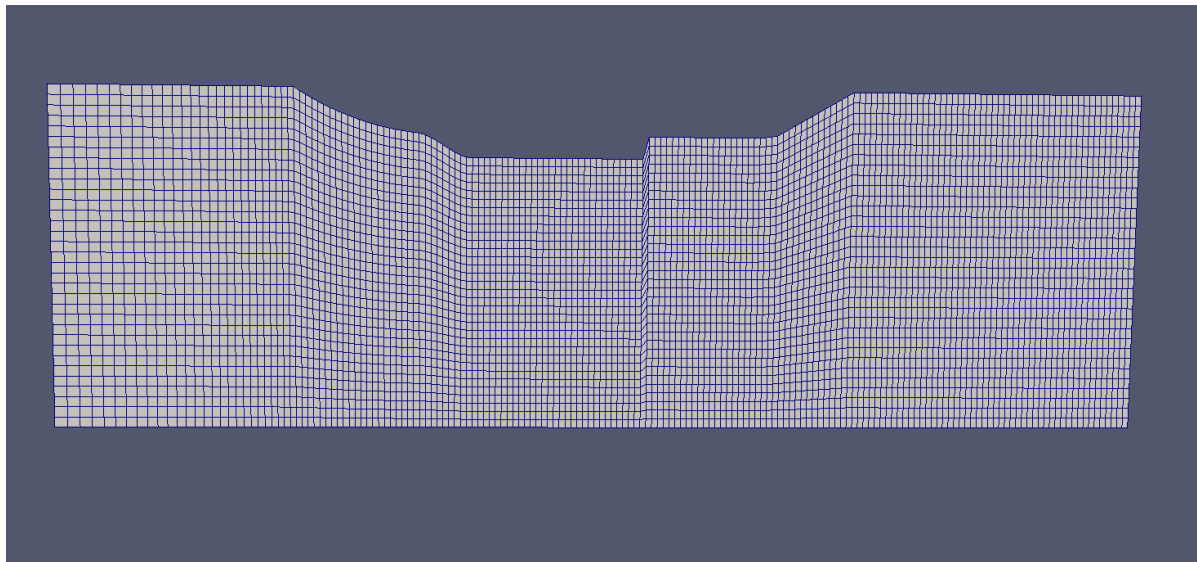
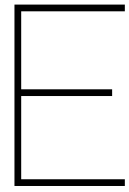


Figure D.23: Free surface grid of the concept with an open aft of a sponson.

A concept study to the influence of the position and shape of the sponson leads to unreliable results. If an difference in outcome of the wave-making resistance calculation with RAPID between two concepts is noticed, the origin of this difference cannot be defined with certainty. The difference may come from the influence of the position of the sponson on the wave-making resistance or from the discretization errors in the free surface grid.

These unpredictable results due to the open aft of the sponson has decided to left the open aft off again.

The aft of the sponson is designed with an eye on the viscous flow, which means that the aft is designed with a longer transition. This is done to avoid separation in practice, as described in chapter 5.



Variation concepts

In this appendix the fifteen concepts as described in paragraph 5.1 are shown with four different views and a top view of the wave pattern. Concept d1 is the concept, which combines the best of the three variations and is added as latest concept.

E.1. Concept a1

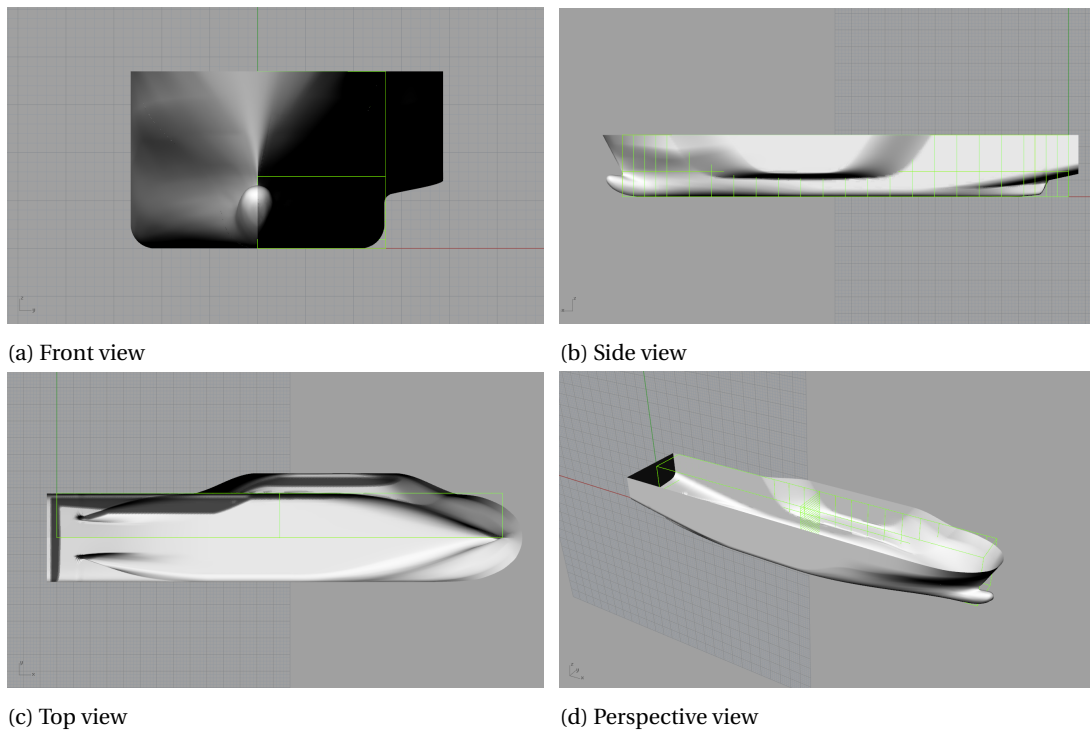


Figure E.1: Rhinoceros 3D model of concept a1.

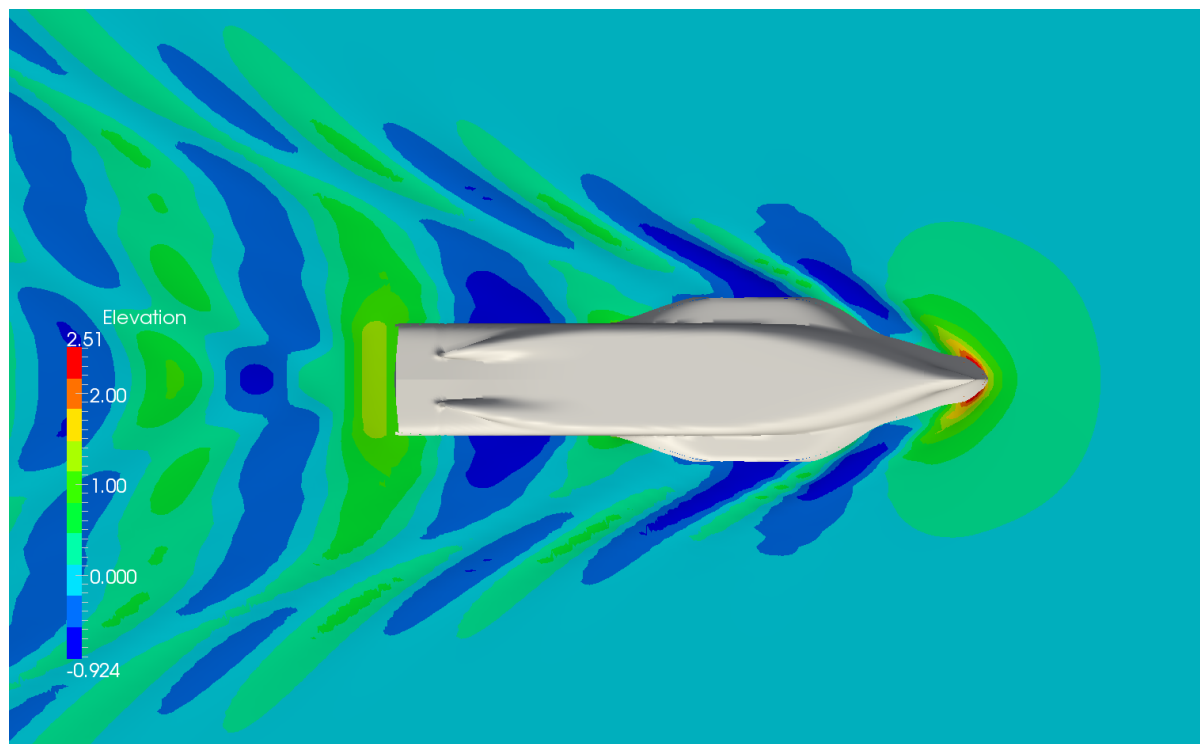


Figure E.2: Wave pattern of concept a1 as calculated with RAPID.

E.2. Concept a2

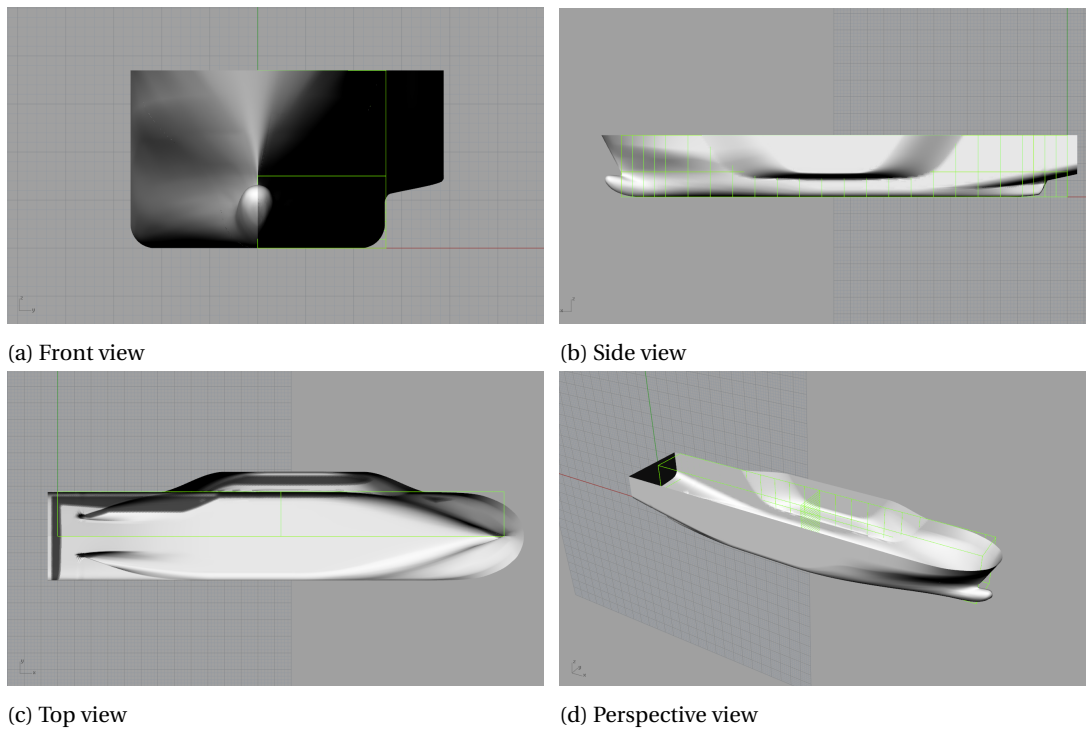


Figure E.3: Rhinoceros 3D model of concept a2.

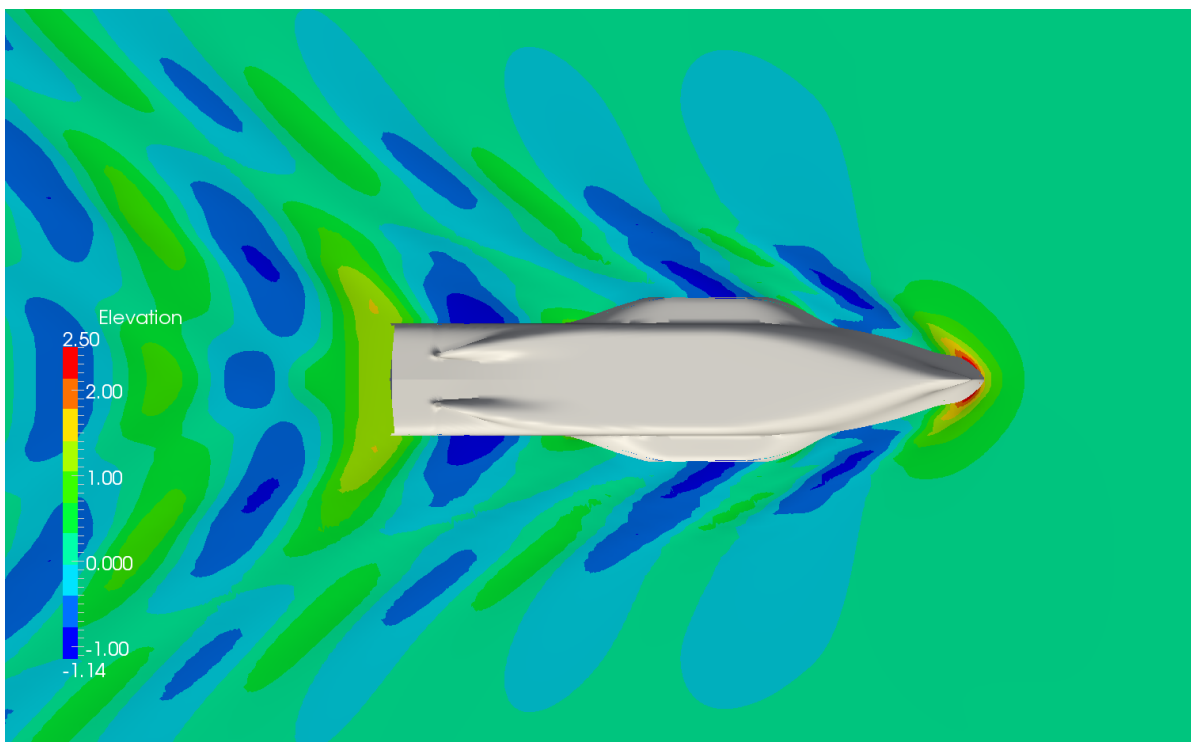


Figure E.4: Wave pattern of concept a2 as calculated with RAPID.

E.3. Concept a3

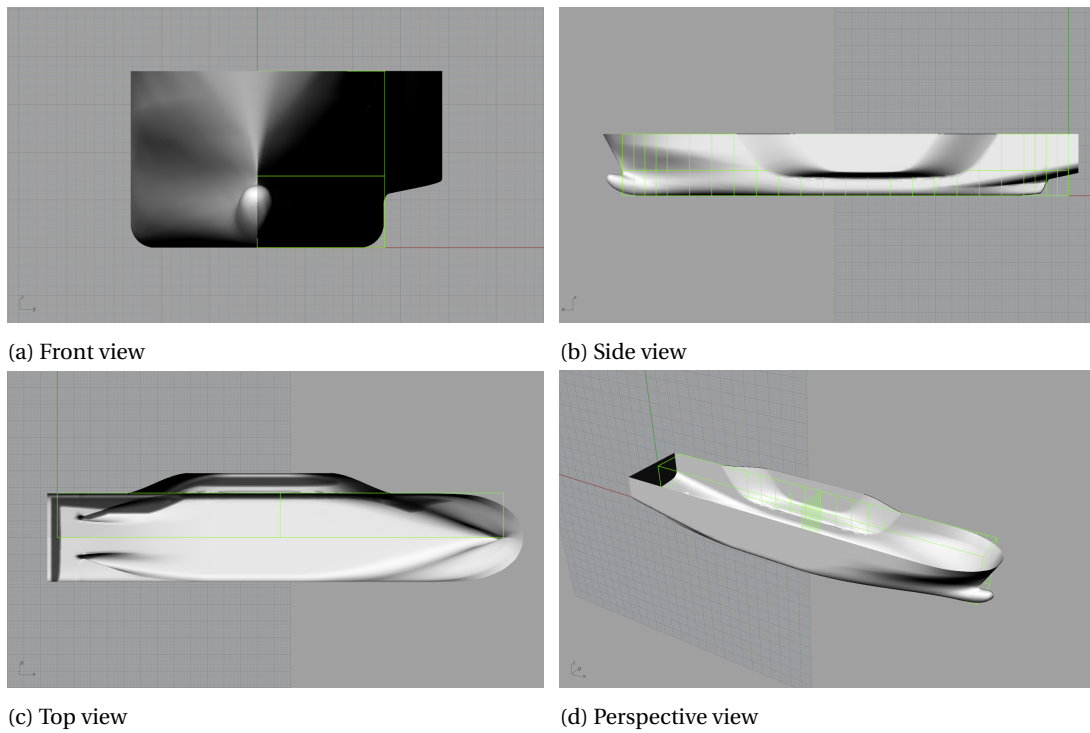


Figure E.5: Rhinceros 3D model of concept a3.

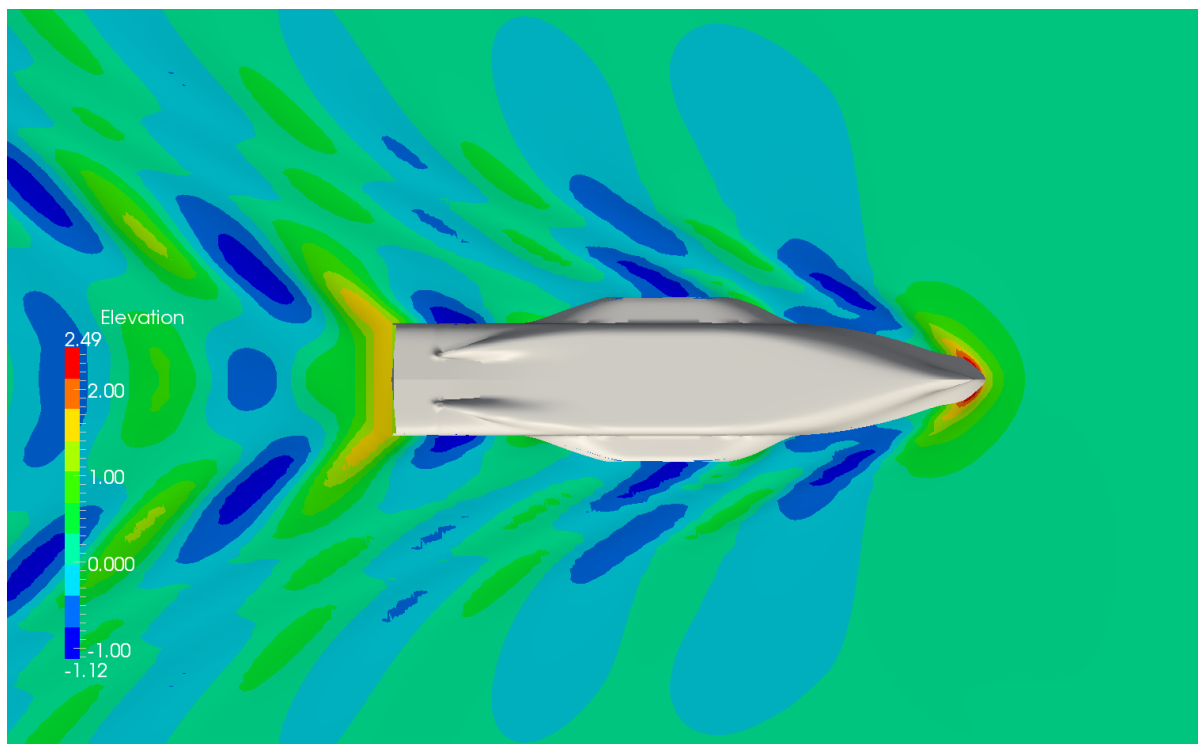


Figure E.6: Wave pattern of concept a3 as calculated with RAPID.

E.4. Concept a4

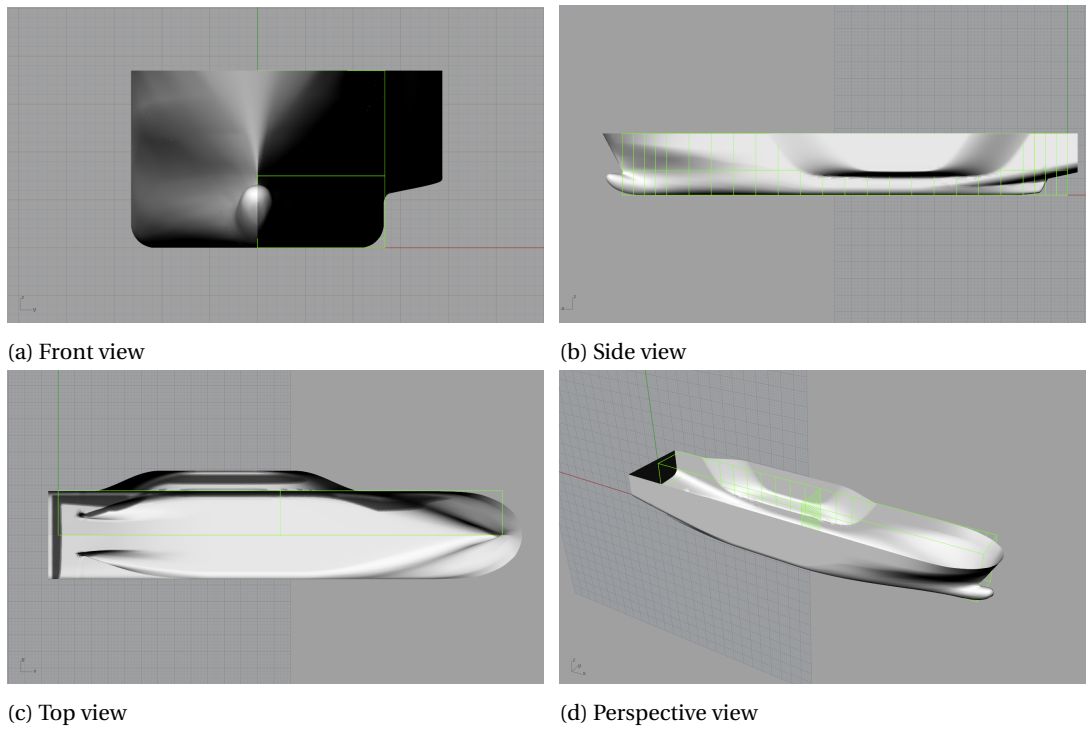


Figure E.7: Rhinoceros 3D model of concept a4.

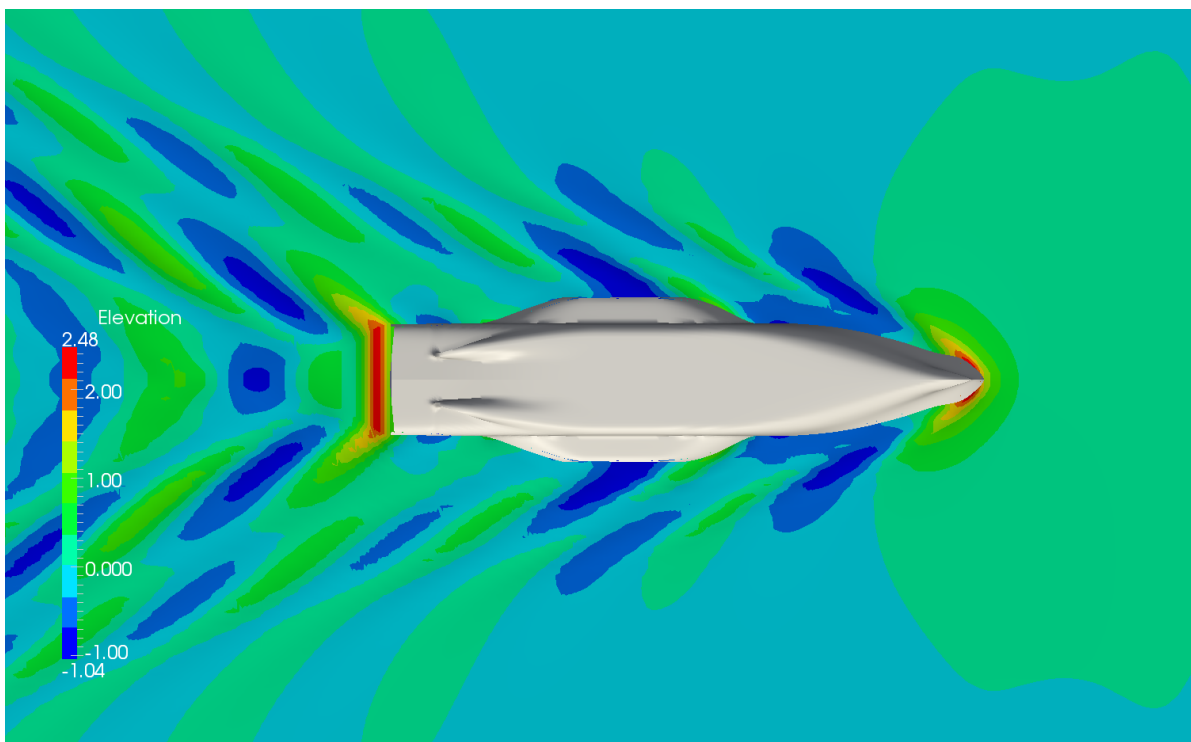


Figure E.8: Wave pattern of concept a4 as calculated with RAPID.

E.5. Concept a5

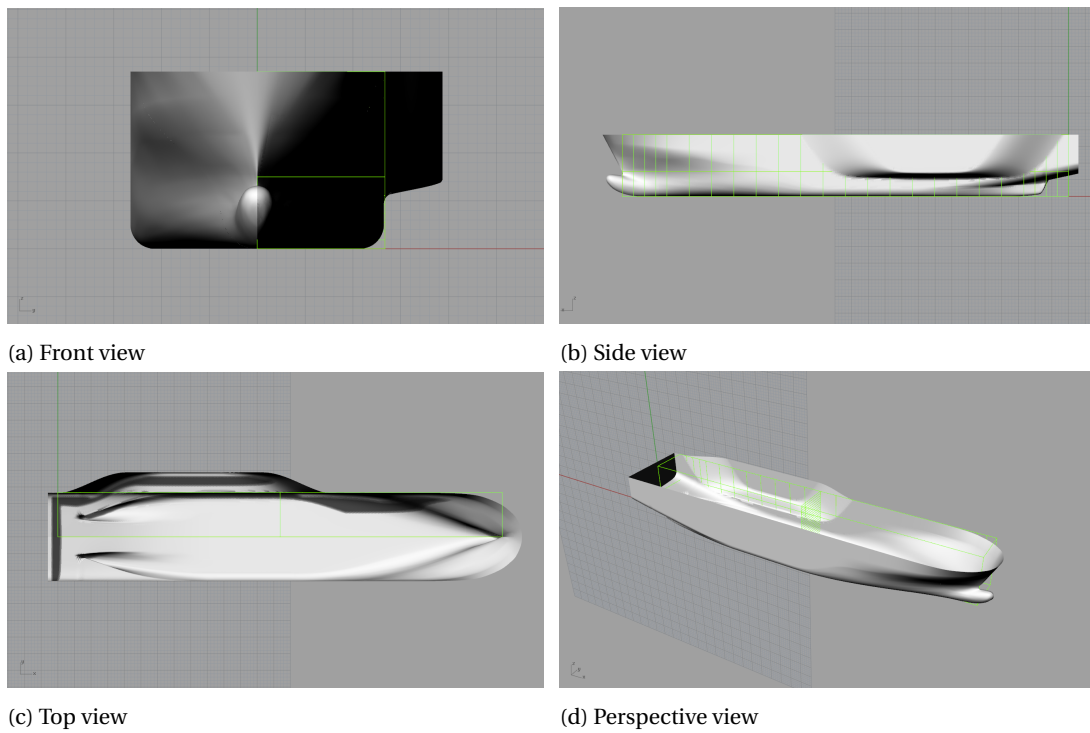


Figure E.9: Rhinoceros 3D model of concept a5.

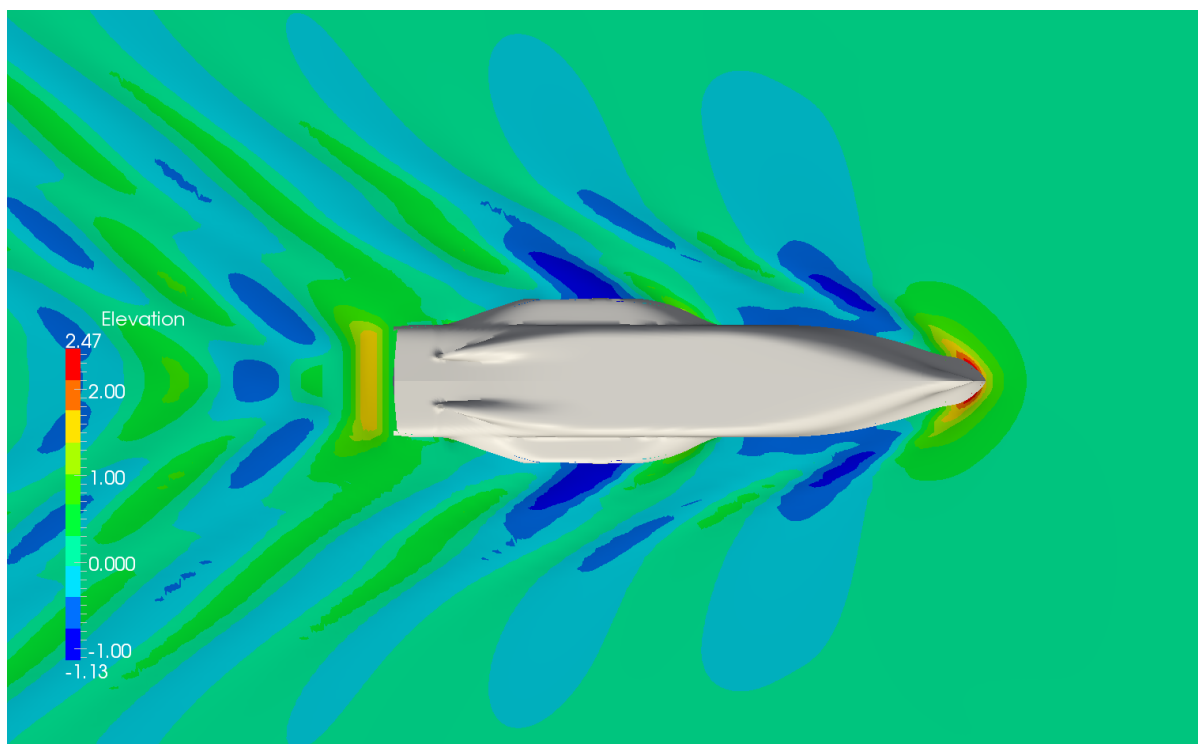


Figure E.10: Wave pattern of concept a5 as calculated with RAPID.

E.6. Concept b1

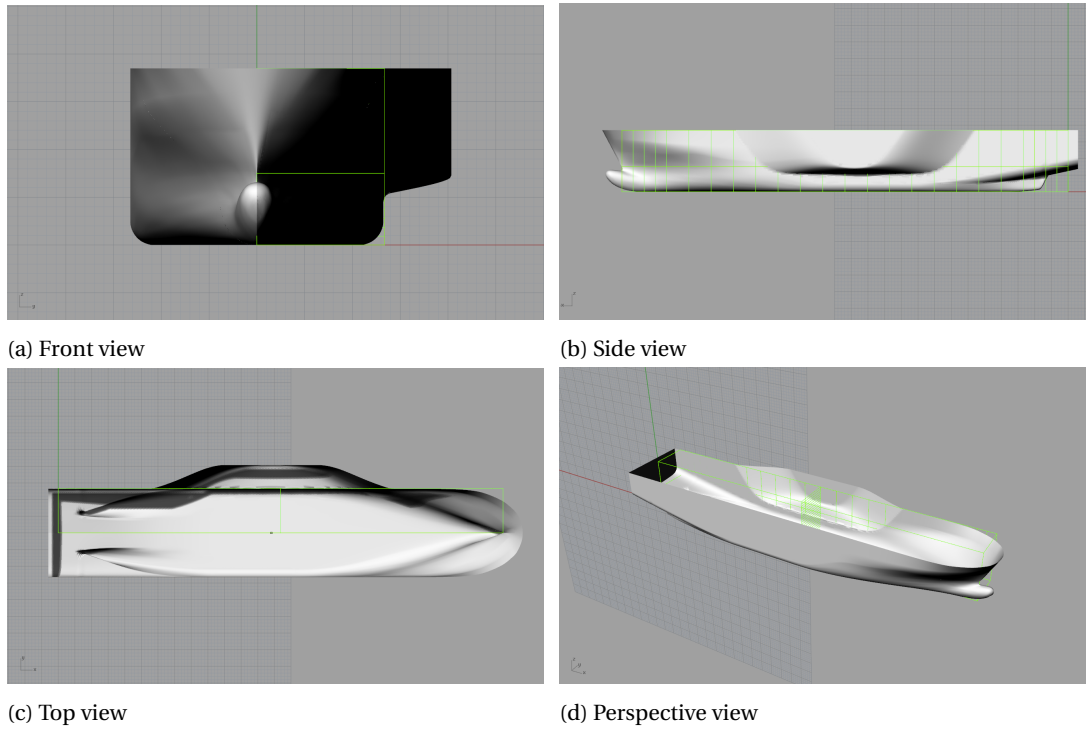


Figure E.11: Rhinoceros 3D model of concept b1.

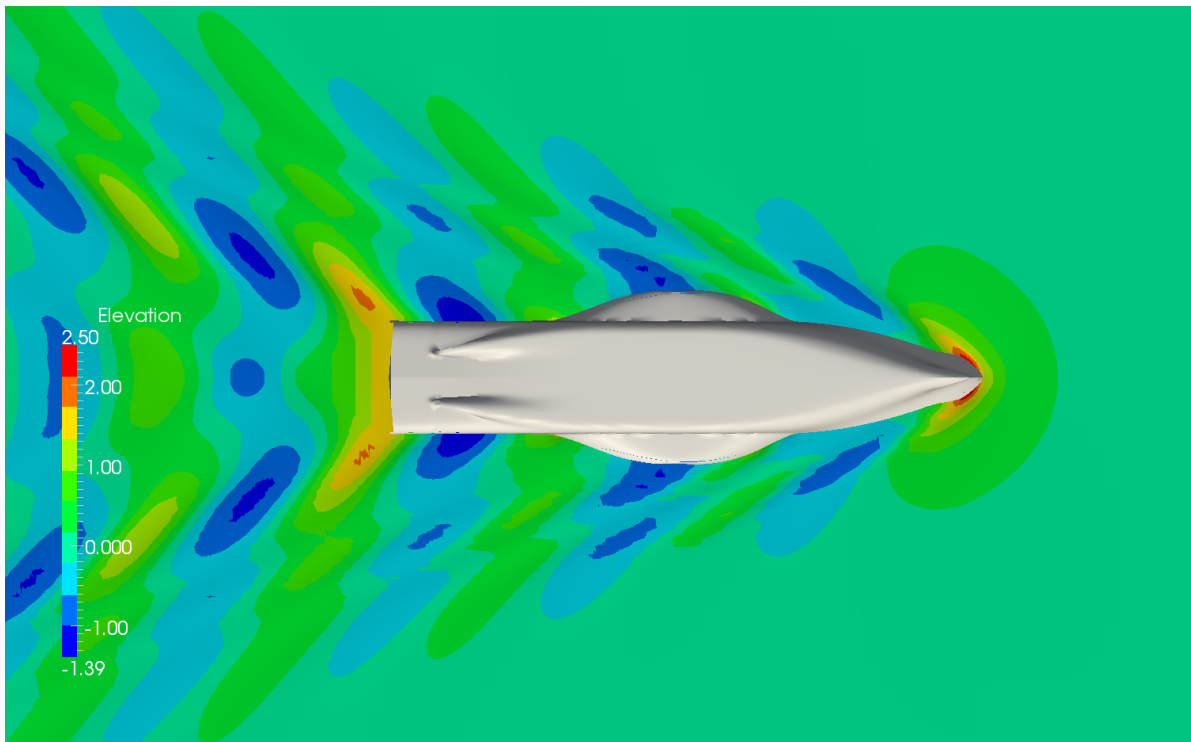


Figure E.12: Wave pattern of concept b1 as calculated with RAPID.

E.7. Concept b2

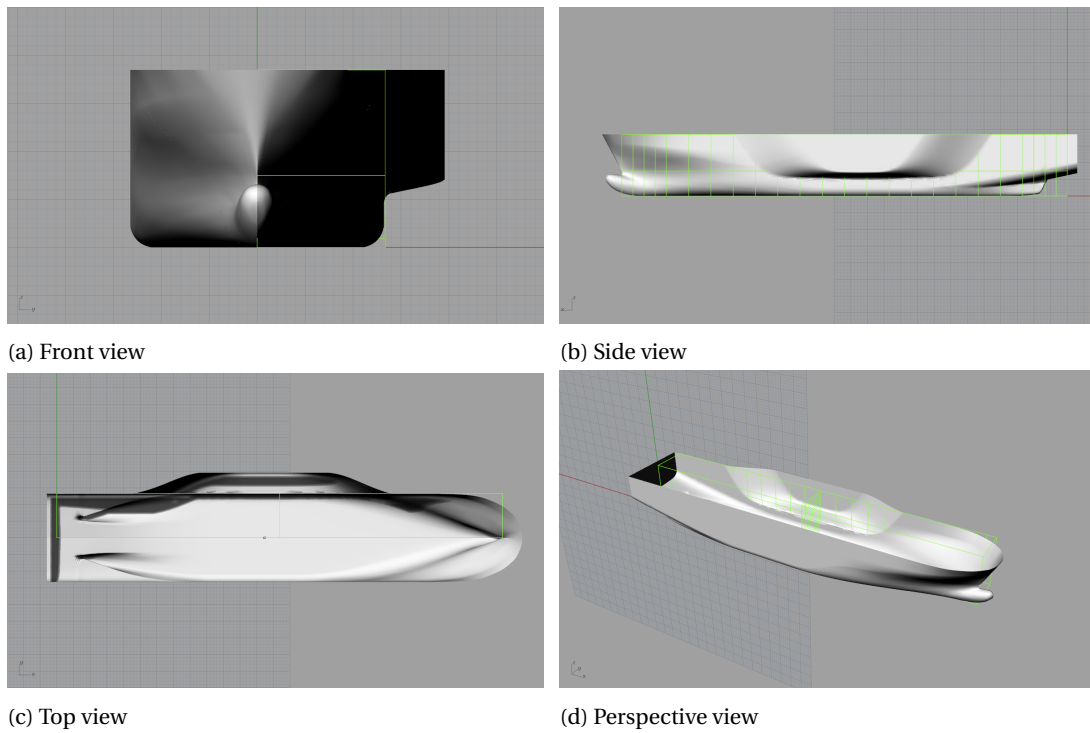


Figure E.13: Rhinceros 3D model of concept b2.

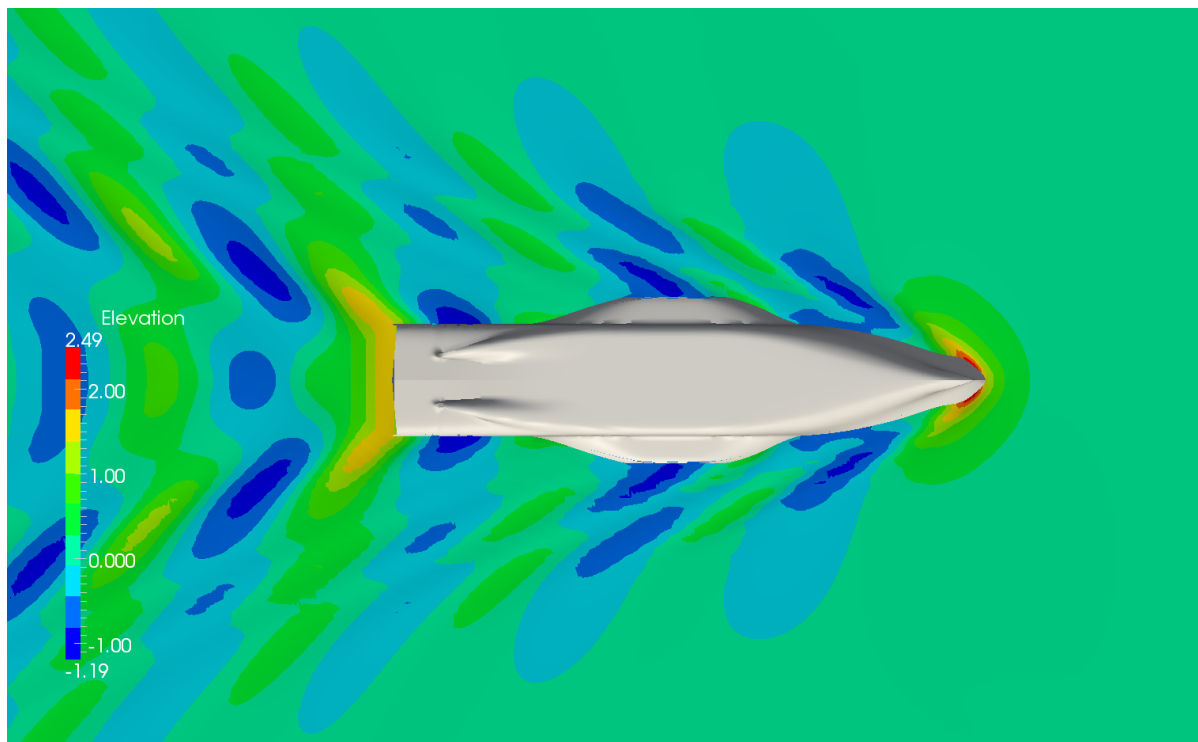


Figure E.14: Wave pattern of concept b2 as calculated with RAPID.

E.8. Concept b3

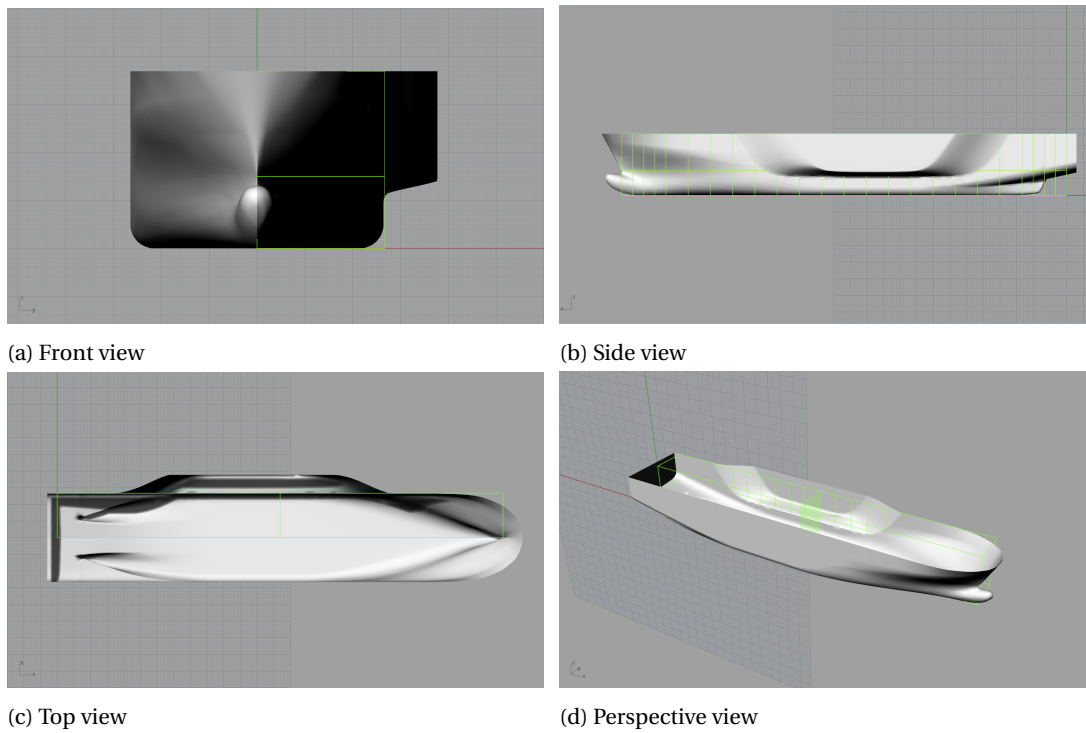


Figure E.15: Rhinoceros 3D model of concept b3.

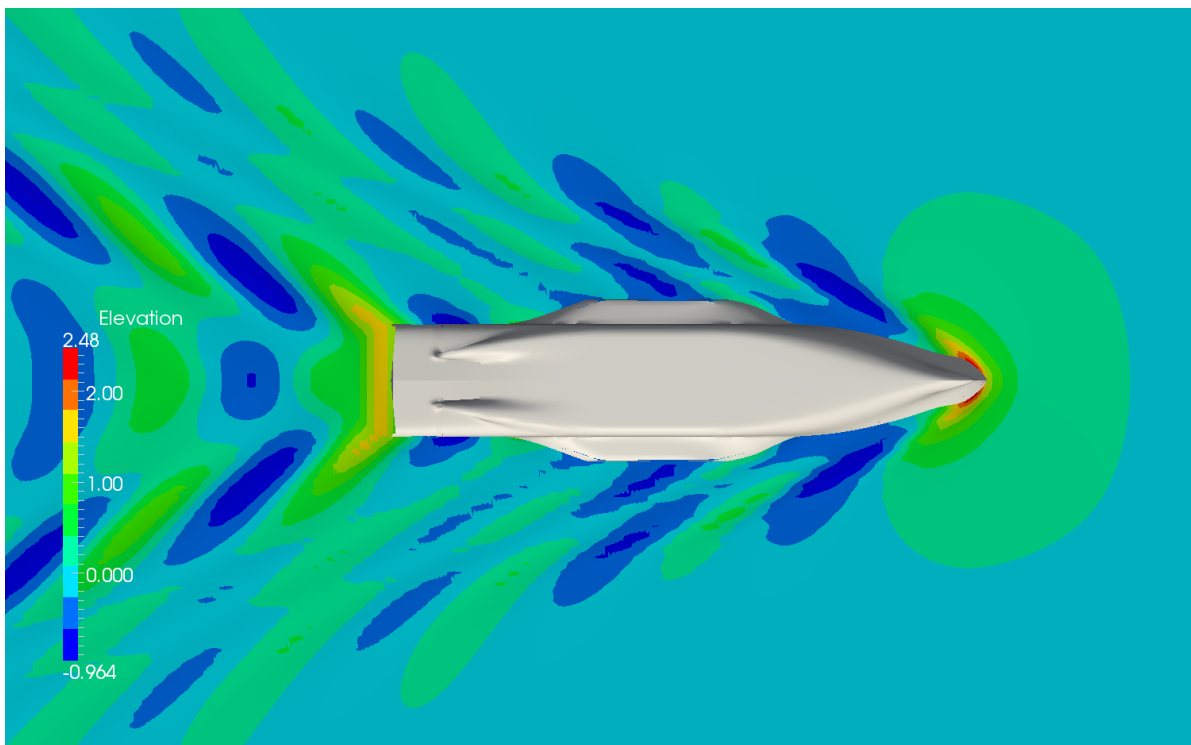


Figure E.16: Wave pattern of concept b3 as calculated with RAPID.

E.9. Concept b4

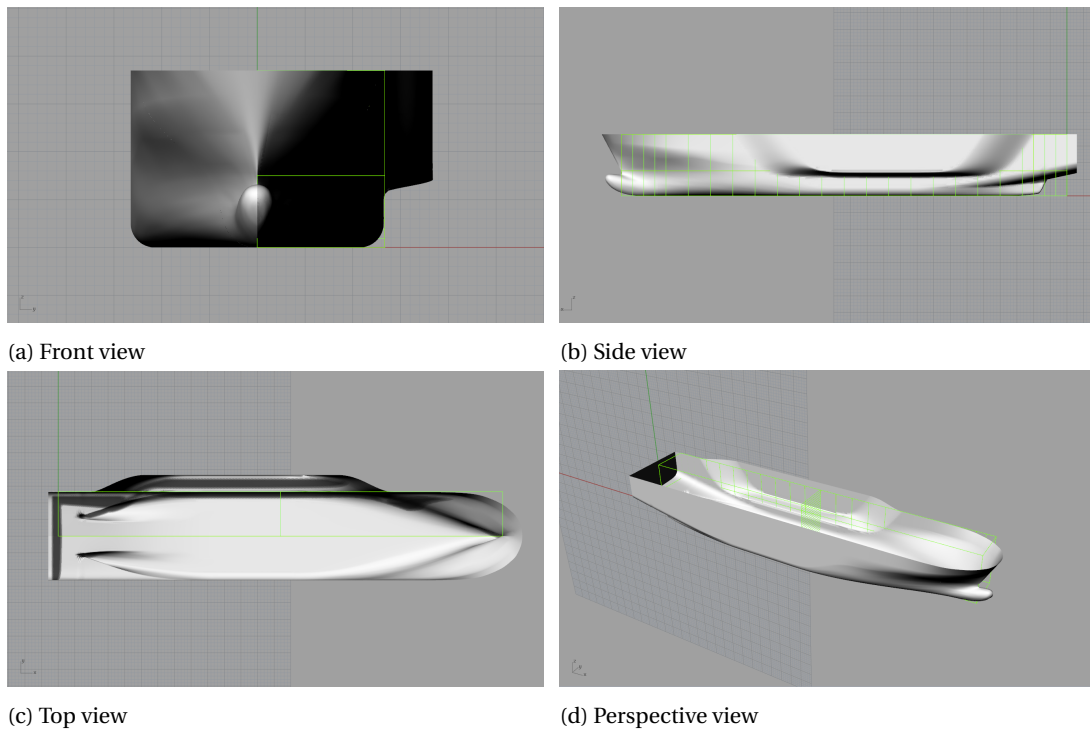


Figure E.17: Rhinceros 3D model of concept b4.

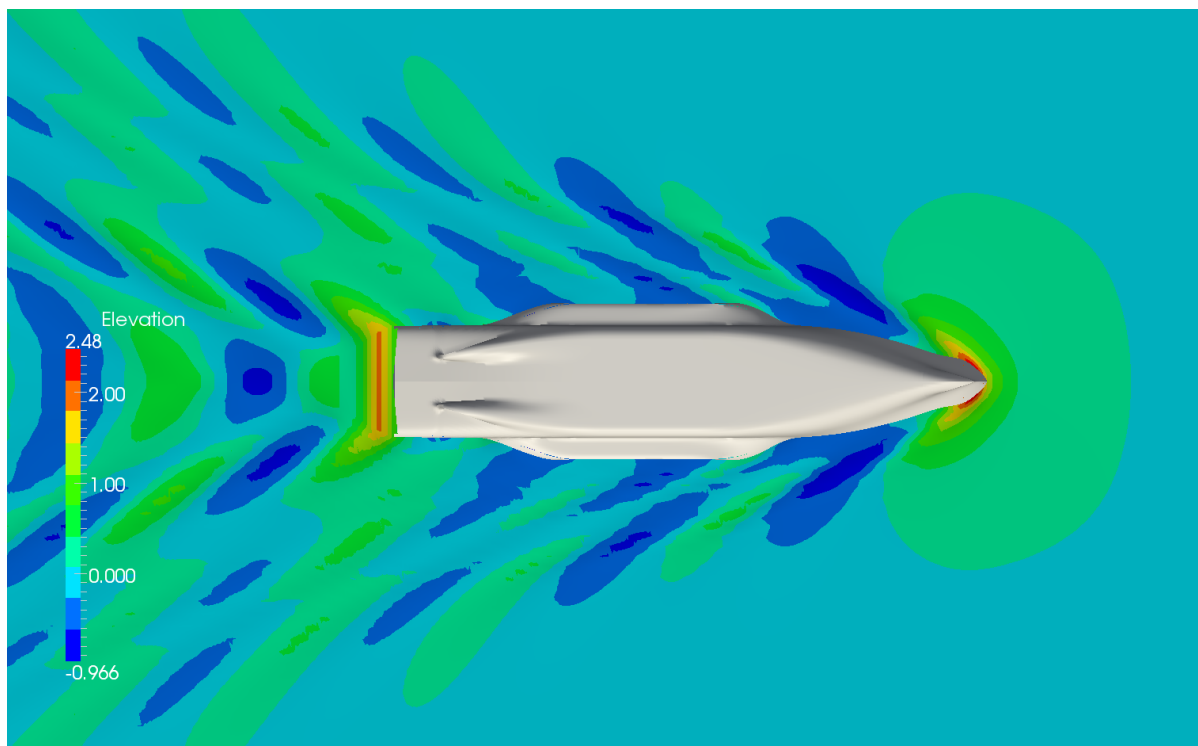


Figure E.18: Wave pattern of concept b4 as calculated with RAPID.

E.10. Concept b5

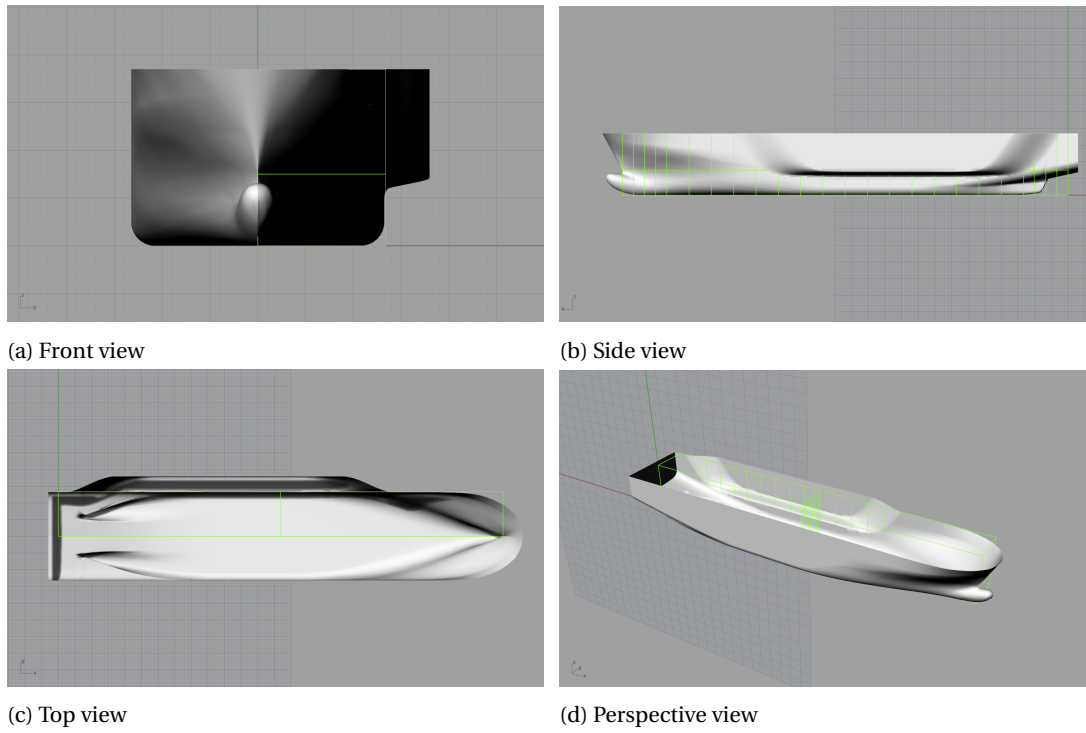


Figure E.19: Rhinoceros 3D model of concept b5.

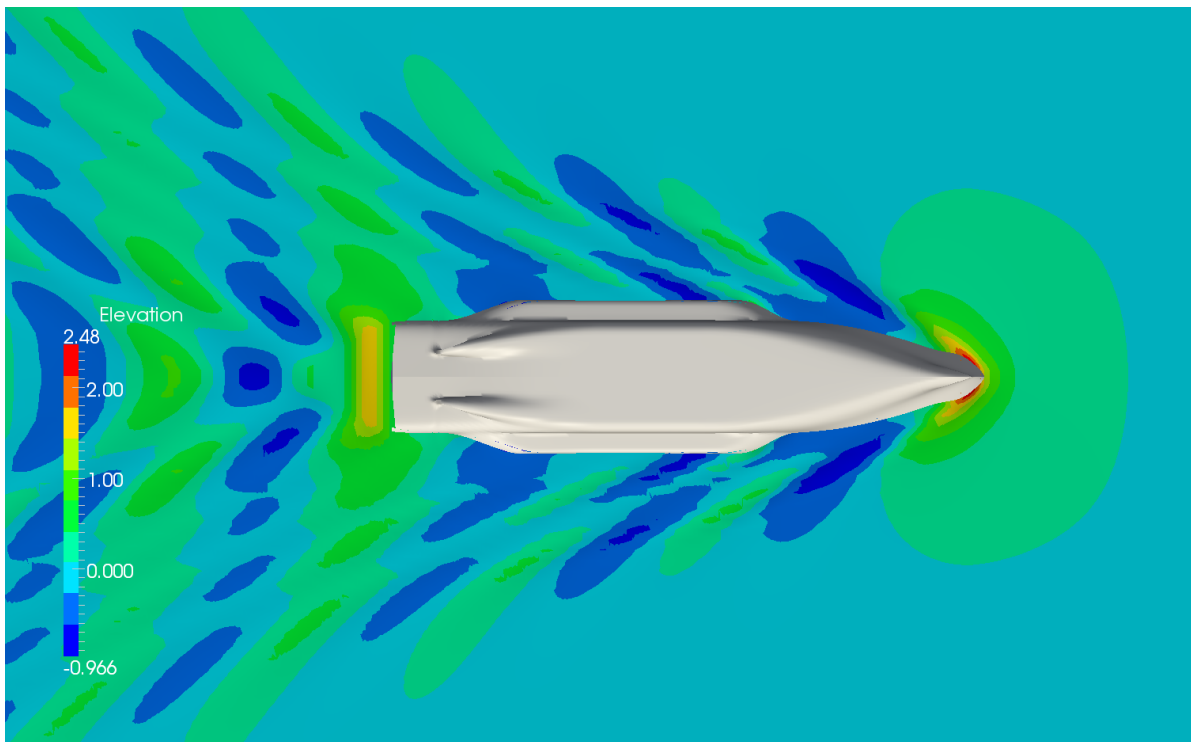


Figure E.20: Wave pattern of concept b5 as calculated with RAPID.

E.11. Concept c1

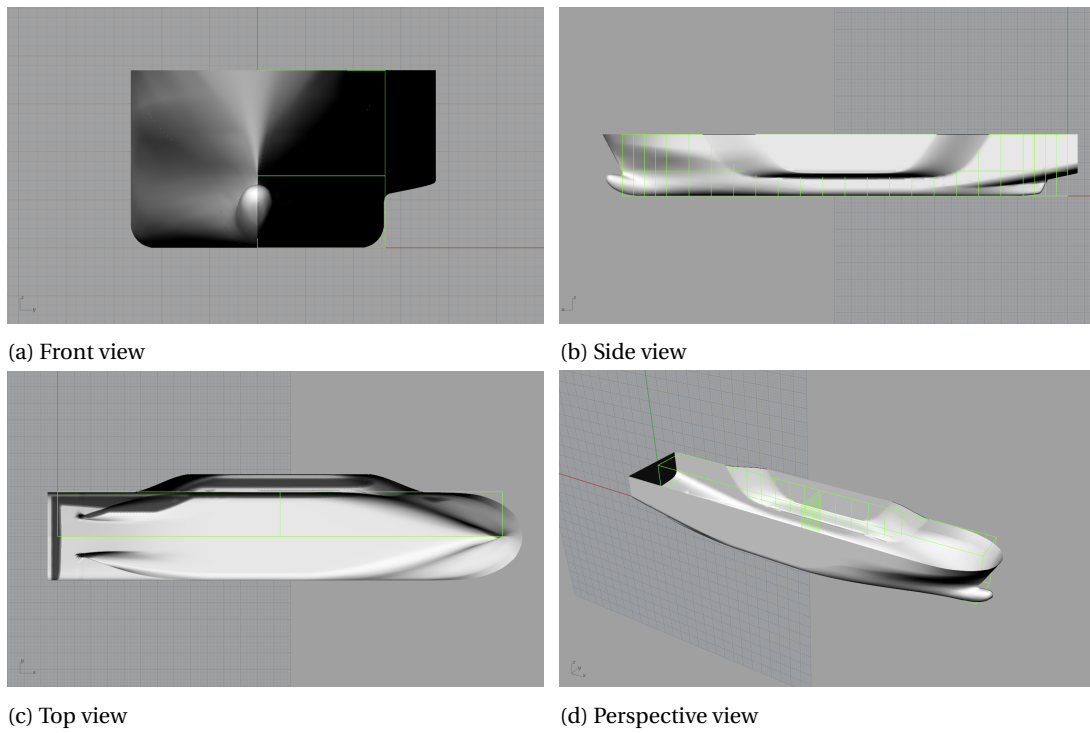


Figure E.21: Rhinoceros 3D model of concept c1.

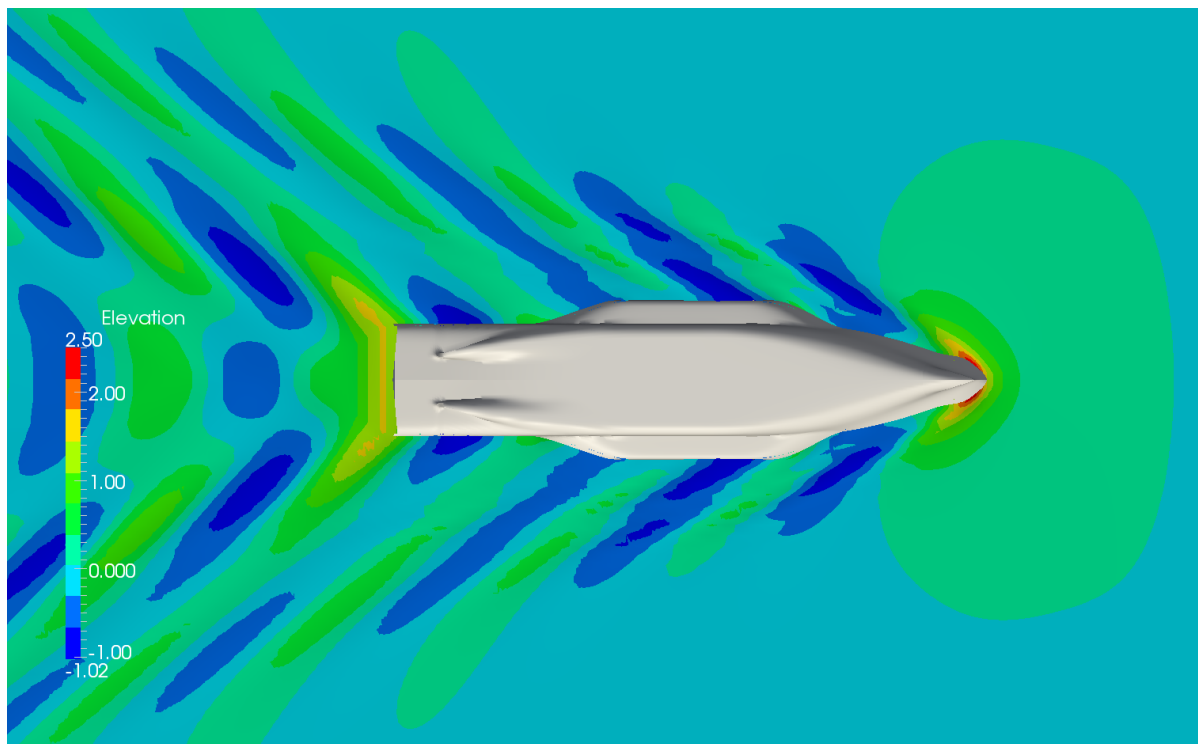


Figure E.22: Wave pattern of concept c1 as calculated with RAPID.

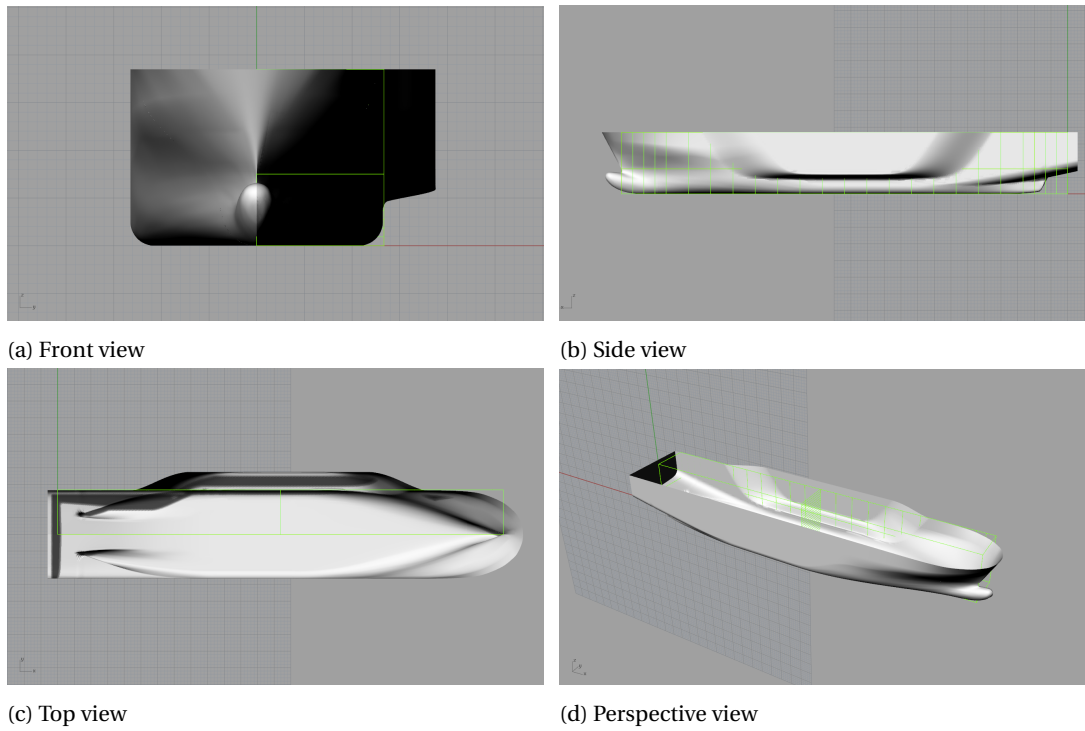
E.12. Concept c2

Figure E.23: Rhinoceros 3D model of concept c2.

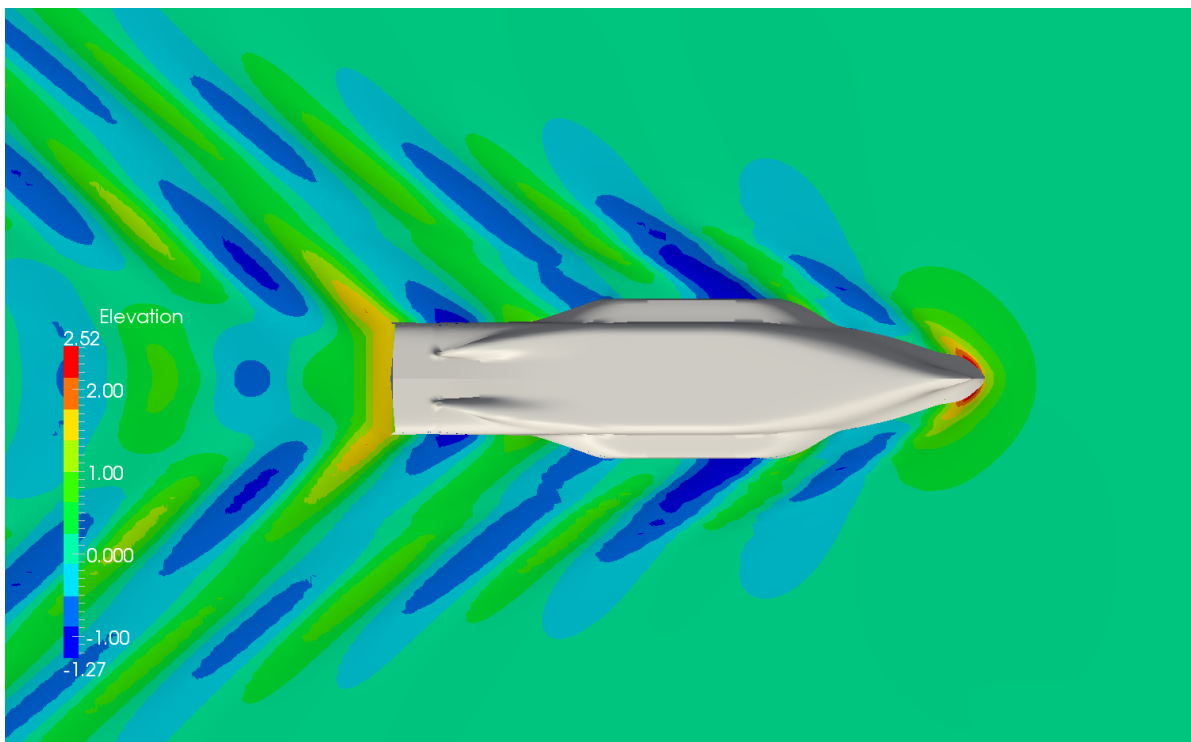


Figure E.24: Wave pattern of concept c2 as calculated with RAPID.

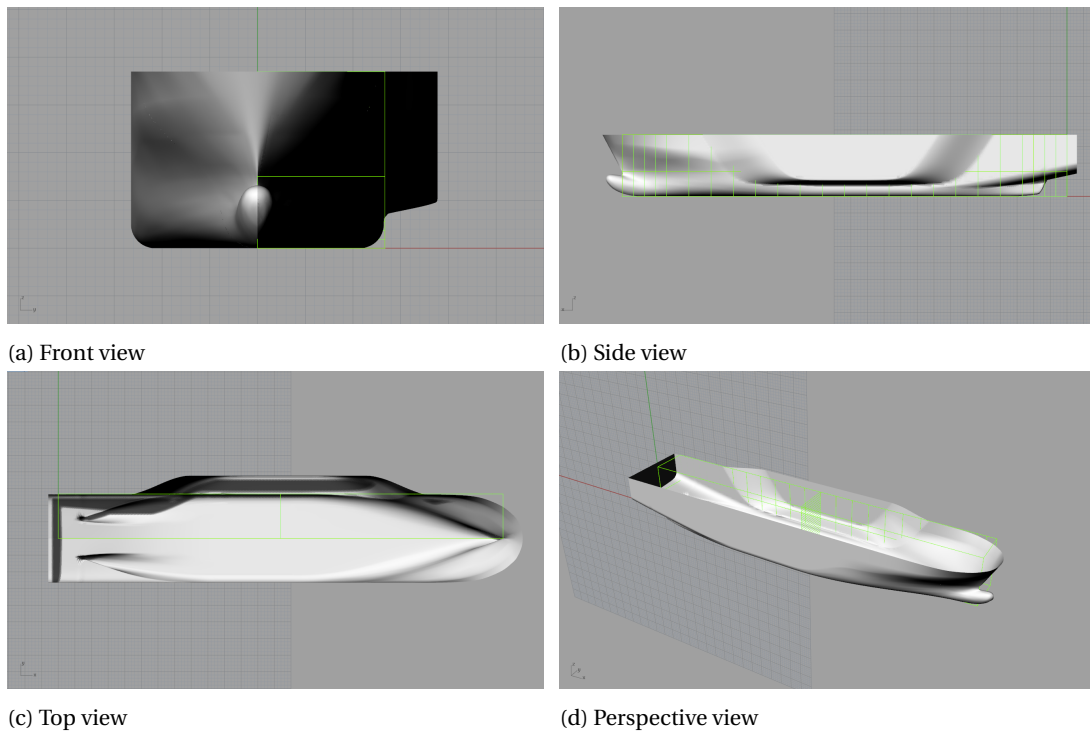
E.13. Concept c3

Figure E.25: Rhinoceros 3D model of concept c3.

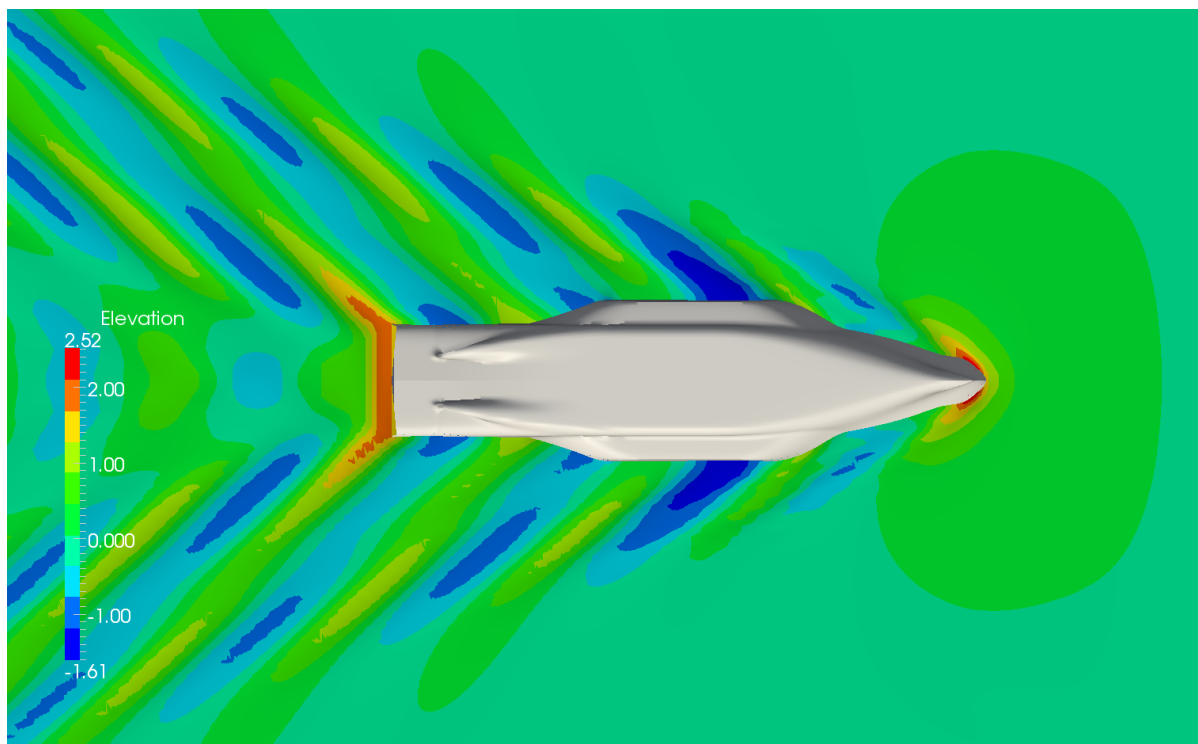


Figure E.26: Wave pattern of concept c3 as calculated with RAPID.

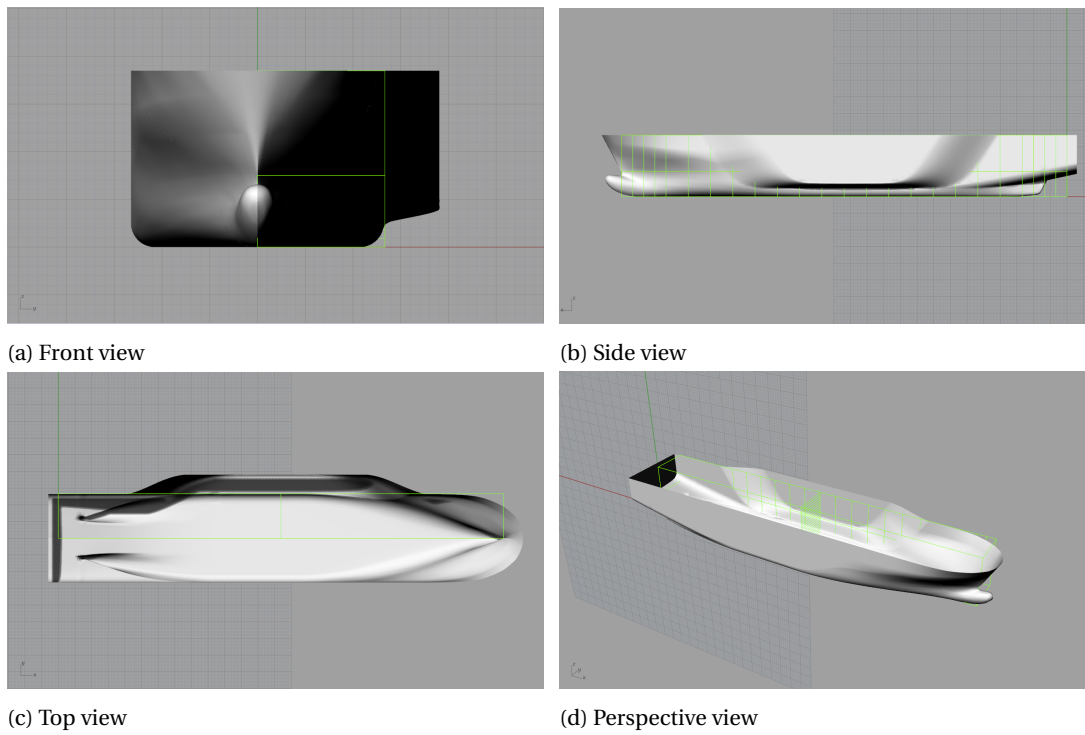
E.14. Concept c4

Figure E.27: Rhinoceros 3D model of concept c4.

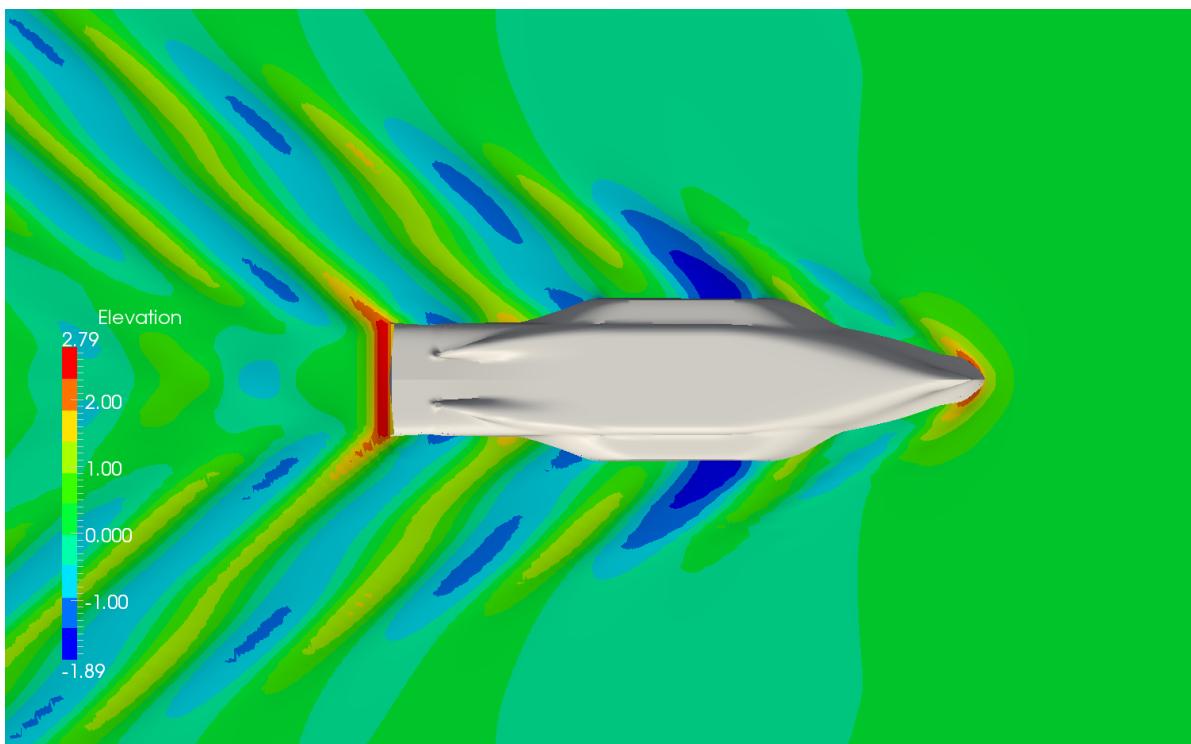


Figure E.28: Wave pattern of concept c4 as calculated with RAPID.

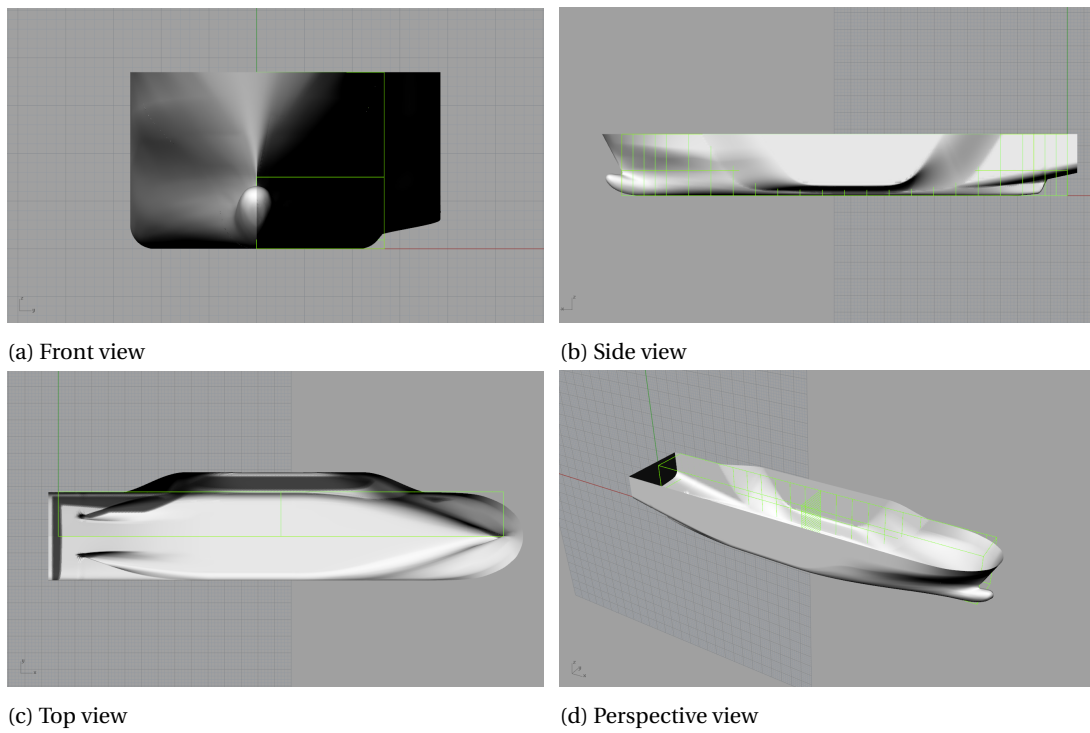
E.15. Concept c5

Figure E.29: Rhinoceros 3D model of concept c5.

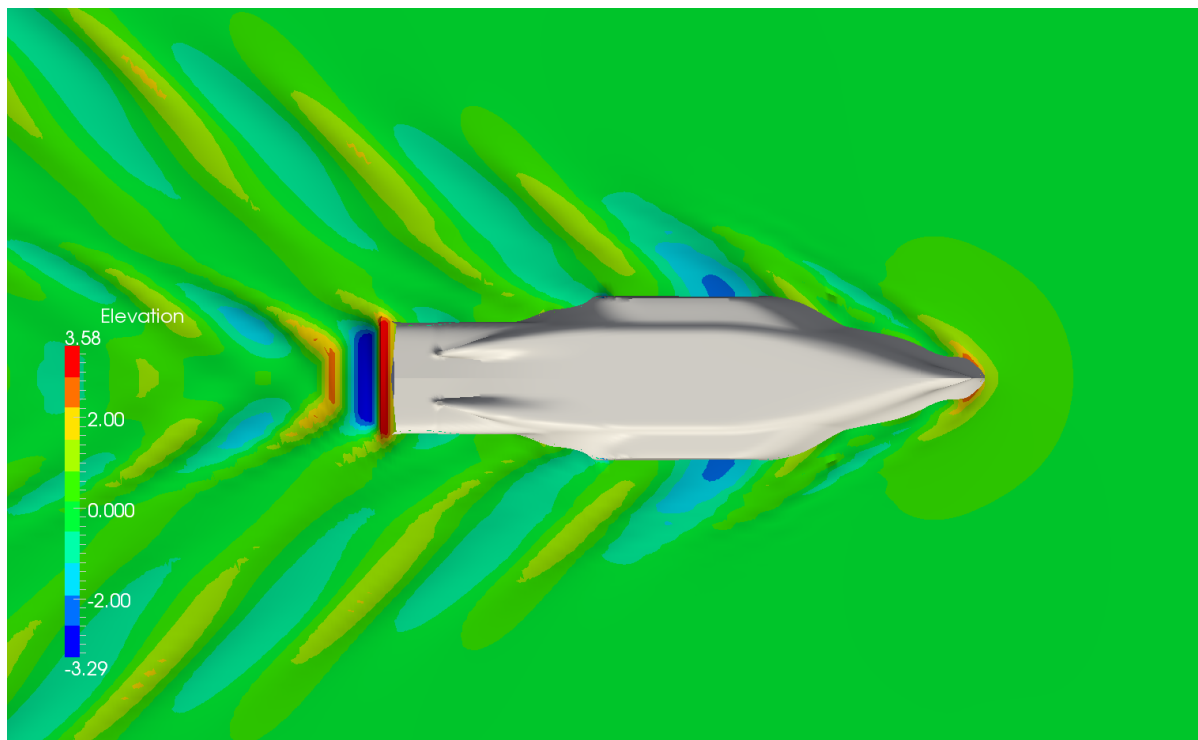


Figure E.30: Wave pattern of concept c5 as calculated with RAPID.

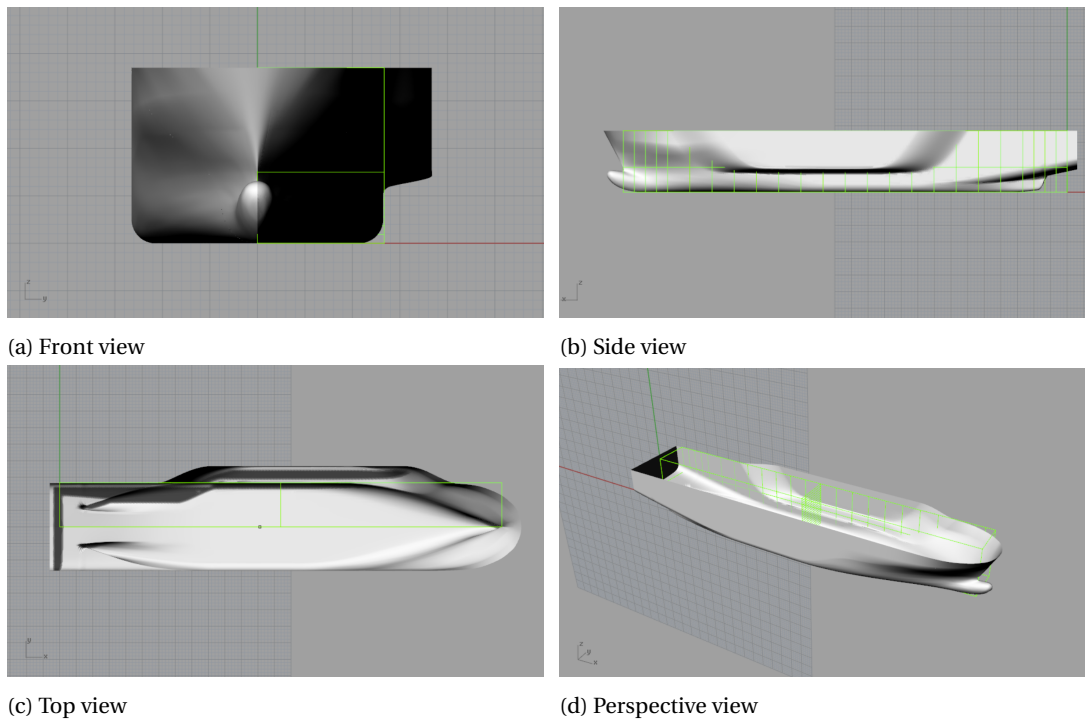
E.16. Concept d1

Figure E.31: Rhinoceros 3D model of concept d1.

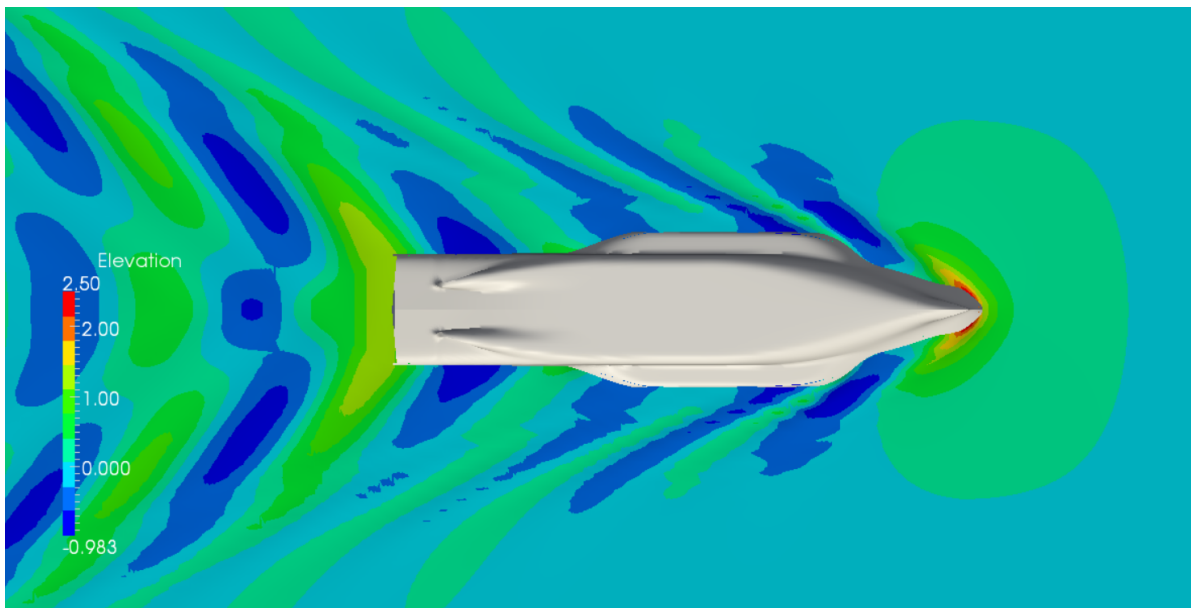
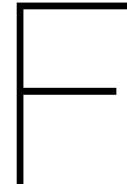


Figure E.32: Wave pattern of concept d1 as calculated with RAPID.



Results of the adjusted Holtrop-Mennen method

In table E1 the percentage increase of the 15 concepts are given with respect to the base case of the Fairplayer. In table E2 the actual values of the 15 concepts are given. As described in paragraph 5.3 an extra iteration is done, which combines the information obtained from the variation study. This resulted in a final concept, namely concept d1, for which the percentage increase in resistance and the actual values of the resistance are given in table E3.

Table E1: Increase of the resistance components as percentage of the Fairplayer for the different concepts.

Variation concept	Frictional resistance [%]	Wave-making resistance [%]	Model-ship correlation resistance [%]	Total resistance [%]
Base case	0.0	0.0	0.0	0.0
a1	8.6	8.5	3.7	8.0
a2	8.5	44.2	3.6	21.2
a3	8.6	42.1	3.6	20.5
a4	8.7	30.4	3.6	16.2
a5	8.7	10.3	3.6	8.7
b1	8.5	79.2	3.3	34.1
b2	8.4	50.8	3.4	23.6
b3	8.4	23.2	3.6	13.4
b4	8.7	5.9	4.0	7.1
b5	9.0	7.1	4.4	7.8
c1	8.8	44.8	4.1	21.6
c2	8.6	91.6	4.3	38.9
c3	8.2	142.0	4.3	57.4
c4	8.0	193.1	4.7	76.4
c5	7.5	168.1	4.9	66.9

Table F2: Values of the resistance components for the different concepts calculated with the adjusted Holtrop-Mennen method.

Variation concept	Frictional resistance [kN]	Wave-making resistance [kN]	Model-ship correlation resistance [kN]	Total resistance [kN]
Base case	389.0	281.2	87.0	757.2
a1	422.4	305.1	90.3	817.8
a2	422.2	405.5	90.2	917.8
a3	422.5	399.5	90.2	912.2
a4	422.9	366.6	90.2	879.7
a5	423.0	310.0	90.2	823.2
b1	422.1	503.8	89.9	1015.7
b2	421.5	424.0	90.0	935.5
b3	421.6	346.5	90.2	858.3
b4	422.9	297.8	90.5	811.2
b5	424.0	301.2	90.8	816.1
c1	423.2	407.2	90.6	921.1
c2	422.3	538.7	90.7	1051.7
c3	420.8	680.3	90.8	1191.9
c4	420.1	824.1	91.1	1335.3
c5	418.2	753.9	91.3	1263.4

Table E3: Resistance components for the extra iteration of the concept from the Fairplayer with a sponson.

Variation concept	Frictional resistance [%]	Wave-making resistance [%]	Model-ship correlation resistance [%]	Total resistance [%]
d1	8.9	34.8	4.2	18.0
Variation concept	Frictional resistance [kN]	Wave-making resistance [kN]	Model-ship correlation resistance [kN]	Total resistance [kN]
d1	423.6	379.1	90.7	893.5